Free Surface Problems for Jet Impact on Solid Boundaries

Weidong Peng

Thesis presented for the degree of

Doctor of Philosophy

University of Edinburgh

1994

Abstract

Impinging jets are used in a number of cooling and drying systems generally because the thin boundary layer near the centre of impingement provides a high local heat transfer coefficient. Industrial uses of impinging jets include the tempering of glass, drying of paper and textiles, and the cooling of metal sheets, turbine blades and electronic components.

In this thesis the impact of fluid jets on various objects is analysed. For a jet incident on a porous wall at which normal fluid speed is specified, it is found that the problem of determining the free surface of the jet is governed by a system of nonlinear integral equations relating the flow angles on the boundary, on the free surface and on the porous wall. With constant normal speed at the porous wall, the system reduces to an integral equation for the flow angle. We also show how this formulation may be extended to include the action of gravity.

A nonlinear two-dimensional free surface problem of an ideal jet impinging on an uneven wall is studied using complex variable and transform techniques. A relation between the flow angle on the free surface and the wall angle is first obtained. Then, by using a Hilbert transform and the generalised Schwartz-Christoffel transformation technique, a system of nonlinear integro-differential equations for the flow angle and the wall angle is formulated. For the case in which the wall geometry is symmetric, a compatibility condition for the system is automatically satisfied. Some numerical solutions are presented, showing the shape of the free surface corresponding to a number of different wall shapes. For the case in which the wall geometry is asymmetric, a pair of conditions which determine the position of the stagnation point are revealed, using the integral form of the momentum equation. Thus the shapes of the free surface of the jet impinging on a few asym-

metric uneven walls are shown. The stagnation point is located for each of the different cases.

A flow passing through a porous film and then impinging on a flat solid boundary is analysed. Since the pressure field and fluid velocity are discontinuous along the film, the flow region is divided into two parts. At the film, by analogy with Darcy's law, the pressure difference is taken to be proportional to the flow rate. The free surface problem for this transpiration flow is formulated as a system of three coupled integral equations using a boundary integral method. As the system is solved numerically, the normal speeds at the film and the shapes of the free surface for different permeability coefficients are presented.

Acknowledgements

I would like to thank my supervisor Prof. David. F. Parker for his encouragement, guidance and helpful discussion. I would also like to thank Dr. A. M. Davie for his help.

I would take this opportunity to acknowledge University of Edinburgh for financial support through a Postgraduate Studentship and a Overseas Research Studentship.

I would like to thank my mother Hu Xin and my brothers for their love, support and patience.

Finally, I would like to express my gratitude to the staff and students of the Department of Mathematics and Statistics for providing an excellent working environment.

Table of Contents

Chapter 1

Introduction

The fluid motions considered in this thesis have in common the presence of a surface separating two fluids of different densities. As one fluid is air, with negligible density so that pressure changes are small, the interface may be idealized as a free surface. In addition the flows also have in common the presence of an uneven rigid surface as part of the boundary of the whole flow region. In all cases, the steady two-dimensional flow of an incompressible, inviscid and irrotational fluid is treated.

Free surface flows over some kinds of obstacles have been studied for at least a century. Early work in this area was characterised by the use of a linearized free surface condition and perturbation procedures such as the infinitesimal wave approximation and the shallow water approximation. A review of the two methods is due to Wehausen and Laitone [1960]. In 1886, Kelvin considered the stationary wave pattern caused by finite elevations or depressions in the bed of a stream and also developed expressions for the hydrodynamic forces acting on these obstacles. For the case of free surface flows past curved barriers, the calculation was first performed by Brodetsky[1923], who developed a method of trigonometric interpolation to successfully treat the plane infinite flow past circular and elliptical arcs, later extended by Birkhoff and Zarantonello[1957]. Later this method, com-

bined with finite Hilbert transforms, was modified by Olmstead and Raynor[1964] to consider depressions in a liquid surface due to an impinging two-dimensional potential jet. In this work, the authors treated the interface as an obstacle of unknown shape along which some boundary condition holds. All the above-cited work was based upon the adaptation of the classical hodograph method to flow around a body with a curved boundary. A direct formulation of this problem as a nonlinear integro-differential equation for the angle made by the fluid velocity vector was derived by Villat[1911] and also by Nekrasov[1922] to prove both existence and uniqueness of flows around a small circular arc. Nekrasov also found approximate solutions to the equations. For the case of the free surface flow of a stream obstructed by a bump or even an arbitrary bed topography, many types of such problem have been analysed using approximate nonlinear theories of similar accuracy to the cnoidal theory of Benjamin and Lighthill[1954]. Amongst these are a sluice gate projecting into the free surface [Benjamin, 1956], and the effects of arbitrary bumps on the bottom of a stream[Gerber, 1955]. The general theory of the shallow water approximation for problems of interface waves and surface waves in a fluid bounded by a rigid bottom surface was given in Wehausen and Laitone [1960].

The increasing availability of high speed digital computers, combined with the advanced state of the general theory, in both the obstructed free surface problem (in which a stream is obstructed by some bumps on the stream bed) and the problem of a jet flowing steadily over an arbitrarily curved wall, has fostered the development of numerical methods.

Stokes[1880] first introduced the velocity potential ϕ, and stream function ψ as independent variables so as to generate series expansions for the position (x,y) of the free surface of a steady wave. Many authors have successfully used this method. Schwartz[1974] extended Stokes' infinitesimal wave expansion, using a

computer to evaluate the coefficients. The radius of convergence of the series was extended by the use of Padé approximants so improving the estimates of the highest wave. A similar method was used by Longuet-Higgins[1975] to consider large amplitude waves in deep water, and by Cokelet[1977] for all steady, irrotational waves in water of any uniform depth. Another approach used by Long[1956] was extended by Byatt-Smith[1970] to obtain the vertical independent variable y of the free surface in terms of the velocity potential ϕ along the free surface $\psi = \psi_s$ and to give an exact integral equation for the elevation of the free surface using a generalized Hilbert transform. The equation can apply to all waves, including solitary waves and waves of maximum height. Forbes[1981] studied free-surface flows over a semi-elliptical bump obstruction. The problem was formulated inversely, by allowing the velocity potential and stream function to be independent variables. The physical region was conformally mapped to a plane in which the bottom streamline becomes a straight line, so that it was only necessary to set numerical grid points directly at the free surface. Then the profiles of curved free-surface profiles were calculated. The author predicted that the nonlinear drag vanishes for some ellipse lengths. A similar analysis of an obstructed free surface flow in which the exact free surface condition was retained is given by Forbes and Schwartz[1982], who considered flow over a semi-circular bump in the bed of a stream of finite depth. In their work, a Joukowski transformation was used to remove the stagnation point at the front of the obstruction and an integro-differential equation for the transformed free surface elevation was obtained using a (ϕ, ψ)-coordinate system. The free-surface height in the physical plane together with other quantities of interest, for instance, the drag force on the semicircle, were then calculated from the solution to the integro-differential equations.

The conformal mapping methods applied in free surface flow problems usually employ transformations on to some appropriate region of the complex potential plane, typically simple polygons or strips. In order to map them to even simpler

shapes such as a half-plane or unit disk, the transformations are given through the Schwartz-Christoffel formula. However, in some cases the relevant regions of the complex potential planes are complicated, so more elaborate mapping techniques are needed to treat the problem. Some generalisations of the Schwartz-Christoffel formula were demonstrated in Woods' work [1958,1961], where applications to incompressible fluid motion were given. Dobroval[1969] derived a nonlinear singular integral equation for the water wedge entry problem using a generalisation of the Schwartz-Christoffel formula in an implicit way. Bloor[1978] has successfully used one of the generalisations to solve the problem of capillary-gravity surface waves. The physical flow region, rather than the complex potential plane, was directly mapped into a half-plane. An exact nonlinear integro-differential equation for the free surface angle was then obtained. Some known results such as the linearized solution and the Stokes solution were recovered by expanding the integro-differential equation in terms of the amplitude, and numerical solutions for large amplitude waves were computed.

King and Bloor[1987] used a similar transformation technique to examine the problem of steady free surface flow of an ideal fluid over a semi-infinite step in the bed. A nonlinear integro-differential equation for the slope of the free surface was obtained. The authors found that the solutions to this equation have a number of different characteristics depending on the step height and the upstream Froude number. Linearized solutions, based upon small step height were given. Numerical nonlinear solutions to the integro-differential equation were obtained and comparison of the accuracy of the numerical solutions with an asymptotically exact hydraulic theory was made. The free surface flow of a stream, obstructed by a semi-elliptical bump was considered by Forbes [1981], and obstructed by a triangular bump by Boutrous and El-Malek[1987]. A more general problem of steady free surface flow involving gravity and arbitrary bottom topography was examined by Gerber[1955]. The formulation of this problem involved coupled integral and

integro-differential equations for the four variables: flow speed on the free surface and at the bottom, the angle of the free surface, and the arclength along the bottom, using the classical hodograph method. The existence and uniqueness of the solution to these equations was shown. The same problem was also considered by Naghdi and Vonsarnpigoon[1986], who formulated the problem as a nonlinear ordinary differential equation for the wave height using an approximate theory; a director theory for a constrained fluid sheet. The bed topography was assumed to be compact and the flow region was divided into three parts; the upstream region I with a level bottom , the region II bound by the obstacle region II and a downstream region III. The equation for the downstream region was integrated up to an undetermined constant.

King and Bloor[1988] studied the same problem, using a more versatile method, again based upon a generalization of the Schwartz-Christoffel formula, to formulate this obstructed flow. A pair of coupled integral and integro-differential equations holding on the free surface and the bottom topography were derived. The linear theory developed was compared with that obtained by Lamb[1932] and the linear solution is found to be as accurate as that given by Lamb. Some numerical solutions of such flows for a variety of bottom topographies were shown. Their computations showed that the effects of nonlinearity on the problem are very dependent upon the form of the bottom topography. Later, another problem of computing a free streamline with condition of constant speed, the steady flow of a jet of ideal fluid against an arbitrary curved wall, was also investigated by King and Bloor[1990] using a similar technique. Moreover, Tuck[1987] studied the flow of a stream of water falling under gravity from a simple slit orifice in a vertical wall. He used a conformal mapping method and a Cauchy principal-value singular integral to write the logarithmic flow speed and y-coordinate in terms of the tangential angle of the free-surface in a reference half-plane. Thus the whole problem was reduced to a nonlinear integral equation. It was shown that the flow

exists only for Froude number exceeding 0.496 at which the limiting flow has a stagnation point at the upper edge of the orifice. This formulation is equivalent to that of King and Bloor[1988] which used the Schwartz-Christoffel formula.

Although we have mainly surveyed above the obstructed free-surface flows with bottom topography, there are other obstructed free-surface problems such as weir flow, flow over a submerged body, flows over sluice and waterfalls, flows due to a submerged source and sink, among other free-surface problems. Vanden-Broeck and Keller[1989] considered the steady motions of a flat surfboard driven by a solitary wave. The complex potential plane was conformally mapped into the interior of the unit circle in the t-plane. Thus the logarithm of the complex velocity was expanded inside the circle. The solutions for the flow past a horizontal and an inclined flat surfboard without a spray or splash were constructed numerically. The problem was further investigated by Vanden-Broeck and Dias[1991] to consider the gravitational free-surface flow past a submerged inclined flat plate. Here x and ψ were chosen as the independent variables. The flow region is then a strip of height h in the x-ψ plane. The components of velocity u and v were given in terms of derivatives of ψ with respect to x and y. A finite difference scheme was used to calculate the solutions for the inclined plate placed in the fluid and numerical results were presented. The problem for the flow past a horizontal plate and for flow past a semi-infinite plate were also investigated where, in the former case, they found that, as the plate is gradually moved upward from the bottom toward the free surface at a constant Froude number, the maximum height of the free surface first increases, then reaches a maximum and finally decreases. Another interesting classic obstructed free-surface flow of a fluid, that induced by a submerged source or sink with gravity acting as the restoring force has been examined by many authors.

In addition to the above extensively-studied problems of fluid flow over topography, the free surface problems of jet impact are interesting problems.

Jet impingement is much applied in many cooling and drying system in industrial process. Many applications in industry require localized heating or cooling. An effective way to accomplish this is through the use of impinging gas jets or liquid jets. Industrial uses of impinging jets include the tempering of glass, drying of paper and textiles, and the cooling of metal sheets, turbine blades and electronic components. When a flow passes through a wall, we say the fluid transpires through the surface. In transpiration cooling a relatively cold fluid enters through a porous wall. This flow could be used to cool a wall over which hot combustion gases flow. In heat transfer, jet impingements are used because the thin boundary layer near the centre of the impingement has high local heat transfer coefficient. After the points of maximum temperature are located, the jets are directed towards them, to maximise the heat transfer.

The mathematical problem is the first stage of idealization of the complicated fluid motion. The classic problems in this field can be found in Birkhoff and Zarantonello[1957]. General methods for formulating the problems of jets impinging on various objects were developed. Olmstead and Raynor[1965] studied the depression due to a jet impinging on a fluid surface, in order to describe the experimentally observed appearance of lips on the liquid surface. They assumed potential flow of a two dimensional gas jet impinging symmetrically on an infinite liquid surface. They used Birkhoff and Zarantonello's method to formulate this problem.

However, mathematical modelling of a jet impinging unsymmetrically on a object is not much studied. In many cases the location of the point where the jet splits into two parts around the object is unknown beforehand.

In the manufacture of 'glassy' metals, a jet of molten metal is aimed onto a

moving wheel or substrate where it is solidified extremely rapidly. Even when the viscous and thermal effects are neglected, the remaining outer inviscid flow problem results in a difficult free-surface problem. After taking the fluid as incompressible and inviscid and the fluid motion as irrotational and steady, Jenkins & Barton [1989] gave an analysis of the impact of a jet on a porous wall at which the normal velocity is prescribed. By using fixed-domain methods the computation of the shape of the inviscid jet was developed. Numerical results were presented. In seeking a simpler computation method, King [1990], using an extension of the classical hodograph method, reduced the problem of finding the free surface of a jet incident on a porous wall to a first order ordinary differential equation. The solution of this equation also provided independent confirmation of the result of Jenkins and Barton. This method, however, is restricted to the case in which the normal speed through the wetted portion of the wall is constant. In the case that the normal speed is not constant, finding a transformation which maps the hodograph plane to an upper half plane will be difficult. Moreover, whenever the specified normal speed is changed, a new transformation has to be determined.

In this thesis we investigate the free surface problems of jets impinging on uneven walls, of jet impact on a porous wall with specified distribution of normal speed and of a jet passing through a porous film. The remainder of this thesis is organized as follows. In Chapter 2, some fundmental aspects of fluid dynamics and a few methods used in studying the interaction of a fluid with obstacles are given, including the generalized Schwartz-Christoffel formula. The solution of an integral equation which will appear in the Chapter 4 is also found. We then use capillary-gravity waves as an example, in the last section of Chapter 2, to illustrate that in some cases, a simple conformal mapping, rather than a complicated transformation, can be employed to formulate the problem. In Chapter 3, the free surface problem of a jet incident on a porous wall is studied. A system of integral equations is derived to formulate this problem by use of the Cauchy formula. In

the case of constant normal speed, the system reduces to a single nonlinear integral equation. The asymptotic behaviour of the free surface is analyzed and a numerical method is used to determine the shape of the jet. The formulation is also extended to include the effect of gravity. In Chapter 4, a jet impinging on a rough wall is considered. Using the generalized Schwartz-Christoffel formula, we map the physical plane onto an upper half plane. Based on the method for solution of an integral equation given in Chapter 2, a class of analytic solutions is found. The classic result is revisited, which forms a check on the numerical method. For some wall shapes, numerical results are presented. In Chapter 5, we further consider a jet impinging on an asymmetric wall surface. The condition determining the position of the stagnation point is found using the momentum equation in an integral form. A numerical method is developed. Chapter 6 contains the mathematical model of a jet passing through a porous film where the fluid pressure and velocity have a jump across the film. An analogue of Darcy's law applies to the film. Using the Cauchy integral formula, we formulate the problem through a system of integral equations. The singularities in this model are analysed and a few numerical solutions to the system corresponding to different parameters are presented. The conclusions and some remarks are given in Chapter 7.

Chapter 2

Mathematical Formulations

2.1 Overview

This chapter is mainly concerned with several typical mathematical treatments which reveal general formulations of obstructed free surface flows. The model equations for incompressible inviscid flow are briefly summarized. The momentum equation in integral form is provided. Some generalizations of the Schwartz-Christoffel formula are derived. By transforming variables, an integral equation is solved. All techniques developed in this chapter will be applied in some problems considered in later chapters.

2.2 The Governing Equations

To represent the velocity vector field, we adopt the usual bold type-face, thus $\mathbf{u}=(u,v,w)$ with magnitude q. The divergence of $\mathbf{u}$ is defined as the resulting rate of change of volume per unit volume

$$div\mathbf{u} = \nabla \cdot \mathbf{u} = \frac{\partial u}{\partial x_1} + \frac{\partial v}{\partial x_2} + \frac{\partial w}{\partial x_3} \tag{2.1}$$

Supposing that we have an incompressible Newtonian fluid of constant density ρ and constant kinematic viscosity ν, its motion is governed by the Navier-Stokes

equations

$$\frac{\partial \mathbf{u}}{\partial t} + (\mathbf{u}\cdot\nabla)\mathbf{u} = -\frac{1}{\rho}\nabla p + \nu\nabla^2\mathbf{u} + \mathbf{F}, \tag{2.2}$$

$$\nabla\cdot\mathbf{u} = 0 \tag{2.3}$$

where p represents pressure and may be a function of position within the fluid, $\mathbf{F}$ denotes the vector resultant of the volume forces per unit mass of fluid and ∇^2 denotes the Laplace operator $\partial^2/\partial x_1^2+\partial^2/\partial x_2^2+\partial^2/\partial x_3^2$. If the fluid is further assumed to be inviscid, i.e., $\mu = 0$, the second term in the right hand side of (2.2) can be neglected. Then we have the Euler equations

$$\frac{\partial \mathbf{u}}{\partial t} + (\mathbf{u}\cdot\nabla)\mathbf{u} = -\frac{1}{\rho}\nabla p + \mathbf{F}, \tag{2.4}$$

$$\nabla\cdot\mathbf{u} = 0. \tag{2.5}$$

If the only volume force per unit mass acting on the fluid is gravitational, then, $\mathbf{F}$, being conservative, can be written as the gradient of a potential: $\mathbf{F} = -\nabla f$. Using the vector identity

$$(\mathbf{u}\cdot\nabla)\mathbf{u} = (\nabla\wedge\mathbf{u})\wedge\mathbf{u} + \nabla(\frac{1}{2}\mathbf{q}^2), \tag{2.6}$$

where $\mathbf{q}^2 = |\mathbf{u}|^2$, the momentum equation can be cast into the form

$$\frac{\partial \mathbf{u}}{\partial t} + (\nabla\wedge\mathbf{u})\wedge\mathbf{u} = -\nabla\left(\frac{p}{\rho} + \frac{1}{2}\mathbf{q}^2 + f\right). \tag{2.7}$$

Since inviscid fluids allow irrotational motion, with $\mathbf{u} = \nabla\Phi$ for some velocity potential $\Phi(\mathbf{x}, t)$, equation (2.7) yields for these motions

$$\nabla\left(\frac{\partial\Phi}{\partial t} + \frac{p}{\rho} + \frac{1}{2}\mathbf{q}^2 + f\right) = \mathbf{0} \tag{2.8}$$

where $\mathbf{q} = |\nabla\Phi|$. This may be integrated, without loss of generality, to give

$$\frac{\partial\Phi}{\partial t} + \frac{p}{\rho} + \frac{1}{2}|\nabla\Phi|^2 + f = 0, \tag{2.9}$$

the unsteady equivalent of Bernoulli's equation.

For steady, two-dimensional motions, the formulation is further simplified by taking $\Phi = \Phi(\mathbf{x})$, which through (2.5) satisfies Laplace's equation

$$\nabla^2\Phi = 0. \tag{2.10}$$

Moreover, a stream function Ψ exists defined by

$$u = \frac{\partial\Psi}{\partial x_2}, \quad v = -\frac{\partial\Psi}{\partial x_1}. \tag{2.11}$$

Since Ψ is the harmonic conjugate to $\Phi = \Phi(x_1, x_2)$, the complex potential $W = \Phi + i\Psi$ is an analytic function of the complex variable $Z = x_1 + ix_2$.

In this case the momentum equation (2.4) is reduced to Bernoulli's equation

$$\frac{p}{\rho} + \frac{1}{2}|\nabla\Phi|^2 + f = \text{constant}. \tag{2.12}$$

If the flow has a free streamline $x_2 = Y_s(x_1)$ at which surface tension is neglected, the pressure p there equals the constant air pressure p_0.

We shall largely be concerned with flows having a free streamline at which the fluid pressure p equals the uniform air pressure p_0. If gravitational effects are included, the x_2 axis is taken as vertically upward, so that $f = gx_2$. Then, Bernoulli's equation becomes

$$\frac{p}{\rho} + \frac{1}{2}|\nabla\Phi|^2 + gx_2 = \frac{p_0}{\rho} + \frac{1}{2}U^2 + gH \tag{2.13}$$

where U is the speed on the free streamline at a point where $x_2 = H$. In particular, at the free surface $\Psi = \Psi_0$ (say) Bernoulli's equation becomes

$$\frac{1}{2}\left(U^2 - |\nabla\Phi|^2\right) = g(x_2 - H). \tag{2.14}$$

A non-dimensionalization based on typical length H and typical speed U may be introduced by

$$z = x + iy = \frac{x_1 + ix_2}{H}, w = \phi + i\psi = \frac{\Phi + i\Psi}{UH}. \tag{2.15}$$

Bernoulli's equation on the free surface is written as

$$\frac{F^2}{2}|\nabla\phi|^2 + y_s = \frac{F^2}{2} + 1 \tag{2.16}$$

where $F = \frac{U}{\sqrt{gH}}$ is the Froude number. The case when gravity is neglected corresponds to infinite Froude number, so that the fluid speed along the free surface has the constant value $|\nabla\phi|^2 = 1$.

When the influence of surface tension is considered, there is a pressure difference across the surface, proportional to the surface tension force T and inversely proportional to the radius of curvature R of the surface l with R chosen as positive when the surface is concave towards the fluid. Thus the fluid pressure p on the surface is related to the uniform air pressure p_0 by

$$p = p_0 + \frac{T}{R}. \tag{2.17}$$

In this case, Bernoulli's equation at the surface becomes

$$\frac{T}{\rho R} + \frac{1}{2}|\nabla\phi|^2 - \frac{1}{2}U^2 = g(x_2 - H) = 0. \tag{2.18}$$

In dimensionless form with $r = R/H$, this becomes

$$\frac{F^2}{2}(|\nabla\phi|^2 - 1) = 1 - y_s - \frac{\hat{T}}{r}, \tag{2.19}$$

where $\hat{T} = T/\rho g H^2$. After division by $F^2/2$, the above equation can be written further as

$$|\nabla\phi|^2 - 1 = \frac{2}{F^2}(1 - y_s) - \frac{\bar{T}}{r}, \tag{2.20}$$

where $\bar{T} = 2T/\rho U^2 H$. This form is appropriate for treatment of capillary-gravity waves. Alternatively, if gravity can be neglected the appropriate form is

$$|\nabla\phi|^2 - 1 + \bar{T}r^{-1} = 0. \tag{2.21}$$

In 1957, Crapper found an exact expression for pure capillary periodic waves on deep water. The velocity potential ϕ and stream function ψ were taken to

be the independent variables in his formulation of an analytic solution. Later, Kinnersley[1976] extended this exact solution to capillary waves on fluid of uniform finite depth.

2.3 The Momentum Equation in Integral Form

The differential form of the momentum equation (2.4) is largely used in considering obstructed free surface flow, but in some important cases, an integral relation specifying the momentum balance for a certain region of fluid leads directly to the required information. We have

$$\int_v \frac{\partial \rho \mathbf{u}}{\partial t} dV = -\int_s \rho \mathbf{u}\mathbf{u} \cdot \mathbf{n} dA + \int_v \mathbf{F} \rho dV + \int_s \sigma \mathbf{n} dA \tag{2.22}$$

where $\mathbf{n}$ is a unit vector directed out of the volume v, $\sigma = (\sigma_{ij})$ is the stress tensor and the two volume integrals are taken over the volume bounded by s which is referred to as the control surface.

If the body force per unit mass is a conservative field, $\rho\mathbf{F}$ can be written as the gradient of a scalar quantity

$$\rho \mathbf{F} = -\nabla(\rho f). \tag{2.23}$$

Then the contribution from the volume force can be put in the form of a surface integral. Thus we obtain

$$\int_v \frac{\partial \rho \mathbf{u}}{\partial t} dV = -\int_s \rho \mathbf{u}\mathbf{u} \cdot \mathbf{n} dA + \int_s (-\rho f \mathbf{n} + \sigma \cdot \mathbf{n}) dA. \tag{2.24}$$

In the important case of steady motion the remaining volume integral, on the left-hand side of (2.21) is zero. Thus the above equation can be reduced to

$$\int_s \rho \mathbf{u}\mathbf{u} \cdot \mathbf{n} dA = \int_s (-\rho f \mathbf{n} + \sigma \cdot \mathbf{n}) dA \tag{2.25}$$

which states that the convective flux of momentum out of the region bounded by A is equal to the sum of the resultant contact force exerted at the boundary by the surrounding matter and the resultant force at the boundary arising from the stress system which is equivalent to the body force. The boundary surface A may be chosen freely in particular flow fields. This integral form of the momentum equation may be specialized for an incompressible inviscid fluid in steady motion under gravity as

$$\int_s \rho \mathbf{u}\mathbf{u} \cdot \mathbf{n} dA = \int_s (\rho \mathbf{g} \cdot \mathbf{x} - p)\mathbf{n} dA. \tag{2.26}$$

In order to show explicitly that gravity may be ignored when components of the momentum flux and resultant force in a horizontal plane are under consideration, the first term containing $\mathbf{g}$ may be transformed to a volume integral, then giving

$$\int_s \rho \mathbf{u}\mathbf{u} \cdot \mathbf{n} dA = \rho \mathbf{g} V - \int_s p\mathbf{n} dA. \tag{2.27}$$

However this equation is the vectorial form of momentum equation. The momentum equation in integral form, in more general case, is one projected on a special axis , says, $\bar{l} = (l_1, l_2, l_3)$ with $|\bar{l}| = 1$.

Let velocities in the direction of $\bar{l}$ be denoted by $\tilde{u} = \mathbf{u} \cdot \bar{l}$. Similar to (2.22), we have

$$\int \frac{D\rho\tilde{u}}{Dt} d\tau = \int \mathbf{F} \cdot \bar{l} \rho d\tau + \int \Sigma_{i=1}^{3} l_i \frac{\partial \sigma_{ij}}{\partial x_j} d\tau \tag{2.28}$$

The right hand side of (2.28) can be written

$$\begin{aligned}
\int_v \frac{D\rho\tilde{u}}{Dt} d\tau &= \int_v \rho \left(\frac{\partial \tilde{u}}{\partial t} + \mathbf{u} \cdot \nabla \tilde{u} \right) \quad d\tau \\
&= \int_v \left(\frac{\partial \tilde{u}}{\partial t} - \tilde{u} \frac{\partial \rho}{\partial t} + \rho \mathbf{u} \cdot \nabla \tilde{u} \right) d\tau \\
&= \int_v \left(\frac{\partial \rho\tilde{u}}{\partial t} + \rho \tilde{u} \nabla \cdot \mathbf{u} + \rho \mathbf{u} \cdot \nabla \tilde{u} \right) d\tau \\
&= \int_v \left(\frac{\partial \tilde{u}}{\partial t} + \rho \nabla \cdot \tilde{u}\mathbf{u} \quad d \right) \tau.
\end{aligned} \tag{2.29}$$

Consideration of the balance of momentum for the fluid contained within a fixed surface S is more convenient in use. Therefore substituting (2.29) into (2.28) and using the divergence theorem yields

$$\int_v \frac{\partial \rho \tilde{u}}{\partial t} d\tau = -\int_s \rho \tilde{u} u_j n_j dS + \int_v \mathbf{F} \cdot \bar{l} \rho d\tau + \int_v \Sigma_{i=1}^3 l_i \sigma_{ij} n_j dS \tag{2.30}$$

If the body force $\mathbf{F}$ is due to gravity, the stress is an isotropic pressure $\sigma_{ij} = -P\delta_{ij}$ and the speed of uniform oncoming flow is assumed to be sufficiently large, the effect of gravity is negligible. Thus, in steady motion, we obtain

$$\rho \int_s (\mathbf{u} \cdot \vec{l}) \mathbf{u} \cdot \mathbf{n} dS = -\int_s \rho (\vec{l} \cdot \mathbf{n}) dS \tag{2.31}$$

Equation (2.31) is the integral form of momentum equation in the direction $\vec{l}$ for an incompressible inviscid fluid in steady motion. An application of the momentum will be made in Chapter 5 concerning an ideal jet of liquid impinging on an uneven wall.

2.4 Conformal Mapping, Integral-Equation and Hodograph Methods

A few typical methods applied in obstructed free-surface flows are introduced in this section.

2.4.1 Transformation of a boundary into an infinite straight line

Directly mapping the region occupied by the fluid into a somewhat simpler region, the lower-half of the ζ-plane say, can reduce the problem of some obstructed free-surface flows to finding a complex potential satisfying the appropriate boundary conditions. The steady two-dimensional free-surface flow of an ideal fluid

over arbitrary bottom topography is used to illustrate the transformation. The transformation, given by King and Bloor[1989], can be written as

$$\frac{dz}{d\zeta} = \frac{-1}{\pi\zeta} \exp\left\{-\frac{1}{\pi}\int_{-\infty}^{+\infty} \frac{\theta(t)}{\zeta - t} dt\right\} \tag{2.32}$$

where $\theta(t)$ is the angle made by the tangent to the free surface or bottom with the x-axis at the point which corresponds to $\zeta = \xi + i0$. The point $\zeta = 0$ corresponds to the downstream flow at infinity. As ζ approaches the real axis, the limiting form of (2.32) is written as

$$\frac{dz}{d\xi} = \frac{-1}{\pi\xi} \exp\left\{-\frac{1}{\pi}\int_{-\infty}^{+\infty *} \frac{\theta(t)}{\xi - t} dt + i\theta(\xi)\right\} \tag{2.33}$$

where the integral sign with an asterisk denotes the Cauchy principal value. The complex potential in the ζ-plane can be treated as a sink at the origin of strength $1/\pi$, so that

$$W(\zeta) = -\frac{1}{\pi}\log\zeta. \tag{2.34}$$

Therefore the complex velocity can be given as

$$u - iv = qe^{-i\Theta} = \frac{dW}{dz} = \exp\left\{\frac{1}{\pi}\int_{-\infty}^{+\infty} \frac{\theta(t)}{\zeta - t} dt\right\} \tag{2.35}$$

where Θ is the angle made by the fluid velocity vector at the point corresponding to ζ. As ζ approaches to the real axis the limiting form of (2.35) is

$$qe^{-i\Theta} = exp\left\{\frac{1}{\pi}\int_{-\infty}^{+\infty *} \frac{\theta(t)}{\xi - t} dt - i\theta(\xi)\right\}, \tag{2.36}$$

that is

$$q = exp\left\{\frac{1}{\pi}\int_{-\infty}^{+\infty *} \frac{\theta(t)}{\xi - t} dt\right\}, \Theta = \theta. \tag{2.37}$$

Equations (2.33) and (2.37) can be used in the derivative of the free-surface Bernoulli condition, which is

$$F^2 q\frac{dq}{d\xi} + \frac{dy_s}{d\xi} = 0. \tag{2.38}$$

Equation (2.38) is a nonlinear integro-differential equation for $\theta(\xi)$. To solve a coupled set consisting of (2.38) and $\tan\theta = f'(x)$, a numerical scheme has been developed and applied by King and Bloor to the solution of a variety of obstructed free-surface flows.

The transformation of the region occupied by fluid in the complex potential plane, rather than the region of the physical plane, to an upper (or lower)-half plane is another technique used in considering obstructed free-surface flows.

In many cases, the flow region in the complex potential plane is a simple shape, such as that considered in the above example, which is the strip $-1 \leq \psi \leq 0$. It then can be mapped into an upper-half plane by a standard conformal mapping. This idea will be fully developed in the next Chapter. Tuck[1986] considered a flow in which a stream of water emerging from a simple slit orifice in a vertical wall then falling under gravity. The flow region then corresponds to the strip $-1 \leq \psi \leq 0$ in the w-plane, which is mapped to the lower-half ζ-plane by

$$\zeta = -e^{-\pi w}. \tag{2.39}$$

After introducing the logarithmic hodograph

$$\Omega = \log\frac{dw}{dz} = \tau - i\theta, \tag{2.40}$$

where $q = e^{\tau}$ is the flow speed and θ the flow direction, the variable

$$\chi = \Omega + \log\zeta + i\frac{\pi}{2} \tag{2.41}$$

is defined. Since this vanishes at infinity in the lower-half ζ-plane, the Hilbert transform was used to give, for real ζ,

$$\chi(\zeta) = -\frac{1}{\pi i}\int_{-\infty}^{\infty *}\frac{\chi(\xi)d\xi}{\xi-\zeta}, \tag{2.42}$$

After some manipulations, this yields the demanded relationship, namely

$$\tau(\zeta) = -\frac{1}{2}\log|\xi_0-\zeta| - \frac{1}{2}\log|\xi_N-\zeta| + \frac{1}{\pi i}\int_{\xi_0}^{\xi_{N}*}\frac{\theta(\xi)d\xi}{\xi-\zeta}, \tag{2.43}$$

where ξ_0 and ξ_N correspond to the two points at the edges of the orifice.

The y-coordinate is needed for use in the Bernoulli condition. Integrating (2.40) gives

$$z = \int e^{-\Omega} dw \tag{2.44}$$

which is written, in terms of ξ, as

$$z(\zeta) = \int_{\xi_0}^{\zeta} e^{-\tau(\xi)+i\theta(\xi)} \frac{d\xi}{(-\pi\xi)}, \tag{2.45}$$

where the top edge $\zeta = \xi_0$ is chosen as the origin in the z-plane. Thus, taking the real part of (2.45) yields

$$y(\zeta) = \int_{\xi_0}^{\zeta} e^{-\tau(\xi)} \sin\theta(\xi) \frac{d\xi}{(-\pi\xi)}. \tag{2.46}$$

This then reduces the whole problem to a nonlinear integral equation for $\theta = \theta(\xi), \xi_0 < \xi < \xi_N$.

However, the flow region in the complex potential plane is not always so simple. The boundary of the flow region in the complex potential plane may include an unknown portion of curve such as in the problem of the impact of an ideal jet on a porous wall. Since the complex potential is unknown along the wetted portion of the porous wall, the problem seems to be difficult by the classical hodograph method. Based on the Baiocchi transformation, a numerical scheme was developed by Jenkins and Barton[1989]. King[1990] used a conformal mapping approach, an extension of the classical hodograph method to reduce the problem to a first order differential equation. In King's formulation, the region occupied by the flow in the complex potential plane is a semi-infinite strip bounded by two parallel lines and an unknown curve. The fact that this curve is undetermined arises because neither speed nor stream function is knowen on the porous wall. In this case, again, a generalization of the Schwartz-Christoffel formula is used to transform the w-plane into the upper-half of the ζ-plane. The fluid velocity along the wet

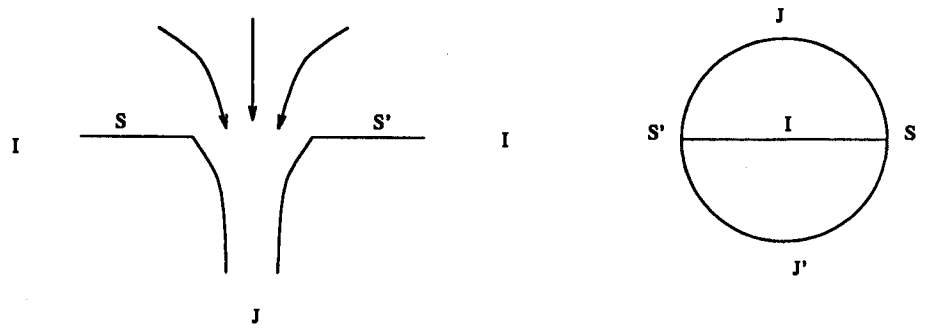

(a) Physical plane of a jet flow from a slot. (b) t-plane

Figure 2–1: The physical-plane of a jet flow from a slot and a reference t-plane.

portion of the porous wall, together with the mapping between the hodograph plane and upper-half of the ζ-plane then can be obtained. That the fluid velocity is not assumed to be constant at the porous wall makes for difficulty in finding the transformation between the region occupied by the fluid in the dw/dz-plane and in the ζ-plane.

2.4.2 Conformal mapping of a boundary into a circle

In the previous section we have introduced the conformal mapping technique by which some problems of obstructed free surface flows were formulated. In this section, we adopt the Birkhoff and Zarantonello method, an analogue of that of Levi-Civita [1907], for finding ideal steady plane flows in a gravity field, bounded by a free streamline and by polygonal fixed boundaries to illustrate how the conformal mapping of a boundary into a semicircle is used. We take the formulation of the symmetric jet from a slot as an example, for brevity. The flow considered can be mapped conformally and symmetrically onto the unit semicircle

$$\Gamma : |t| \leq 1, \Im\{t\} \geq 0 \tag{2.47}$$

in a reference t-plane. The fixed walls are mapped into the real diameter and the free streamlines onto the circumference $t = e^{i\sigma}$ of Γ, as indicated in Fig. 2–1. In order to determine the complex potential W, the conformal transformation

$T = -(t + t^{-1})/2$ is used to map Γ on to the upper half-plane so that

$$W = C \ln T, \quad \frac{dW}{dT} = \frac{C}{T}, \tag{2.48}$$

for some scale factor C.

Since $\zeta = dW/dz$, we have $z = \int \zeta^{-1} dW$. To determine the flow, we need to find $\zeta(t)$. The flow is assumed to be stagnant at I, hence ζ vanishes at $t = 0$. ζ is also real on the real diameter. From the Reflection Principle, ζ can be extended to a function analytic in the unit circle $|t| < 1$. Since ζ is imaginary when t is imaginary, we have

$$\zeta = a_1 t + a_3 t^3 + a_5 t^5 + \cdots \qquad \text{on} \quad |t| < 1. \tag{2.49}$$

$\zeta(t)$ is analytic on the unit circle $t = e^{i\sigma}$, except at the separation point $t = \pm 1$, where $\zeta = \pm 1$, and at $t = \pm i$ where $\zeta = \pm\infty$. From the Bernoulli condition $|\zeta|^2 = 2gy$, we have

$$\zeta \sim (2igz)^{\frac{1}{2}}, \qquad \text{asymptotically, near } J \text{ at infinity,} \tag{2.50}$$

hence

$$W \sim \int (2igz)^{\frac{1}{2}} dz = \frac{(8g)^{\frac{1}{2}}(iz)^{\frac{3}{2}}}{3}. \tag{2.51}$$

Substituting $T = -(t + t^{-1})/2$ into the first equation in (2.48), we find

$$W = C \ln T = C \ln[-(t + t^{-1})/2] \sim \begin{cases} \ln(1 + it), & \text{near } J \\ \ln(1 - it), & \text{near } J' \end{cases} \tag{2.52}$$

Thus near J, we obtain

$$\zeta \sim (2igz)^{\frac{1}{2}} \sim W^{\frac{1}{3}} \sim [\ln(1 + it)]^{\frac{1}{3}}. \tag{2.53}$$

Consequently, for $0 < C < 0.5$, the function

$$\frac{\zeta(t)}{t[\ln C(1 + it)]^{\frac{1}{3}}} \tag{2.54}$$

is bounded away from zero and infinity throughout $|t| \leq 1$. We can then write

$$\zeta = t[\ln C(1+it)]^{\frac{1}{3}} e^{\Omega(t)}. \tag{2.55}$$

Since $\Omega(t)$ is bounded and continuous in $|t| \leq 1$, and analytic in the interior, we can have

$$\Omega(t) = a_0 + a_1 t^1 + a_2 t^2 + \cdots. \tag{2.56}$$

In this symmetric case of ζ, we further obtain

$$\Omega(t) = a_0 + a_2 t^2 + a_4 t^4 + \cdots. \tag{2.57}$$

where the coefficients a_{2j} are to be determined. Substituting (2.57) back into the Bernoulli condition on the free surface then gives rise to an integral equation. The integral equation is solved numerically by truncation of the expanded series for $\Omega(t)$. Recently Vanden-Broeck and Keller[1987] used a very similar technique to construct the problem of of weir flow.

2.5 Transformations and Integral Equations

In this section, some generalizations of the Schwartz-Christoffel Formula which transform special regions into an upper-half plane are given. The application of these transformations to the obstructed free surface problem will be presented in the following chapters.

2.5.1 Generalizations of the Schwartz-Christoffel formula

A mapping is sought to transform the singly-connected region bounded by the contour $ABCDEF$ shown in Fig. 2–2 on to the upper-half of the ζ-plane, in such a way that $ABCDEF$ maps on to the real axis $\eta = 0, -\infty < \xi < \infty$.

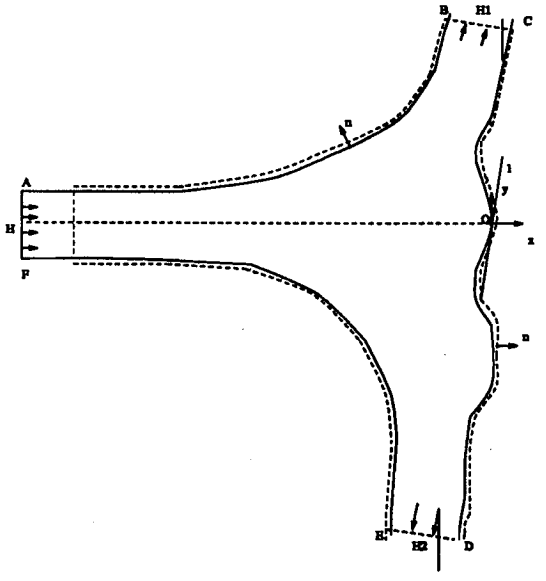

Figure 2–2: The physical-plane of a jet impinging on an asymmetric wall

The contour is assumed to have a continuously turning tangent except at a finite number of points, where simple discontinuities in the slope α of the contour may exist. The generalization of the Schwartz-Christoffel formula, in the form given by Woods[1961], is used for this purpose. It is written as

$$\frac{dz}{d\zeta} = K \exp\left\{-\frac{1}{\pi}\int_{-\infty}^{+\infty} \log(\zeta - t)\alpha'(t)dt\right\}. \tag{2.58}$$

The relation between the slope α of the contour and the flow angle θ made with the real axis is

$$\theta(t) = \begin{cases} \alpha(t) & -\infty < t < -1 \\ \alpha(t) - \pi & -1 < t < a \\ \alpha(t) & a < t < 1 \\ \alpha(t) - \pi & 1 < t < \infty \end{cases} \tag{2.59}$$

where a corresponds to the stagnation point in the physical region, at which the flow angle has discontinuity π. The integration in equation (2.58) can be split into

five parts as

$$\int_{-\infty}^{+\infty} \log(\zeta - t)d\alpha(t) = \int_{-\infty}^{-1-\epsilon} + \int_{-1-\epsilon}^{-1+\epsilon} + \int_{-1+\epsilon}^{1-\epsilon} + \int_{1-\epsilon}^{1+\epsilon} + \int_{1+\epsilon}^{+\infty} \log(\zeta - t)d\alpha(t) \tag{2.60}$$

and the integration taken with respect to θ instead of α using the relation (2.59), where appropriate. Then, using integration by parts:

i)

$$\begin{aligned}
\int_{-\infty}^{-1-\epsilon} \log(\zeta - t)d\alpha(t) &= \int_{-\infty}^{-1-\epsilon} \log(\zeta - t)d\theta(t) \\
&= \theta(t)\log(\zeta - t)|_{-\infty}^{-1-\epsilon} + \int_{-\infty}^{-1-\epsilon} \frac{\theta(t)}{\zeta - t}dt \\
&= -\frac{\pi}{2}\log(\zeta + 1 + \epsilon) + \int_{-\infty}^{-1-\epsilon} \frac{\theta(t)}{\zeta - t}dt
\end{aligned} \tag{2.61}$$

ii)

$$\int_{-1+\epsilon}^{-1-\epsilon} \log(\zeta - t)d\alpha(t) = \pi\log(\zeta + 1) + O(\epsilon) \tag{2.62}$$

iii)

$$\begin{aligned}
\int_{-1+\epsilon}^{1-\epsilon} \log(\zeta - t)d\alpha(t) &= \alpha(t)\log(\zeta - t)|_{-1+\epsilon}^{1-\epsilon} + \int_{-1+\epsilon}^{1-\epsilon} \frac{\alpha(t)}{\zeta - t}dt \\
&= \frac{\pi}{2}\log\frac{\zeta - 1 + \epsilon}{\zeta + 1 - \epsilon} + \int_{-1+\epsilon}^{a} \frac{\alpha(t)}{\zeta - t}dt + \int_{a}^{1-\epsilon} \frac{\theta(t)}{\zeta - t}dt \\
&= \frac{\pi}{2}\log\frac{\zeta - 1 + \epsilon}{\zeta + 1 - \epsilon} + \int_{-1+\epsilon}^{a} \frac{\theta(t) + \pi}{\zeta - t}dt + \int_{a}^{1-\epsilon} \frac{\theta(t)}{\zeta - t}dt \\
&= \frac{\pi}{2}\log\frac{\zeta - 1 + \epsilon}{\zeta + 1 - \epsilon} + \pi\log\frac{\zeta + 1 - \epsilon}{\zeta - a} + \int_{-1+\epsilon}^{1-\epsilon} \frac{\theta(t)}{\zeta - t}dt \\
&= \frac{\pi}{2}\log\frac{\zeta^2 - (1 - \epsilon)^2}{(\zeta - a)^2} + \int_{-1+\epsilon}^{1-\epsilon} \frac{\theta(t)}{\zeta - t}dt
\end{aligned} \tag{2.63}$$

iv)

$$\int_{1-\epsilon}^{1+\epsilon} \log(\zeta - t)d\alpha(t) = \pi\log(\zeta - 1) + O(\epsilon), \tag{2.64}$$

v)

$$\begin{aligned}
\int_{1+\epsilon}^{+\infty} \log(\zeta - t)d\alpha(t) &= \int_{1+\epsilon}^{+\infty} \log(\zeta - t)d\theta(t) \\
&= -\frac{\pi}{2}\log(\zeta - 1 + \epsilon) + \int_{1+\epsilon}^{+\infty} \frac{\theta(t)}{\zeta - t}dt.
\end{aligned} \tag{2.65}$$

Substituting these equations into (2.57) yields

$$\begin{aligned}\int_{-\infty}^{+\infty}\log(\zeta-t)d\alpha(t) &= -\frac{\pi}{2}\log(\zeta+1+\epsilon)+\int_{-\infty}^{-1-\epsilon}\frac{\theta(t)}{\zeta-t}dt+\pi\log(\zeta+1)\\ &+\frac{\pi}{2}\log\frac{\zeta^2-(1-\epsilon)^2}{(\zeta-a)^2}+\int_{-1+\epsilon}^{1-\epsilon}\frac{\theta(t)}{\zeta-t}dt\\ &+\pi\log(\zeta-1+\epsilon)-\frac{\pi}{2}\log(\zeta-1+\epsilon)+\int_{1+\epsilon}^{+\infty}\frac{\theta(t)}{\zeta-t}dt+O(\epsilon).\end{aligned} \tag{2.66}$$

Then, letting $\epsilon \to 0$ gives the required relation

$$\int_{-\infty}^{+\infty}\log(\zeta-t)d\alpha(t)=\pi\log\frac{\zeta^2-1}{\zeta-a}+\int_{-\infty}^{+\infty}\frac{\theta(t)}{\zeta-t}dt. \tag{2.67}$$

Inserting (2.64) into (2.55) gives

$$\begin{aligned}\frac{dz}{d\zeta} &= K\exp\left\{-\frac{1}{\pi}\left[\pi\log\frac{\zeta^2-1}{\zeta-a}+\int_{-\infty}^{+\infty}\frac{\theta(t)}{\zeta-t}dt\right]\right\}\\ &= K\frac{\zeta-a}{\zeta^2-1}\exp\left\{-\frac{1}{\pi}\int_{-\infty}^{+\infty}\frac{\theta(t)}{\zeta-t}dt\right\}.\end{aligned} \tag{2.68}$$

As $|\zeta| \to \infty$, we have

$$\frac{\zeta-a}{\zeta^2-1}\exp\left\{-\frac{1}{\pi}\int_{-\infty}^{+\infty}\frac{\theta(t)}{\zeta-t}dt\right\}\sim\frac{1}{\zeta}. \tag{2.69}$$

This allows the constant K to be determined so that the width of the incoming flow has the assumed value 2: integrating (2.67) along a large semi-circle using (2.68) then yields $K=-2/\pi$. Thus we obtain

$$\frac{dz}{d\zeta}=-\frac{2}{\pi}\frac{\zeta-a}{\zeta^2-1}\exp\left\{-\frac{1}{\pi}\int_{-\infty}^{+\infty}\frac{\theta(t)}{\zeta-t}dt\right\}. \tag{2.70}$$

In the above, the upstream flow is assumed parallel to the physical x-axis. If instead it is inclined at an angle γ_0 to the x-axis, we similarly obtain

$$\frac{dz}{d\zeta}=-\frac{2e^{i\gamma_0}}{\pi}\frac{\zeta-a}{\zeta^2-1}\exp\left\{-\frac{1}{\pi}\int_{-\infty}^{+\infty}\frac{\theta(t)}{\zeta-t}dt\right\}. \tag{2.71}$$

2.5.2 An integral equation and its solution

In this subsection, we discuss an integral equation and find its analytic solution. This result will be used in Chapter 4 in formulating a free surface problem of a jet impinging on certain objects.

To solve

$$\frac{1}{\pi}\int_{-\infty}^{-1*}\frac{\theta(t)}{\xi-t}dt+\frac{1}{\pi}\int_{1}^{\infty*}\frac{\theta(t)}{\xi-t}dt=F(\xi),\quad F(\xi)\in L_2[-\infty,-1]\cup[1,\infty],\quad (2.72)$$

we make the change of variables $t=r^{-1}$, $s=\xi^{-1}$ in (2.71) and obtain

$$\begin{aligned}F(s^{-1}) &= \frac{1}{\pi}\int_{-1}^{0*}\frac{s\theta(r^{-1})r^{-1}}{r-s}dr+\frac{1}{\pi}\int_{0}^{1*}\frac{s\theta(r^{-1})r^{-1}}{r-s}dr\\ &= s\frac{1}{\pi}\int_{-1}^{1*}\frac{\theta(r^{-1})r^{-1}}{r-s}dr, \qquad 0<|s|<1. \end{aligned}\quad (2.73)$$

Let $g(s)=s^{-1}F(s^{-1})$, $g(s)\in L_2[-1,1]$. Then equation (2.72) reduces to the so-called *aerofoil equation*

$$g(s)=\frac{1}{\pi}\int_{-1}^{1*}\frac{\phi(r)}{s-r}dr\quad , \qquad 0<|s|<1, \quad (2.74)$$

which here relates $g(s)$ defined above in terms of the flow angle on the wall to $\phi(r)\equiv r^{-1}\theta(r^{-1})$. The integral equation (2.73) may be inverted using the formula (see Hochstadt [1973] p.165) as

$$\phi(s)=\frac{c}{\sqrt{1-s^2}}-\frac{1}{\pi}\int_{-1}^{1*}\sqrt{\frac{1-r^2}{1-s^2}}\frac{g(r)}{s-r}dr, \quad (2.75)$$

where c is a constant to be determined later. Moreover, there is an alternative representation

$$\phi(s)=-\frac{1}{\pi}\int_{-1}^{1*}\sqrt{\frac{1-s^2}{1-r^2}}\frac{g(r)}{s-r}dr \quad (2.76)$$

valid subject to the compatibility condition

$$\int_{-1}^{1}\frac{g(s)}{\sqrt{1-s^2}}ds=0. \quad (2.77)$$

Reinterpreting (2.74) in terms of the free streamline angle $\theta(s^{-1}) = s\phi(s)$ gives

$$s^{-1}\theta(s^{-1})\sqrt{1-s^2} = c - \int_{-1}^{1*} \sqrt{1-r^2}\frac{g(r)}{s-r}dr. \tag{2.78}$$

Since θ remains finite as $s \longrightarrow \pm 1$, we obtain the two expressions

$$c = \int_{-1}^{1} \sqrt{1-r^2}\frac{g(r)}{1-r}dr = -\int_{-1}^{1} \sqrt{1-r^2}\frac{g(r)}{1+r}dr. \tag{2.79}$$

Thus we find that

$$0 = \int_{-1}^{1} \sqrt{1-r^2}\left(\frac{1}{1-r} + \frac{1}{1+r}\right) g(r)dr = 2\int_{-1}^{1} \frac{g(r)}{\sqrt{1-r^2}}dr. \tag{2.80}$$

The constant c is determined using (2.79) as

$$c = \frac{1}{2}\int_{-1}^{1} \sqrt{1-r^2}\left(\frac{1}{1-r} - \frac{1}{1+r}\right) g(r)dr = \frac{1}{2}\int_{-1}^{1} \frac{2rg(r)}{\sqrt{1-r^2}}dr. \tag{2.81}$$

Consequently, condition (2.76) is satisfied for all cases. Equation (2.77) may be rewritten in terms of $\theta(t)$ ($|t| > 1$) as

$$\theta(t) = \pm\frac{1}{\pi}\frac{\sqrt{t^2-1}}{t}\left(\int_{-\infty}^{-1*} - \int_{1}^{\infty*}\right) \frac{1}{\sqrt{\xi^2-1}}\frac{\xi F(\xi)}{\xi - t}d\xi, \qquad |t| > 1, \tag{2.82}$$

where the positive sign applies for $t > 1$ and the negative sign for $t < -1$.

2.6 Capillary-Gravity Waves of Finite Amplitude

In this section, we intend to use simple complex variable transformation techniques, rather than the generalized Schwartz-Christoffel formula, to study the mathematical formulation of the steady, two-dimensional, free surface flow of a stream which is obstructed by an arbitrarily curved bed topography.

2.6.1 Formulation

Two dimensional steady capillary-gravity waves of finite amplitude are investigated, on a flowing stream of water of finite depth over an uneven bed. The waves

are subject to the effects of gravity, surface tension and a corrugated bottom. The progressive gravity waves are in an irrotational incompressible inviscid fluid with surface tension acting at the free surface.

The X-axis is horizontal, Y-axis vertically upwards. A potential function $\Phi(X,Y)$ and a stream function $\Psi(X,Y)$ are introduced. We assume that the stream function $\Psi(X,Y)$ takes the values Q on the free surface and 0 on the bottom respectively. Let C denote the fluid speed upstream where the flow is uniform with undisturbed depth H. Then we have $HC = Q$ and

$$\Psi \to CY, \qquad X \to -\infty. \tag{2.83}$$

Within the fluid the velocity potential Φ and stream function are conjugate harmonic functions. We introduce the dimensionless variables

$$x = \frac{X}{H}, \quad y = \frac{Y}{H}, \quad \phi = \frac{\Phi}{Q}, \quad \psi = \frac{\Psi}{Q} \tag{2.84}$$

In terms of complex variables, the standard formulation is

$$\begin{aligned} &w = \phi + i\psi, \qquad z = x + iy, \\ &\frac{dw}{dz} = u - iv = q\ e^{-i\theta}, \quad \tau = \ln q \end{aligned} \tag{2.85}$$

where w is the complex potential, u and v are velocity components, and q and θ the speed and direction of the flow. The shape of the bottom $\Psi = 0$ is specified by $y = f(x)$, and of the free surface $\Psi = 1$ by $y = s(x)$. Bernoulli's equation is

$$\frac{F^2}{2}q^2 + \frac{p}{\rho g H} + y = constant \tag{2.86}$$

where F is the Froude number with $F^2 = C^2/gH$ and p the pressure. In particular, on the free surface, the effects of surface tension T and constant air pressure p_0, give the pressure as

$$p = p_0 + \kappa T, \tag{2.87}$$

so that equation (2.86) becomes

$$\frac{F^2}{2}q^2 + \frac{\kappa T}{\rho g H} + y = \text{constant}, \qquad \Psi = 1 \tag{2.88}$$

where κ is the curvature of the free streamline:

$$\kappa = \frac{d\theta}{ds} = \frac{q}{H}\frac{d\theta}{d\phi}. \tag{2.89}$$

Replacing (2.89) into (2.88), we obtain

$$\frac{F^2}{2}q^2 + \frac{T}{\rho g H^2}\frac{q d\theta}{d\phi} + y = \text{constant}, \qquad \Psi = 1. \tag{2.90}$$

The kinematic conditions are

$$\phi_y = f'(x)\phi_x, \quad \Psi = 0; \qquad \phi_y = s'(x)\phi_x, \quad \Psi = 1 \tag{2.91}$$

on the rigid boundary and the free surface respectively. Corresponding to the flow region in the physical plane, we have the strip $0 \le \psi \le 1, \quad -\infty \le \phi \le \infty$ in the complex potential plane. We transform the strip to the upper half plane using the conformal mapping

$$\zeta = \xi + i\eta = e^{\pi w}, \qquad \xi = e^{\pi\phi}\cos\pi\psi, \qquad \eta = e^{\pi\phi}\sin\pi\psi. \tag{2.92}$$

We introduce $\omega = \tau - i\theta$, which is an analytic function defined in the upper half plane $\zeta = \xi + i\eta (\eta \ge 0)$. Thus, by the Hilbert transform, we have

$$\tau(\xi, 0) = -\frac{1}{\pi}\int_{-\infty}^{\infty *} \frac{\theta(t,0)}{t-\xi}dt, \tag{2.93}$$

$$\theta(\xi, 0) = \frac{1}{\pi}\int_{-\infty}^{\infty *} \frac{\tau(t,0)}{t-\xi}dt. \tag{2.94}$$

After substituting (2.92) into (2.93) and (2.94), we have τ and θ defined on the w-plane. In particular, we let

$$\tau(-e^{\pi\phi}, 0) = \hat{\tau}(\phi), \qquad \theta(-e^{\pi\phi}, 0) = \hat{\theta}(\phi), \quad \Psi = 0; \tag{2.95}$$

$$\tau(e^{\pi\phi}, 0) = \bar{\tau}(\phi), \qquad \theta(e^{\pi\phi}, 0) = \bar{\theta}(\phi), \quad \Psi = 1 \tag{2.96}$$

on the free surface and the rigid bed respectively, where $\hat{\tau}$ and $\hat{\theta}$ correspond to the free surface, $\bar{\tau}$ and $\bar{\theta}$ to the rigid bed. After using (2.95) to replace ξ by ϕ in (2.93), we obtain

$$\begin{aligned}
\hat{\tau}(\phi) &= -\frac{1}{\pi}\left[\int_{-\infty}^{0*}\frac{\theta(t,0)}{t+e^{\pi\phi}}dt+\int_{0}^{\infty}\frac{\theta(t,0)}{t+e^{\pi\phi}}dt\right] \\
&= -\frac{1}{\pi}\left[\int_{\infty}^{-\infty*}\frac{\theta(e^{-\pi s},0)}{-e^{\pi s}+e^{\pi\phi}}\left(-\pi e^{-\pi s}ds\right)\right. \\
&\quad \left.+\int_{-\infty}^{\infty}\frac{\theta(e^{\pi r},0)}{e^{\pi r}+e^{\pi\phi}}\left(\pi e^{\pi r}dr\right)dr\right] \\
&= -\frac{1}{\pi}\left[\pi\int_{-\infty}^{\infty*}\frac{\hat{\theta}(s)}{-1+e^{\pi(\phi-s)}}ds+\pi\int_{-\infty}^{\infty}\frac{\bar{\theta}(r)}{1+e^{\pi(\phi-r)}}dr\right] \\
&= -\left\{\int_{-\infty}^{\infty*}\frac{\hat{\theta}(s)}{e^{\pi(\phi-s)}-1}ds+\int_{-\infty}^{\infty}\frac{\bar{\theta}(s)}{e^{\pi(\phi-s)}+1}ds\right\}. \qquad (2.97)
\end{aligned}$$

Similarly, we have

$$\bar{\tau}(\phi)=\int_{-\infty}^{\infty}\frac{\hat{\theta}(s)}{1+e^{\pi(\phi-s)}}ds-\int_{-\infty}^{\infty*}\frac{\bar{\theta}(s)}{1-e^{\pi(\phi-s)}}ds. \qquad (2.98)$$

Defining $T/\rho gH^2=T_0$, then the derivative of (2.90) with respect to ϕ gives

$$F^2qq'+T_0(q\theta')'+q^{-1}\sin\theta=0, \qquad \psi=1, \quad -\infty<\phi<\infty \qquad (2.99)$$

where a prime denotes $d/d\phi$. Substituting $q=e^{\hat{\tau}(\phi)}$ and $\theta=\hat{\theta}$ into (2.99) yields

$$F^2e^{2\hat{\tau}}\hat{\tau}'+T_0(e^{\hat{\tau}}\hat{\theta}')'+e^{-\hat{\tau}}\sin\hat{\theta}=0, \qquad \psi=1, \quad -\infty<\phi<\infty. \qquad (2.100)$$

On the fluid bed, $y=f(x)$ we have

$$\tan\bar{\theta}=\tan\theta=f'(x). \qquad (2.101)$$

Since

$$\frac{\partial x}{\partial\phi}=q^{-1}\cos\theta, \quad \frac{\partial y}{\partial\phi}=q^{-1}\sin\theta, \qquad (2.102)$$

we have on the streamline $\psi=0$

$$x'(\phi)=\bar{x}'(\phi)=q^{-1}\cos\bar{\theta}=e^{-\bar{\tau}}\cos\bar{\theta}. \qquad (2.103)$$

Equations (2.97), (2.98), (2.100) and (2.101), combined with (2.103), describe a free surface problem for flow over an uneven bottom. For the case $\bar{\theta} = 0$, i.e. for flow over a flat horizontal bottom, the problem was discussed by Bloor[1978], who used the transformation which maps the physical plane to a lower half plane to obtain an exact nonlinear integro-differential equation for the flow angle of the free surface. A generalized Schwartz-Christoffel formula was applied in his study to specify the problem. In this study, rather than mapping the region occupied by the fluid, we transform the complex potential plane into an upper half plane in an explicit form. In the next subsection we present some results concerning some special cases of uneven bottoms.

2.6.2 Flow over a ramp

In this subsection, we discuss a special case: flow over a bottom with a step. Let $\bar{\theta} = \alpha$ on $0 < \phi < b$, with $\bar{\theta} = 0$ otherwise on $\Psi = 0$. Then (2.97) becomes

$$\hat{\tau}(\phi) = -\int_{-\infty}^{\infty *} \frac{\hat{\theta}(s)}{e^{\pi(\phi - s)} - 1} ds - \frac{\alpha}{\pi} \ln \frac{1 + e^{-\pi(\phi - b)}}{1 + e^{-\pi\phi}}. \tag{2.104}$$

To determine the constant b, we need another condition which follows from (2.102) as

$$\epsilon = \sin\alpha \int_0^b e^{-\bar{\tau}(\phi)} d\phi = b \sin\alpha \int_0^1 e^{-\bar{\tau}(bt)} dt \tag{2.105}$$

where ϵ is the height of the step. Then $\bar{\tau}(\phi)$ is given by

$$\bar{\tau}(\phi) = \int_{-\infty}^{\infty} \frac{\hat{\theta}(s)}{e^{\pi(\phi - s)} - 1} ds - \frac{\alpha}{\pi} \ln \frac{e^{\pi b} - e^{\pi\phi}}{e^{\pi\phi} - 1}. \tag{2.106}$$

In this case we only need to solve the nonlinear equations (2.100) and (2.103), combined with (2.105). In order to provide a basis for a numerical scheme for solving the nonlinear equations, as first approximation, we consider the linearized equation of (2.100).

Linearized equation

If the step height and ramp angle α are assumed to be small, then $b = \delta$ and the flow angle is small so that (2.100) can be linearized to become

$$F^2\hat{\tau}' + T_0\hat{\theta}'' + \hat{\theta} = 0, \qquad \psi = 1, \quad -\infty < \phi < \infty. \tag{2.107}$$

The derivative $\hat{\tau}'$ can be approximated to give

$$\frac{d\hat{\tau}}{d\phi} = \frac{d\tau_1}{d\phi} + \alpha\frac{\pi\delta e^{\pi\phi}}{(1+e^{\pi\phi})^2}, \tag{2.108}$$

where

$$\tau_1 = -\int_{-\infty}^{\infty *} \hat{\theta}(s)P(\phi - s)ds \tag{2.109}$$

and $P(\phi) = 1/(e^{\pi\phi} - 1)$.

Substituting (2.108) into (2.107) gives

$$F^2\frac{d\tau_1}{d\phi} + T_0\hat{\theta}'' + \hat{\theta} = -F^2\alpha\frac{\pi\delta e^{\pi\phi}}{(1+e^{\pi\phi})^2}, \tag{2.110}$$

which may be solved using Fourier transforms and the convolution theorem.

If we let $\bar{f}(k) = F\{f(\phi)\}$ denote the Fourier transform of f, then using $F\{\tau'\} = -ik\bar{\tau}(k)$, we obtain

$$ikF^2(2\pi)^{\frac{1}{2}}F\{\hat{\theta}(k)\}\bar{P}(k) + T_0F\{\hat{\theta}''\} + F\{\hat{\theta}(k)\} = -F^2\alpha\pi\delta F\left\{\left(\frac{e^{\pi\phi}}{(1+e^{\pi\phi})^2}\right)\right\}. \tag{2.111}$$

Since

$$F\{\hat{\theta}''\} = -k^2F\{\hat{\theta}(k)\}, \quad \bar{P}(k) = \frac{i}{(2\pi)^{\frac{1}{2}}\tanh k},$$
$$F\left\{\left(\frac{e^{\pi\phi}}{(1+e^{\pi\phi})^2}\right)\right\} = -\frac{k}{(2\pi)^{\frac{1}{2}}\pi\sinh k}, \tag{2.112}$$

it follows that (2.111) becomes

$$\left(\frac{F^2k}{\tanh k} + T_0k^2 - 1\right)F\{\hat{\theta}(k)\} = -\frac{F^2\alpha\delta k}{(2\pi)^{\frac{1}{2}}\pi\sinh k}. \tag{2.113}$$

In the case that k satisfies $F^2k+(T_0k^2-1)\tanh k = 0$, equation (2.113) is singular and we have to consider solution to

$$F^2\frac{d\tau_1}{d\phi} + T_0\hat{\theta}'' + \hat{\theta} = 0. \tag{2.114}$$

This was solved by Bloor [1978] using

$$\int_{-\infty}^{\infty *} \frac{e^{ikx}}{e^{\pi(r-x)}-1}dx = -\frac{ie^{ikr}}{\tanh k}, \tag{2.115}$$

to give general sinusoidal waves of wavenumber k

$$\hat{\theta} = A\cos ks + B\sin ks \tag{2.116}$$

where A and B are arbitrary constants. If $F^2k + (T_0k^2-1)\tanh k \neq 0$, equation (2.113) reduces to

$$F\{\hat{\theta}\} = -\frac{F^2\alpha\delta k}{(2\pi)^{\frac{1}{2}}\pi\cosh k(F^2k+(T_0k^2-1)\tanh k)} \tag{2.117}$$

which is then solved using the inverse Fourier transform as

$$\hat{\theta} = -\int_{-\infty}^{\infty} \frac{F^2\alpha\delta k e^{-ik\phi}dk}{2\pi^2\cosh k(F^2k+(T_0k^2-1)\tanh k)} \tag{2.118}$$

The closed form evaluation of (2.118) generally cannot be obtained. By using the residue theorem and suitably choosing the contour the integral may be evaluated as an infinite series which is fully discussed by Lamb [1932] and King & Bloor [1987]. The pure complex roots of $F^2k + (T_0k^2-1)\tanh k)$ can be determinded. Figure 2–3 shows the graph of $D(k) = F^2k - (T_0k^2+1)\tan k)$ when $F = 1.25$ and $T_0 = 0.85$. All the cusps indicate that $D(k)$ is $\pm\infty$ at $\pm(2n+1)\pi/2$ where $n = 0, 1, 2, \cdots$.

In this Chapter, we have recalled the basic theory of fluid dynamics, the governing equations of free surface problem. We have also introduced some known techniques being used to deal with obstructed free surface problems. We have also presented some results. The integral form of the momentum equation will be used

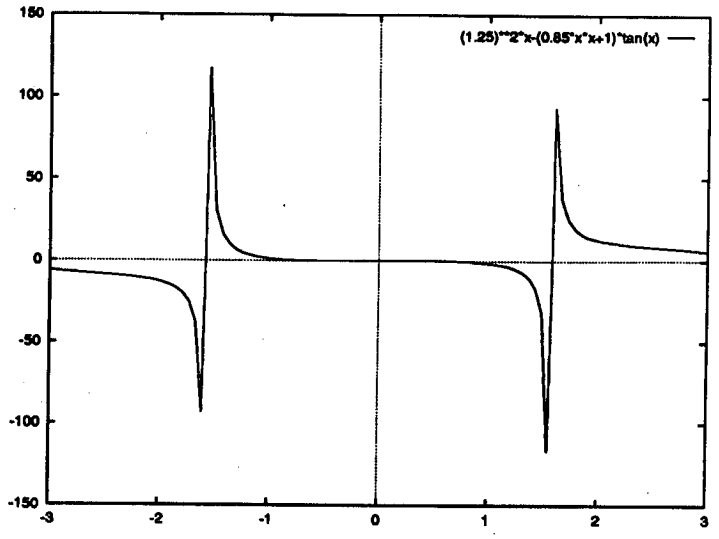

Figure 2–3: $D(k) = F^2k - (T_0k^2 + 1)\tan k$ with $F = 1.25$ and $T_0 = 0.85$.

in Chapter 5 for a jet impinging on an uneven wall. The transformation (2.68) will be used in Chapter 4 and the solution of an integral equation, in the form (2.82), will also be applied in Chapter 4.

Chapter 3

Nonlinear Free Surface Shapes of a Jet Incident on a Porous Wall

3.1 Introduction

The problem of determining the free streamline of a jet of ideal fluid incident on a porous wall was considered in the recent papers of Jenkins and Barton [1989] and King [1990]. Using Bernoulli's law, Jenkins and Barton gave the velocity potential on the free boundary so that an expanded velocity potential was defined on a wider region. Based on the Baiocchi transformation method, the problem was transformed into a fixed-domain problem, then a numerical computation of the various shapes of the free surfaces was provided and the pressure field was also given numerically. King extended the classical hodograph method and obtained an expression for the tangential angle along the curved portion in the complex potential plane in an explicit form. Then he reduced the problem to a first order differential equation, which was solved numerically. In both cases in computing the shapes of the jet the boundary condition assumed on the wetted portion of the wall was that the normal velocity of the fluid was constant. In this case,

King presented a concise numerical approach. However, although the particular boundary condition is not essential to his method, a non-constant normal velocity at the wall would introduce the difficulty of finding a conformal mapping which transforms the domain of the hodograph plane corresponding to the flow region into an upper half plane. As the wall velocity changes, a new conformal mapping has to be found. With the aim of studying the free surface problem when the normal velocity of fluid on the wall is not constant and the desire to give a compact numerical method applied to all the cases considered, in this chapter we use a boundary integral method and obtain a system of nonlinear integral equations relating the flow angle on the free surface and on the porous wall. When the normal velocity along the porous wall is constant, the problem reduces to solving a single nonlinear integral equation, so providing a computation of the shape of the free surface, alternative to those of King and of Jenkins and Barton. Moreover, as the flow angle on the wall is found, the velocity of the jet at the porous wall can be analysed, and then the force exerted on the porous wall by the fluid jet is given. In the last section, we extend this formulation to consider the effect of gravity. The method developed in this chapter can be treated as a complement to King's work and as a further confirmation that conformal mapping techniques can well describe a problem of a jet incident on a porous wall.

3.2 Mathematical Formulation

The physical problem here modelled is shown in Figure 3–1. A two-dimensional steady jet of inviscid fluid incident upon a porous wall, inclined at angle γ to the upstream flow. The fluid occupies the region Ω. Cartesian coordinates (x, y) are introduced, as shown in Figure 3–1. In terms of the velocity potential ϕ, the stream function ψ and the complex potential $w = \phi + i\psi$ which is an analytic

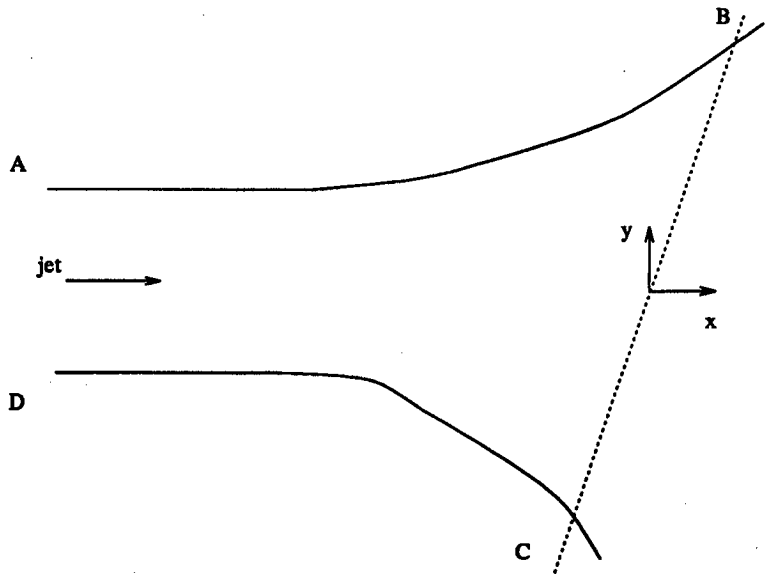

Figure 3–1: The physical-plane of a jet impinging on a porous wall

function of z, the complex velocity is given by

$$\chi = \frac{dw}{dz} = qe^{-i\theta} = u - iv. \tag{3.1}$$

Here q is the fluid speed, θ is the flow angle relative to the x-axis and u, v are the velocity components in the x and y directions.

The stream function ψ is harmonic within the flow satisfying Laplace's equation

$$\Delta^2\psi = 0, \qquad z \in \Omega, \tag{3.2}$$

with the boundary conditions

$$\frac{dw}{dz} \to 1 \quad as \quad x \to -\infty, \quad -1 \leq \psi \leq 1 \tag{3.3}$$

$$Re\left(\frac{dw}{dz}e^{-i\gamma}\right) = G(y) \quad on \quad x = y\tan\gamma, \quad a \leq y \leq b \tag{3.4}$$

$$\left|\frac{dw}{dz}\right| = 1 \quad \text{on} - \infty \leq x \leq y\tan\gamma, \quad \psi = \pm 1. \tag{3.5}$$

The function $G(y)$ specifies the normal component of velocity on wetted portions of the wall, and $y = a, b$ are to be found as positions where the bounding streamlines

Figure 3–2: The images of A,B,C and D in the reference $\zeta = \xi + i\eta$-plane

meet the wall, so that

$$\psi(a\tan\gamma, a) = -1, \;\; \psi(b\tan\gamma, b) = 1. \tag{3.6}$$

The mass conservation law then gives

$$\sec\gamma \int_a^b G(y)dy = 2. \tag{3.7}$$

We introduce a conformal mapping of the flow region onto the upper half of the $\zeta = \xi + i\eta$ plane. The mapping is given by a generalized Schwarz-Christoffel formula, i.e,

$$\frac{dz}{d\zeta} = K \exp\left\{-\frac{1}{\pi}\int_{-\infty}^{\infty} \log(\zeta - t)d\mu(t)\right\} \tag{3.8}$$

where K is a constant to be determined later and $\mu(t)$ is the angle of inclination of the tangent to the boundary of Ω at points which map onto $\xi = t$ on the real axis of the ζ-plane. Since $\psi = \pm 1$ are streamlines and the wall is plane, the angle μ satisfies

$$\begin{cases} \mu = \theta & \text{on} \quad t < -1 \\ \mu = \frac{1}{2}\pi - \gamma & \text{on} \quad |t| < 1 \\ \mu = \theta + \pi & \text{on} \quad t > 1 \end{cases} . \tag{3.9}$$

Since the angle $\mu(t)$ has jumps at points -1 and 1 along the ξ-axis of the ζ-plane, the integration is divided into five parts as

$$\int_{-\infty}^{\infty} \log(\zeta - t)d\mu(t) = \int_{-\infty}^{-1-\epsilon} + \int_{-1-\epsilon}^{-1+\epsilon} + \int_{-1+\epsilon}^{1-\epsilon} + \int_{1-\epsilon}^{1+\epsilon} + \int_{1+\epsilon}^{\infty} \log(\zeta - t)d\mu(t) \tag{3.10}$$

which are evaluated as follows:

$$\int_{-\infty}^{-1-\epsilon} \log(\zeta - t)d\mu(t) = -\alpha\log(\zeta + 1 + \epsilon) + \int_{-\infty}^{-1-\epsilon} \frac{\mu}{\zeta - t}dt \tag{3.11}$$

$$\int_{-1-\epsilon}^{-1+\epsilon} \log(\zeta - t) d\mu(t) = \left(\frac{\pi}{2} - \gamma + \alpha\right) \log(\zeta + 1) + O(\epsilon) \tag{3.12}$$

$$\lim_{\epsilon \to 0} \int_{-1+\epsilon}^{1-\epsilon} \log(\zeta - t) d\mu(t) = 0 \tag{3.13}$$

$$\int_{1-\epsilon}^{1+\epsilon} log(\zeta - t) d\mu(t) = \left(\frac{\pi}{2} + \beta + \gamma\right) \log(\zeta - 1) + O(\epsilon) \tag{3.14}$$

$$\int_{1+\epsilon}^{\infty} \log(\zeta - t) d\mu(t) = -\beta \log(\zeta - 1 - \epsilon) + \int_{1+\epsilon}^{\infty} \frac{\mu - \pi}{\zeta - t} dt. \tag{3.15}$$

After letting $\epsilon \to 0$ in the equations and using (3.9), equation (3.8) is then converted to

$$\begin{aligned} \frac{dz}{d\zeta} &= K \exp\left\{-\frac{1}{\pi}\left[\left(\frac{\pi}{2} - \gamma\right)\log(\zeta + 1) + \left(\frac{\pi}{2} + \gamma\right)\log(\zeta - 1)\right.\right. \\ &\quad \left.\left. + \int_{-\infty}^{-1} \frac{\theta}{\zeta - t} dt + \int_{1}^{\infty} \frac{\theta}{\zeta - t} dt\right]\right\} \\ &= K\left(\zeta^2 - 1\right)^{-\frac{1}{2}} \left(\frac{\zeta - 1}{\zeta + 1}\right)^{-\frac{\gamma}{\pi}} \exp\left\{-\frac{1}{\pi}\left[\int_{-\infty}^{-1} \frac{\theta}{\zeta - t} dt + \int_{1}^{\infty} \frac{\theta}{\zeta - t} dt\right]\right\}. \end{aligned} \tag{3.16}$$

After determining the constant K by the condition at infinity where the upstream flow width is 2, we obtain

$$\frac{dz}{d\zeta} = -\frac{2(\zeta^2 - 1)^{-\frac{1}{2}}}{\pi} \left(\frac{\zeta - 1}{\zeta + 1}\right)^{-\frac{\gamma}{\pi}} \exp\left(-\frac{1}{\pi}\left[\int_{-\infty}^{-1} \frac{\theta(t)}{\zeta - t} dt + \int_{1}^{\infty} \frac{\theta(t)}{\zeta - t} dt\right]\right), \quad \eta > 0 \tag{3.17}$$

where $\theta(t)$ is the flow angle on the free surface while t is a parameter along the real ξ-axis, and $\zeta = -1$, $\zeta = 1$ correspond to $z = ia \sec\gamma e^{-i\gamma}$, $z = ib \sec\gamma e^{-i\gamma}$, respectively.

Since $\ln\chi$ is an analytic function of ζ in $\eta > 0$, then on $\eta = 0$, $\ln q$ and θ are related through Hilbert transformation as

$$q(\xi) = \exp\left(-\frac{1}{\pi} \int_{-\infty}^{\infty *} \frac{\theta(t)}{t - \xi} dt\right) \tag{3.18}$$

$$|\xi| < +\infty,$$

$$\theta(\xi) = \frac{1}{\pi} \int_{-\infty}^{\infty *} \frac{\ln q(t)}{t - \xi} dt \tag{3.19}$$

where the $*$ above the integral indicates a principal-value integral.

After using the boundary conditions (3.5), (3.18) and (3.19) then reduce to

$$-\frac{1}{\pi}\int_{-\infty}^{\infty *}\frac{\theta(t)}{t-\xi}dt = 0, \quad \text{for} \quad |\xi| > 1, \tag{3.20}$$

$$\theta(\xi) = \frac{1}{\pi}\int_{-1}^{1*}\frac{\ln q(t)}{t-\xi}dt, \quad \text{for} \quad |\xi| < +\infty. \tag{3.21}$$

3.3 The Boundary Equations

Let $\theta_w = \theta(\xi)$ ($|\xi| < 1$) denote the flow angle at the porous wall, so that from (3.4) we have

$$q\cos(\theta_w + \gamma) = G(y). \tag{3.22}$$

Hence, for $|\xi| < 1$, we have $\ln q = \ln G(y) - \ln\cos(\theta_w + \gamma)$, which may be inserted into (3.21) to give

$$\theta_w(\xi) = \frac{1}{\pi}\int_{-1}^{1*}\frac{\ln G(y) - \ln\cos(\theta_w+\gamma)}{t-\xi}dt, \quad \text{for} \quad |\xi| < 1. \tag{3.23}$$

Also, since $q(t) = 1$ for $|t| > 1$, equation (3.19) gives

$$\theta(\xi) = \frac{1}{\pi}\int_{-1}^{1}\frac{\ln G(y) - \ln\cos(\theta_w+\gamma)}{t-\xi}dt, \quad \text{for} \quad |\xi| > 1. \tag{3.24}$$

In order to use the above equations to find $\theta_w(\xi)$, it is necessary to relate y to ξ for $|\xi| < 1$. By letting $\zeta \to \xi$ in (3.17) for $|\xi| < 1$, we obtain

$$\frac{dz}{d\xi} = -ie^{-i\gamma}\frac{2}{\pi}(1-\xi^2)^{-\frac{1}{2}}\left(\frac{1-\xi}{1+\xi}\right)^{-\frac{\alpha}{\pi}}\exp\left\{-\frac{1}{\pi}\left(\int_{-\infty}^{-1}+\int_{1}^{\infty}\right)\frac{\theta(t)}{\xi-t}dt\right\}, \quad |\xi| < 1. \tag{3.25}$$

Since $z = (\tan\gamma + i)y = iye^{-i\gamma}\sec\gamma$ on the wetted wall, we have the relation between y and ξ as

$$\frac{dy}{d\xi} = -\frac{2\cos\gamma}{\pi}(1-\xi^2)^{-\frac{1}{2}}\left(\frac{1-\xi}{1+\xi}\right)^{-\frac{\gamma}{\pi}}\exp\left\{-\frac{1}{\pi}\left(\int_{-\infty}^{-1}+\int_1^{\infty}\right)\frac{\theta(t)}{\xi-t}dt\right\}, \quad |\xi|<1. \tag{3.26}$$

Consequently, determination of the flow reduces to solving the system (3.23), (3.24) and (3.26). An iterative method is given later. Since formula (3.24) the flow angle at the free surface also involves $G(y)$ the problem is complicated. We need an explicit relation between the flow angle at the wall and on the free surface. This is provided by inverting equation (3.20) as

$$\theta(t) = \pm\frac{1}{\pi}\frac{\sqrt{t^2-1}}{t}\left(\int_{-\infty}^{-1*}-\int_1^{\infty*}\right)\frac{1}{\sqrt{\xi^2-1}}\frac{\xi F(\xi)}{\xi-t}d\xi, \qquad |t|>1, \tag{3.27}$$

where the positive sign applies for $t>1$ and the negative sign for $t<-1$, while

$$F(\xi) = \frac{1}{\pi}\int_{-1}^{1}\frac{\theta_w(t)}{\xi-t}dt, \qquad 1<|\,\xi\,|<\infty. \tag{3.28}$$

This allows (3.26) to be integrated as

$$y(\xi) = b-\int_1^{\xi}\frac{2\cos\gamma}{\pi}(1-\xi^2)^{-\frac{1}{2}}\left(\frac{1-\xi}{1+\xi}\right)^{-\frac{\gamma}{\pi}}\exp\left\{-\frac{1}{\pi}\left(\int_{-\infty}^{-1}+\int_1^{\infty}\right)\frac{\theta(t)}{\xi-t}dt\right\}d\xi, \tag{3.29}$$

with $\theta(t)$ related to $\theta_w(t)$ through (3.27) and (3.28). Substitution into $G(y)$ in (3.23) then forms an integral equation for θ_w. An alternative way to solve this problem is to consider (3.18), in the form

$$q(\xi)\exp\left\{-\frac{1}{\pi}\int_{-1}^{1}\frac{\theta(t)}{\xi-t}dt\right\} = \exp\left\{\frac{1}{\pi}\left(\int_{-\infty}^{-1}+\int_1^{\infty}\right)\frac{\theta(t)}{\xi-t}dt\right\}, \quad |\xi|<+\infty. \tag{3.30}$$

Substituting this into (3.29) yields

$$y(\xi) = b-\int_1^{\xi}\frac{2\cos\gamma}{\pi}(1-\xi^2)^{-\frac{1}{2}}\left(\frac{1-\xi}{1+\xi}\right)^{-\frac{\gamma}{\pi}}\frac{1}{q(\xi)}\exp\left\{\frac{1}{\pi}\int_{-1}^{1}\frac{\theta(t)}{\xi-t}dt\right\}d\xi, \quad |\xi|<1. \tag{3.31}$$

Then evaluating y in (3.22) using (3.31) yields

$$q(\xi)\ \cos(\theta_w(\xi)+\gamma) = G\left(b-\int_1^{\xi}\frac{2\cos\gamma}{\pi}(1-\xi^2)^{-\frac{1}{2}}\left(\frac{1-\xi}{1+\xi}\right)^{-\frac{\gamma}{\pi}}\frac{1}{q(\xi)}\exp\left\{\frac{1}{\pi}\int_{-1}^{1}\frac{\theta_w(t)}{\xi-t}dt\right\}d\xi\right). \tag{3.32}$$

Thus we consider (3.21) (for $\theta(\xi)=\theta_w(\xi), |\xi|<1$) and (3.32) to obtain a pair of integral equations.

However, this problem simplifies if the normal velocity on the wetted portion of the porous wall is a constant, $G(y)=\cos\alpha$, where α is the flow angle to the x-axis at points where the fluid on the free surface meets the wall. Equation (3.23) then reduces to the integral equation

$$\theta_w(t)=\frac{1}{\pi}\int_{-1}^{1*}\frac{\ln\cos\alpha-\ln\cos(\theta_w(t)+\gamma)}{t-\xi}dt, \quad \text{for} \quad |\xi|<1 \tag{3.33}$$

where as $t\to\pm1$, $\cos(\theta_w(t)+\gamma)\to\cos\alpha$. Alternatively, equation (3.33) may be expressed as

$$\theta_w(\xi)+\frac{1}{\pi}\int_{-1}^{1*}\frac{\ln\cos(\theta_w(t)+\gamma)}{t-\xi}dt=\frac{1}{\pi}\ln\cos\alpha\ln\frac{1-\xi}{1+\xi}, \quad \text{for} \quad |\xi|<1. \tag{3.34}$$

Once this has been solved, the flow angles on the upper and lower free boundaries are found by solving (3.24) as

$$\theta(\xi)=\frac{1}{\pi}\left\{\ln\cos\alpha\ln\frac{\xi-1}{\xi+1}-\int_{-1}^{1*}\frac{\ln\cos(\theta_w(t)+\gamma)}{t-\xi}dt\right\}, \quad \text{for} \quad |\xi|>1. \tag{3.35}$$

Then by integrating (3.24) we may obtain the the shape of the free surfaces. We should note that equations (3.21) and (3.22) indicate an alternative way to of solving this problem.

Letting $\zeta\to\xi$ on $|\xi|>1$ and then examining the singularity along the ξ axis in (3.17) gives

$$\frac{dz}{d\xi}=-\frac{2(\xi^2-1)^{-\frac{1}{2}}}{\pi}\left(\frac{\xi-1}{\xi+1}\right)^{-\frac{\gamma}{\pi}}\exp\left(-\frac{1}{\pi}\left[\int_{-\infty}^{-1*}\frac{\theta(t)}{\xi-t}dt+\int_{1}^{\infty*}\frac{\theta(t)}{\xi-t}dt-i\pi\theta(\xi)\right]\right). \tag{3.36}$$

Expressing equation (3.20) in an alternative form yields

$$\frac{1}{\pi}\int_{-\infty}^{-1*}\frac{\theta(t)}{t-\xi}dt+\frac{1}{\pi}\int_{1}^{\infty*}\frac{\theta(t)}{t-\xi}dt=-\frac{1}{\pi}\int_{-1}^{1}\frac{\theta_w(t)}{t-\xi}dt,\quad \text{for}\quad |\xi|>1. \tag{3.37}$$

Substituting (3.37) into (3.36) yields an equation for determining the free streamline in the form

$$\frac{dz}{d\xi}=-\frac{2(\xi^2-1)^{-\frac{1}{2}}}{\pi}\left(\frac{\xi-1}{\xi+1}\right)^{-\frac{\gamma}{\pi}}\exp\left(-\frac{1}{\pi}\left[\int_{-1}^{1}\frac{\theta_w(t)}{t-\xi}dt-i\pi\theta(\xi)\right]\right),\quad |\xi|>1. \tag{3.38}$$

Taking the real and imaginary parts of (3.38) and integrating each leads, for $r>1$, to

$$x^+(r) = -\int_1^r\frac{2(s^2-1)^{-\frac{1}{2}}\cos\theta(s)}{\pi}\left(\frac{s-1}{s+1}\right)^{-\frac{\gamma}{\pi}}\exp\left(-\frac{1}{\pi}\int_{-1}^{1}\frac{\theta_w(\xi)}{\xi-s}d\xi\right)ds, \tag{3.39}$$

$$y^+(r) = b-\int_1^r\frac{2(s^2-1)^{-\frac{1}{2}}\sin\theta(s)}{\pi}\left(\frac{s-1}{s+1}\right)^{-\frac{\gamma}{\pi}}\exp\left(-\frac{1}{\pi}\int_{-1}^{1}\frac{\theta_w(\xi)}{\xi-s}d\xi\right)ds, \tag{3.40}$$

where the ' + ' above x and y indicates the upper free surface. Similarly, for $r<-1$, we obtain

$$x^-(r) = -\int_{-1}^r\frac{2(s^2-1)^{-\frac{1}{2}}\cos\theta(s)}{\pi}\left(\frac{s-1}{s+1}\right)^{-\frac{\gamma}{\pi}}\exp\left(-\frac{1}{\pi}\int_{-1}^{1}\frac{\theta_w(\xi)}{\xi-s}d\xi\right)ds, \tag{3.41}$$

$$y^-(r) = a-\int_{-1}^r\frac{2(s^2-1)^{-\frac{1}{2}}\sin\theta(s)}{\pi}\left(\frac{s-1}{s+1}\right)^{-\frac{\gamma}{\pi}}\exp\left(-\frac{1}{\pi}\int_{-1}^{1}\frac{\theta_w(\xi)}{\xi-s}d\xi\right)ds, \tag{3.42}$$

where the ' − ' above x and y indicates the lower free surface. The asymptotic behaviour of $\theta(\xi)$ as $\xi\to\pm\infty$ can be derived from (3.23) as

$$\begin{aligned}\theta(\xi) &\sim -\frac{1}{\pi\xi}\int_{-1}^{1}(\ln G(y)-\ln\cos(\theta_w+\gamma)dt\\ &= -\frac{1}{\pi\xi}\int_{-1}^{1}\ln q\,dt=-\frac{c_0}{\pi\xi},\end{aligned} \tag{3.43}$$

where

$$c_0 = \int_{-1}^{1} \ln q dt. \tag{3.44}$$

Consequently, as $\xi \to \pm\infty$, the flow angle at the free surface tends to 0 like ξ^{-1}. Also, the behaviour of the integrands in (3.39) and (3.40) as $\xi \to \infty$ are

$$\frac{2(s^2-1)^{-\frac{1}{2}}\cos\theta(s)}{\pi}\left(\frac{\xi-1}{\xi+1}\right)^{-\frac{\gamma}{\pi}}\exp\left(-\frac{1}{\pi}\int_{-1}^{1}\frac{\theta_w(\xi)}{\xi-s}d\xi\right) \to \frac{2}{\pi s} \tag{3.45}$$

$$\frac{2(s^2-1)^{-\frac{1}{2}}\sin\theta(s)}{\pi}\left(\frac{\xi-1}{\xi+1}\right)^{-\frac{\gamma}{\pi}}\exp\left(-\frac{1}{\pi}\int_{-1}^{1}\frac{\theta_w(\xi)}{\xi-s}d\xi\right) \to -\frac{2c_0}{\pi^2 s^2}. \tag{3.46}$$

Thus if r is very large in (3.32) and (3.33) we may obtain

$$\begin{aligned} x^+(r) \sim & -\int_1^{r_0}\frac{2(s^2-1)^{-\frac{1}{2}}\cos\theta(s)}{\pi}\left(\frac{\xi-1}{\xi+1}\right)^{-\frac{\gamma}{\pi}}\exp\left(-\frac{1}{\pi}\int_{-1}^{1}\frac{\theta_w(\xi)}{\xi-s}d\xi\right)ds \\ & -\int_{r_0}^{r}\frac{2ds}{\pi s} \\ = & -\frac{2}{\pi}\left[\int_1^{r_0}(s^2-1)^{-\frac{1}{2}}\cos\theta(s)\left(\frac{\xi-1}{\xi+1}\right)^{-\frac{\gamma}{\pi}}\exp\left(-\frac{1}{\pi}\int_{-1}^{1}\frac{\theta_w(\xi)}{\xi-s}d\xi\right)ds\right. \\ & \left.+\log\frac{r}{r_0}\right]. \end{aligned} \tag{3.47}$$

Similarly, we have

$$\begin{aligned} y^+(r) \sim & \; b-\frac{2}{\pi}\left[\int_1^{r_0}(s^2-1)^{-\frac{1}{2}}\cos\theta(s)\left(\frac{\xi-1}{\xi+1}\right)^{-\frac{\gamma}{\pi}}\exp\left(-\frac{1}{\pi}\int_{-1}^{1}\frac{\theta_w(\xi)}{\xi-s}d\xi\right)ds\right. \\ & \left.+\frac{c_0}{\pi}\left(\frac{1}{r}-\frac{1}{r_0}\right)\right]. \end{aligned} \tag{3.48}$$

From these approximations we can see that as $r \to \infty$, $x^+ \to -\infty$ and $y^+ \to$ constant. Similar conclusions apply for x^- and y^-.

The pressure along the porous wall is given by Bernoulli's equation in the form

$$p + \frac{q^2}{2} = p_\infty + \frac{1}{2} \tag{3.49}$$

where p_∞ represents the pressure within the jet where it is in uniform flow far away from the wall. The force exerted on the porous wall by the fluid jet is

$$\mathbf{R} = \int_a^b p\mathbf{n}dy \tag{3.50}$$

where $\mathbf{n}$ is an outward normal to Ω. Substituting p, given by (3.49), into (3.50) gives

$$\mathbf{R} = \int_a^b \left[p_\infty + \frac{1}{2} - \frac{q^2}{2} \right] \mathbf{n} dy \tag{3.51}$$

Changing the variable y to ξ in (3.40) and using $G(y) = q\cos\theta_w$, gives

$$\mathbf{R} = \int_{-1}^{1} \left[p_\infty + \frac{1}{2} - \frac{G(y)^2}{2\cos^2(\theta_w + \gamma)} \right] \mathbf{n} \wp(\xi) d\xi \tag{3.52}$$

where $\wp(\xi)$ is defined in the form

$$\wp(\xi) = \frac{2}{\pi}(1-\xi^2)^{-\frac{1}{2}} \exp\left\{ -\frac{1}{\pi} \left(\int_{-\infty}^{-1} + \int_1^{\infty} \right) \frac{\theta(s)}{\xi - s} ds \right\}, \quad |\xi| < 1. \tag{3.53}$$

3.4 The Numerical Scheme

3.4.1 Symmetric problem

$g(y)$ =**constant**

In the symmetric case, with $G(y)$ =constant, equation (3.33) was simplified as

$$\theta_w(t) + \frac{2t}{\pi} \int_0^1 \frac{\log\cos\theta_w(\xi)}{\xi^2 - t^2} d\xi = \log\cos\alpha \log\frac{1-t}{1+t}, \quad 0 < t < 1. \tag{3.54}$$

The integration range $(0,1)$ was discretized on a mesh

$$0 = \xi_0 < \cdots < \xi_N = 1. \tag{3.55}$$

The integration, at $t = \xi_i$, has a singularity, so the interval $(0,1)$ had to be divided into three subdomains $(0, \xi_{i-1}], [\xi_{i-1}, \xi_{i+1}]$ and $[\xi_{i-1}, 1)$. The Trapezoidal rule was applied on $(0, \xi_{i-1}]$ and $[\xi_{i-1}, 1)$ respectively. For $[\xi_{i-1}, \xi_{i+1}]$, the integral was treated using

$$\begin{aligned} \int_{\xi_{i-1}}^{\xi_{i+1}} \frac{\log\cos\theta_w(\xi)}{\xi^2 - \xi_i^2} d\xi &= \int_{\xi_{i-1}}^{\xi_{i+1}} \frac{\log\cos\theta_w(\xi) - \log\cos\theta_w(\xi_i)}{\xi^2 - \xi_i^2} d\xi \\ &+ \int_{\xi_{i-1}}^{\xi_{i+1}} \frac{\log\cos\theta_w(\xi_i)}{\xi^2 - \xi_i^2} d\xi \end{aligned} \tag{3.56}$$

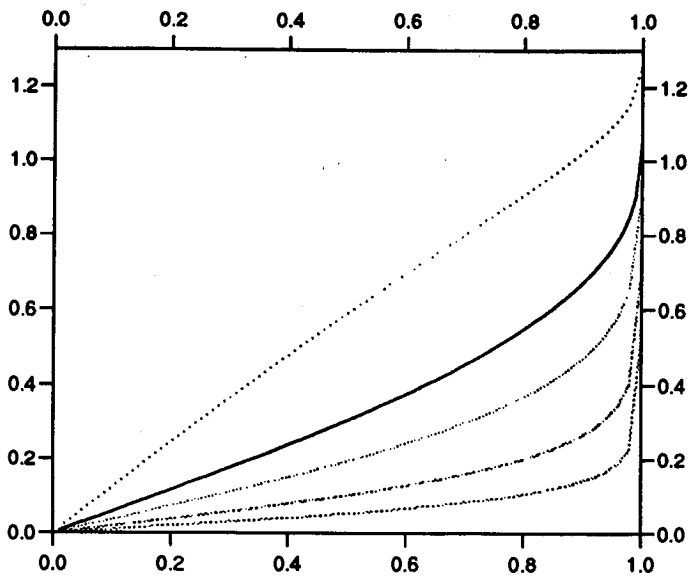

Figure 3–3: The flow angles along the porous wall

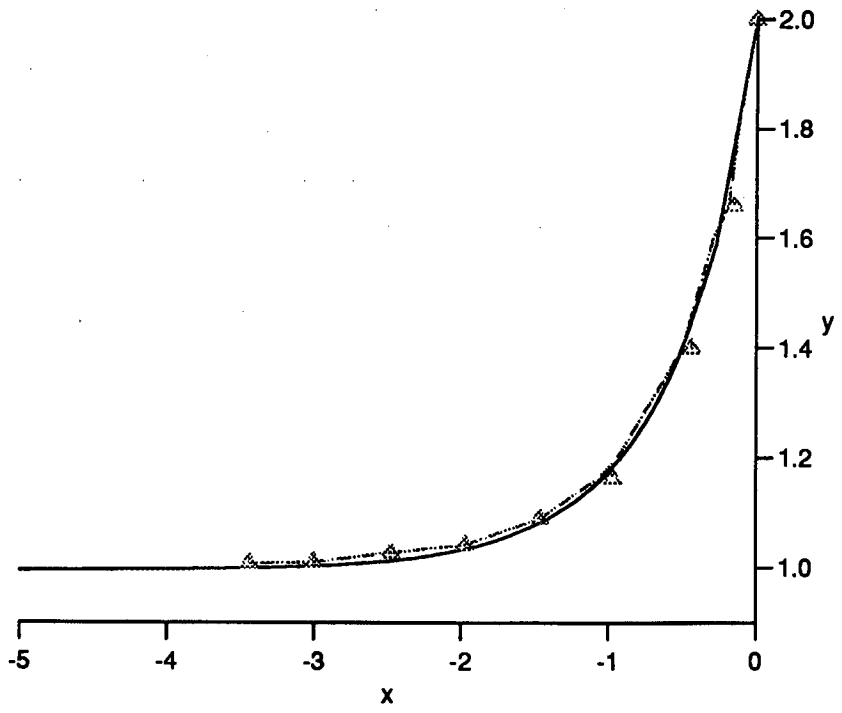

Figure 3–4: The shape of the free surface with constant normal speed $U = 0.5$ along porous wall where the broken line (····) is a polygonal approximation to the curve of King [1990], the triangular markers (Δ) are taken from Jenkins and Barton's [1989] and the result of present computation is shown by solid line (—)

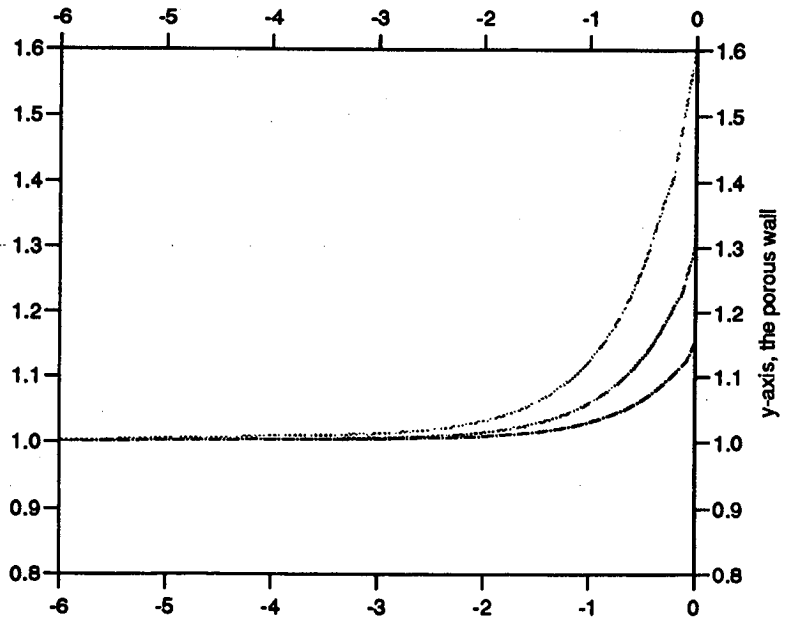

Figure 3–5: The three computed shapes of the free surfaces for the different constant normal speeds $U = 0.625$, 0.769 and 0.87 are shown respectively by the curves from the top to the bottom(Note the differing scales on the two axes).

The first integral of the right side of (3.56) was evaluated using Taylor series. With step length h, one obtains

$$\begin{aligned}
&\int_{\xi_{i-1}}^{\xi_{i+1}} \frac{\log\cos\theta_w(\xi) - \log\cos\theta_w(\xi_i)}{\xi^2 - \xi_i^2} d\xi \\
&= \int_{\xi_{i-1}}^{\xi_{i+1}} \frac{1}{\xi + \xi_i} \left[\theta'_w \tan\theta_w + (\theta'_w \tan\theta_w)' \frac{\xi - \xi_i}{2} \right] d\xi + O(h^3) \\
&= \theta'_w \tan\theta_w \log\frac{\xi_{i+1} + \xi_i}{\xi_i + \xi_{i-1}} + (\theta'_w \tan\theta_w)' \left(2(\xi_i - \xi_{i-1}) - \xi_i \log\frac{\xi_{i+1} + \xi_i}{\xi_i + \xi_{i-1}} \right) + O(h^3)
\end{aligned} \tag{3.57}$$

The second integration was evaluated

$$\begin{aligned}
\int_{\xi_{i-1}}^{\xi_{i+1}} \frac{\log\cos\theta_w(\xi_i)}{\xi^2 - \xi_i^2} d\xi &= \int_{\xi_{i-1}}^{\xi_{i+1}} \frac{1}{2\xi_i} \left(\frac{1}{\xi - \xi_i} - \frac{1}{\xi + \xi_i} \right) \log\cos\theta_w(\xi_i) d\xi \\
&= -\frac{\log\cos\theta_w(\xi_i)}{2\xi_i} \log\frac{\xi_{i+1} + \xi_i}{\xi_i + \xi_{i-1}}.
\end{aligned} \tag{3.58}$$

Then we have

$$\begin{aligned}
&\theta_{w,i} + \frac{2h\xi_i}{\pi} \left(\sum_{j=1}^{i-1} \frac{\log\cos\theta_{w,j}}{\xi_j^2 - \xi_i^2} + \sum_{j=i+1}^{N} \frac{\log\cos\theta_{w,j}}{\xi_j^2 - \xi_i^2} \right) \\
&\quad + \left(\theta'_{w,i} \tan\theta_{w,i} - \frac{\log\cos\theta_{w,i}}{2\xi_i} \right) \log\frac{\xi_{i+1} + \xi_i}{\xi_i + \xi_{i-1}} + (\theta'_{w,i} \tan\theta_{w,i})' \left(2h - \xi_i \log\frac{\xi_{i+1} + \xi_i}{\xi_i + \xi_{i-1}} \right) \\
&\quad = \log\cos\alpha \log\frac{1 - \xi_i}{1 + \xi i}, \qquad i = 1, \cdots, N
\end{aligned} \tag{3.59}$$

where $\theta_{w,i} = \theta_w(\xi_i)$ and $\theta'_{w,i} = \theta'_w(\xi_i)$. Equation (3.59) is a system of N nonlinear equations with N unknown variables, which is solved using NAG library C05NBF.

As the flow angle on the wall $\theta_{w,i}$, $i = 1, \cdots, N$ is found, the flow angle on the free surface can be calculated from equation (3.35)

$$\theta(s_j) = \frac{1}{\pi} \left[\log\cos\alpha \log\frac{s_j - 1}{s_j + 1} + 2\bar{h} \sum_{i=1}^{N} \frac{s_j}{s_j^2 - \xi_j^2} \log\cos\theta_{w,j} \right], \qquad s_j > 1. \tag{3.60}$$

If we change the variable using $(s^2-1)^{\frac{1}{2}} = l$ and $dl = (s^2-1)^{-\frac{1}{2}}sds$, then we obtain an alternative formula for the computation of flow angle on the free surface

$$\theta((1+l_j^2)^{\frac{1}{2}}) = \frac{1}{\pi}\left[\log\cos\alpha\log\frac{l_j^2}{((1+l_j^2)^{\frac{1}{2}}+1)^2} + 2\tilde{h}\sum_{i=1}^{N}\frac{(1+l_j^2)^{\frac{1}{2}}}{1+l_j^2-\xi_j^2}\log\cos\theta_{w,j}\right], \quad l_j > 0. \tag{3.61}$$

Then using the same transformation, we can avoid the singularity in the equations which now became

$$x_+(s) = x_+((1+l^2)^{\frac{1}{2}}) = -\frac{2}{\pi}\int_0^l \frac{\cos\theta((1+l^2)^{\frac{1}{2}})}{(1+l^2)^{\frac{1}{2}}}F(l)dl \tag{3.62}$$

$$y_+(s) = y_+((1+l^2)^{\frac{1}{2}}) = \sec\alpha - \frac{2}{\pi}\int_0^l \frac{\sin\theta((1+l^2)^{\frac{1}{2}})}{(1+l^2)^{\frac{1}{2}}}F(l)dl \tag{3.63}$$

where

$$F(l) = \exp\left(\frac{1}{\pi}\int_{-1}^{1}\frac{\theta_w(\xi)}{\xi-(1+l^2)^{\frac{1}{2}}}d\xi\right). \tag{3.64}$$

In Figure 3–4, we present the comparison of our result with previous results obtained by different techniques in the case that the normal speed across the wetted wall is constant. The broken line $(- \cdot\cdot -)$ is a polygonal approximation to the curve of King [1990] and the triangular markers is taken from Jenkins and Barton [1989]. The solid line is my result. The agreement of mine with others is very good, as shown in Figure 3–4.

$G(y)$ specified

In the case that $G(y)$ is not a constant and that $\gamma = 0$ equations (3.21) and (3.32) complete the problem. Substituting (3.21) into (3.32) to replace $\theta_w(t)$ for $|\xi| < 1$ yields a single integral equation for $q(\xi)$:

$$\begin{aligned} q(\xi)\ \cos(&\frac{1}{\pi}\int_{-1}^{1^*}\frac{\ln q(t)}{t-\xi}dt) \\ = \ & G\left(b - \int_1^{\xi}\frac{2}{\pi}(1-\xi^2)^{-\frac{1}{2}}\frac{1}{q(\xi)}\exp\left\{\frac{1}{\pi}\int_{-1}^{1}\left\{\int_{-1}^{1^*}\frac{\ln q(s)}{s-t}ds\right\}\frac{dt}{\xi-t}\right\}d\xi\right). \end{aligned} \tag{3.65}$$

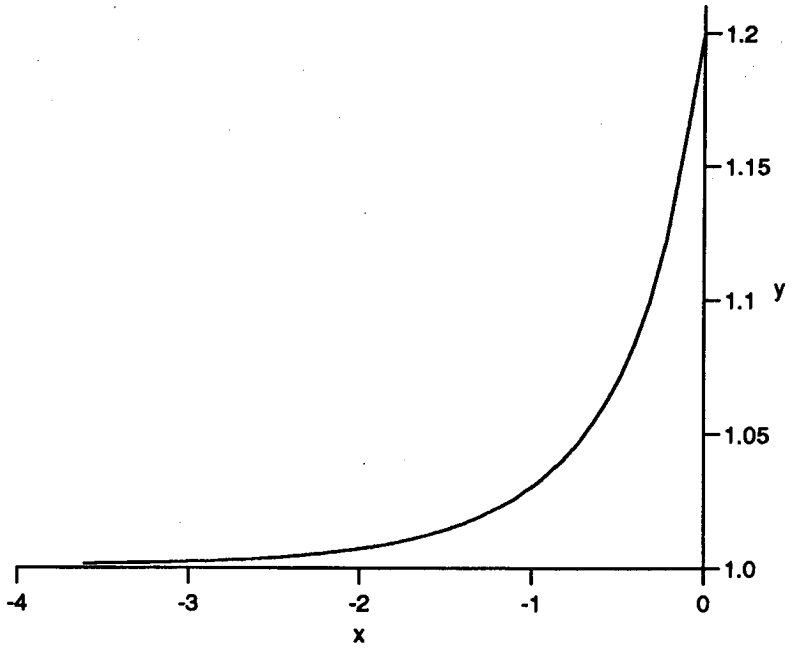

Figure 3–6: The computed free surface shape for normal speed $G(y) = 1 + 3(1 - a)\frac{y^2}{a^3}$ where $a = 1.2$.

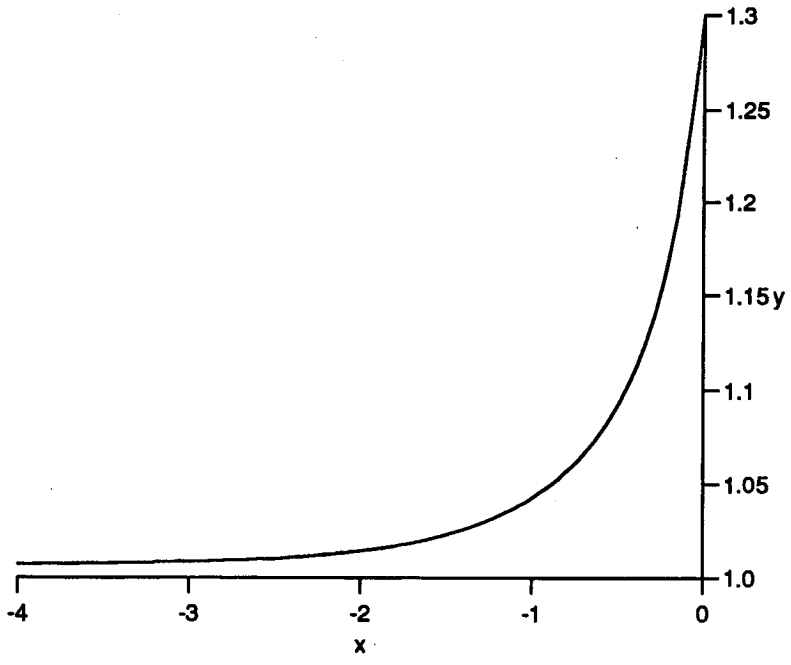

Figure 3–7: The free surface shape for normal speed $G(y) = 1+3(1-a)\frac{y^2}{a^3}$ where $a = 1.3$.

After this equation is solved numerically, the flow angle along the porous wall can be found from (3.21) and y can be determinded from equation (3.31). Thus in this symmetric case the flow angle along the free surace can be found from (3.24), then the shape of the free surface is obtained from equations (3.39) and (3.40). Some numerical results, corresponding to different normal speeds on the porous wall, are presented, shown in Fig. 3–6, 3–7, 3–8 and 3–9.

Alternatively, an iterative scheme can be developed. Equation (3.23) thus becomes

$$\theta_w^{n-1}(t) = \frac{1}{\pi}\int_{-1}^{1*} \frac{\ln G(y_{n-1}) - \ln\cos\theta_w^{n-1}(\xi)}{\xi - t} d\xi, \quad \text{for} \quad |t| < 1 \tag{3.66}$$

while, for $|t| > 1$, from equation (3.24) we obtain

$$\theta^n(s) = \frac{1}{\pi}\int_{-1}^{1} \frac{\ln G(y_{n-1}) - \ln\cos\theta_w^{n-1}(\xi)}{\xi - s} d\xi, \quad \text{for} \quad |s| > 1. \tag{3.67}$$

Equation (3.29) gives

$$y_n(\xi) = y(-1) + \frac{2}{\pi}\int_{-1}^{\xi}(1-\xi^2)^{-\frac{1}{2}} \exp\left\{-\frac{1}{\pi}\left(\int_{-\infty}^{-1} + \int_{1}^{\infty}\right)\frac{\theta^n(s)}{\xi - s} ds\right\} d\xi, \quad |\xi| < 1. \tag{3.68}$$

At both ends of the wetted part of porous wall, $G(y)$ must satisfy the boundary condition

$$\cos\theta_w(\pm 1) = G(y(\pm 1)), \qquad y(\pm 1) = \pm h \tag{3.69}$$

The average normal velocity $G(\bar{y_0}(\xi))$, which satisfies $G(\bar{y})h = 1$, from equation (3.7), can be taken as a first approximation to $G(y)$. We can then, using the same technique, get the first approximation $\theta^1(s)$, and the first approximation of $y_1(\xi)$. In the computation of the integrals in equations (3.66) and (3.67), in addition to the integrals of equations (3.59) and (3.61), both integrals in the right hand side of (3.66) and (3.67) were evaluated. In particular, the integral in (3.66) with singularities must be computed. Thus we have

$$\theta_{w,i}^n + \frac{2h\xi_i}{\pi}\left(\sum_{j=1}^{i-1}\frac{\log\cos\theta_{w,j}^n}{\xi_j^2 - \xi_i^2} + \sum_{j=i+1}^{N}\frac{\log\cos\theta_{w,j}^n}{\xi_j^2 - \xi_i^2}\right)$$

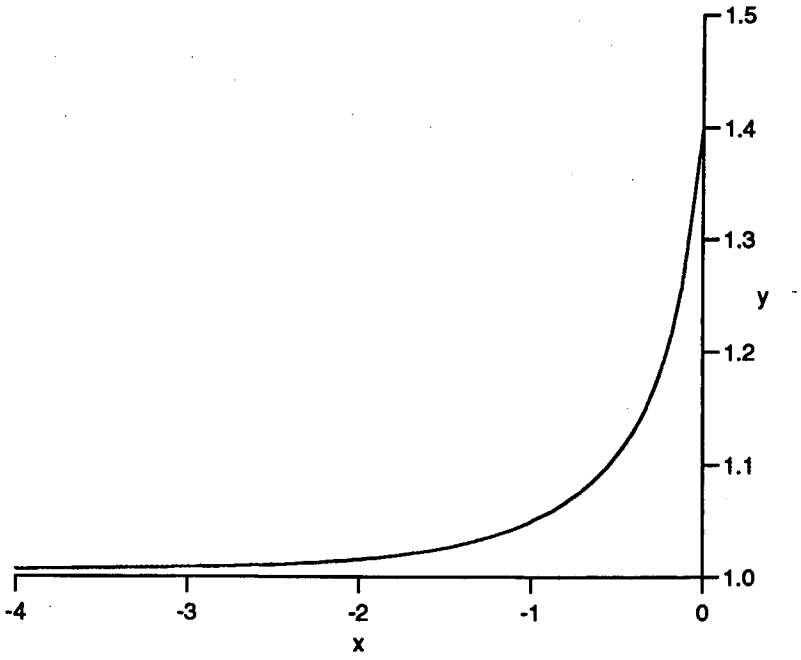

Figure 3–8: The free surface shape for normal speed $G(y) = 1+3(1-a)\frac{y^2}{a^3}$ where $a = 1.4$.

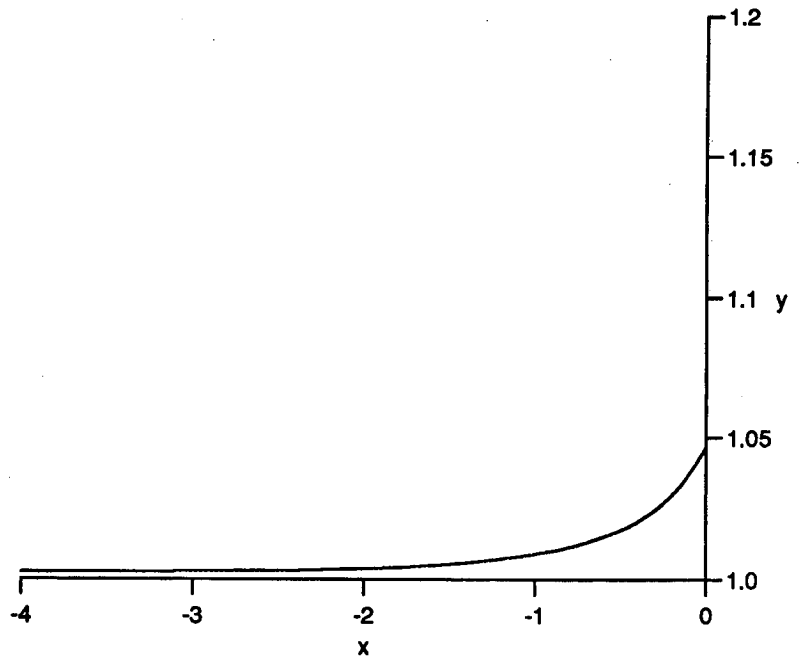

Figure 3–9: The free surface shape for normal speed $G(y) = 1+3(1-a)\frac{y^2}{a^3}$ where $a = 1.04$.

$$+\left(\theta^{n\prime}_{w,i}\tan\theta^{n}_{w,i}-\frac{\log\cos\theta^{n}_{w,i}}{2\xi_i}\right)\log\frac{\xi_{i+1}+\xi_i}{\xi_i+\xi_{i-1}}+(\theta^{n\prime}_{w,i}\tan\theta^{n}_{w,i})'\left(2h-\xi_i\log\frac{\xi_{i+1}+\xi_i}{\xi_i+\xi_{i-1}}\right)$$
$$=h\left(\sum_{j=-N}^{i-1}\frac{\log G(y_{n,j})}{\xi_j-\xi_i}+\sum_{j=i+1}^{N}\frac{\log G(y_{n,j})}{\xi_j-\xi_i}+2(\log G(y_{n,i}))'\frac{dy}{d\xi}\right)$$
$$i=1,\cdots,N \tag{3.70}$$

where $\theta_{w,i}=\theta_w(\xi_i)$, $\theta'_{w,i}=\theta'_w(\xi_i)$ and the $'$ in $(\log G(y_{n,i}))'$ represents differentiation with respect to y. Equation (3.67) was discretized in the form of

$$\theta(s_j)=\frac{\bar{h}}{\pi}\left[\sum_{i=-N}^{i=N}\frac{\ln G(y_{n-1,i})}{\xi_i-s_j}+2\sum_{i=1}^{N}\frac{s_j}{s_j^2-\xi_i^2}\log\cos\theta_{w,i}\right],\qquad s_j>1. \tag{3.71}$$

where $\bar{h}$ is step length, and $y_{n-1,i}=y_{n-1}(\xi_i)$ can be calculated from equation (3.68).

3.5 The Effects of Gravity

A question that will be addressed on the above method is whether it can be extended to apply to similar problem including the effect of gravity. The physical problem which concerns us is a nozzle directed perpendicularly to a wall. The fluid jet comes out of the nozzle with uniform speed U. The physical region is shown in Fig 3–10. Although the problem is altered and the effect of gravity acting on the free surface is considered, the above analysis is still available. After assuming that the air pressure along the free surface is 0, Bernoulli's law that states

$$\frac{F^2q^2}{2}-y=\frac{F^2}{2}-y_0^{\pm} \tag{3.72}$$

on the free surface where F is the Froude number, the $\pm$ signs denote the upper and lower free surfaces and $y_0^{\pm}=\pm1$. On the porous wall we still have

$$q\cos\theta_w=G(y) \tag{3.73}$$

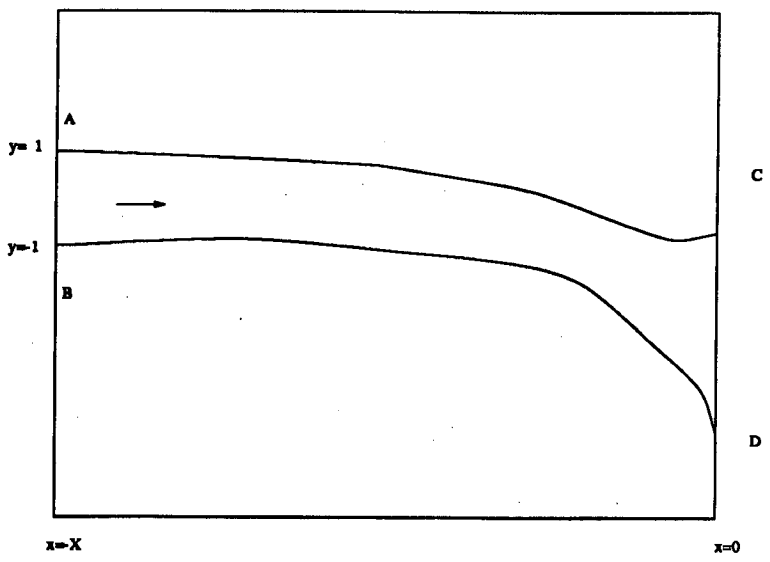

Figure 3–10: A sketch of the physical-plane of a jet impinging on a porous wall with effect of gravity

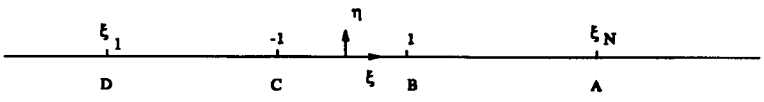

Figure 3–11: The images of A,B,C and D in the reference $\zeta = \xi + i\eta$-plane

If we assume that the nozzle extends to infinity, the transformation from the physical plane to the upper half plane is still available. However, the equations (3.18) and (3.19) change slightly to

$$q(\xi) = \exp\left(-\frac{1}{\pi}\int_{\xi_1}^{\xi_N} \frac{\theta(t)}{t-\xi}dt\right) \qquad (3.74)$$

$$|\xi| < +\infty,$$

$$\theta(\xi) = \frac{1}{\pi}\int_{\xi_1}^{\xi_{N^*}} \frac{\ln q(t)}{t-\xi}dt \qquad (3.75)$$

where ξ_1 and ξ_N correspond to the points showed in Fig 3–11. We have

$$\theta(\xi) = \frac{1}{\pi}\int_{-1}^{1} \frac{\ln q(t)}{t-\xi}dt + H(\xi), \quad \text{for} \quad |\xi| < +\infty, \qquad (3.76)$$

where

$$H(\xi) = \frac{1}{2\pi}\left[\int_{-\infty}^{-1} \frac{\log \frac{y}{F^2}}{t-\xi}d\xi + \int_{1}^{\infty} \frac{\log \frac{y}{F^2}}{t-\xi}d\xi\right]. \qquad (3.77)$$

Similarly to equation (3.24), equation (3.76) reduces to

$$\theta(\xi) = \frac{1}{\pi}\int_{-1}^{1^*} \frac{\ln G(y) - \ln\cos(\theta_w+\gamma)}{t-\xi}dt + H(\xi), \quad \text{for} \quad |\xi| < +\infty. \qquad (3.78)$$

Based on this equation, a numerical iterative scheme , similar to the one developed in section 3.4.1, can also be obtained. However, it is rather complicated and consumes a lot of computing time.

For the purpose of seeking a more concise computing scheme, we consider the coupled equations (3.72) and (3.73), associated with (3.19), (3.30), (3.26) and its analogue

$$\frac{dy}{d\xi} = -\frac{2}{\pi}(\xi^2-1)^{-\frac{1}{2}} \exp\left\{-\frac{1}{\pi}\left(\int_{-\infty}^{-1} + \int_{1}^{\infty}\right)\frac{\theta(t)}{\xi-t}dt\right\}\sin\theta, \quad |\xi| > 1 \qquad (3.79)$$

which yields two expressions: For the upper free surface where $y(\xi_N) = 1$

$$y(\xi) = y(\xi_N) - \frac{2}{\pi}\int_{\xi}^{\xi_N} (\xi^2-1)^{-\frac{1}{2}} \exp\left\{-\frac{1}{\pi}\left(\int_{-\infty}^{-1} + \int_{1}^{\infty}\right)\frac{\theta(t)}{\xi-t}dt\right\}\sin\theta d\xi, \quad |\xi| > 1, \qquad (3.80)$$

while for the lower free surface where $y(\xi_1) = -1$

$$y(\xi) = y(\xi_1) - \frac{2}{\pi}\int_{\xi}^{\xi_1}(\xi^2-1)^{-\frac{1}{2}}\exp\left\{-\frac{1}{\pi}\left(\int_{-\infty}^{-1}+\int_{1}^{\infty}\right)\frac{\theta(t)}{\xi-t}dt\right\}\sin\theta d\xi, \quad |\xi|>1. \tag{3.81}$$

Using (3.75) in (3.80) and (3.81) gives

$$y(\xi) = 1 - \frac{2}{\pi}\int_{\xi}^{\xi_N}(\xi^2-1)^{-\frac{1}{2}}q^{-1}\exp\left\{\frac{1}{\pi}\int_{-1}^{1}\frac{\theta(t)}{\xi-t}dt\right\}\sin\theta d\xi, \quad |\xi|>1, \tag{3.82}$$

and

$$y(\xi) = -1 - \frac{2}{\pi}\int_{\xi}^{\xi_1}(\xi^2-1)^{-\frac{1}{2}}q^{-1}\exp\left\{\frac{1}{\pi}\int_{-1}^{1}\frac{\theta(t)}{\xi-t}dt\right\}\sin\theta d\xi, \quad |\xi|>1. \tag{3.83}$$

Substituting (3.82) and (3.83) into (3.72) and (3.73) yields equations for q and θ. Then we apply (3.75) and obtain an equation for q. However the two parameters ξ_1 and ξ_N are determined using

$$x(\xi_N) = -X, \qquad x(1) = 0; \tag{3.84}$$

$$x(\xi_1) = -X, \qquad x(-1) = 0, \tag{3.85}$$

Although we have not got any further numerical results for this extended formulation for a jet impacting on a porous wall including effects of gravity, it is ready for further exploration without any extra technique involved.

Chapter 4

An Ideal Fluid Jet Impinging on an Uneven Wall

4.1 Introduction

The problem of determining the free surface of a jet of two dimensional ideal fluid impinging on an uneven wall is considered. The classical problem of free streamline flow of an ideal fluid has been studied by many authors. Early work in this area is characterised by the use of the hodograph method and the Schwarz-Christoffel formula, which can deal with flows which have a polygon boundary geometry or whose hodograph plane is a polygon of simple shape. Surveys of the hodograph method applied to jet theory can be found in Birkhoff and Zarantonello [1957], Gurevich [1965] and Woods [1961]. The requirement of polygonal geometry shape limits the application of the method in practical problems. Woods [1961] gave some generalizations of the Schwarz-Christoffel formula which can be used to transform a half plane into a domain with boundary which combines a polygon and a smooth curve. By using the generalized formula, Dobroval [1969] derived a nonlinear singular integral equation for the water wedge entry problem, Bloor

[1978] obtained an integro-differential equation for studying the problem of large amplitude periodic water waves and, more recently, King and Bloor considered various flow problems such as free surface flows over a step [1987], free surface flows over an arbitrary bed topography, and the cusped free surface flows due to a submerged source [1990]. A general feature of their work in the cited papers is that the complex potential must be determined in the reference ζ-plane corresponding to the fluid domain. Some numerical solutions describing an ideal jet issuing from polygonal containers and free streamline problems can be found in the work of Dias, Ekrat and Trefethen [1987]. Fluid, under gravity, emerging from a two-dimensional nozzle at an angle is considered in the work of Dias and Vanden-Broeck [1990]. In the case of a jet of ideal fluid with other boundary conditions, Jenkins & Barton [1989], based on the Baiocchi transformation, gave a numerical treatment of the impact of a jet on a porous wall. King [1990] extended the classical hodograph method and reduced this problem to a first order differential equation.

A two-dimensional ideal jet impinging on an uneven wall is studied in this chapter. Motivation comes from the need to study an ideal jet impinging on hemispherical cups and to better understand the symmetric jet impinging on an uneven wall. After use of the Hilbert transform, the condition of constant speed on the free streamlines results in a relation between the flow angle on the free surface and the wall angle, when expressed in terms of the coordinate along the real axis of an appropriate reference plane. Then, by combining this with application of the generalized Schwarz-Christoffel transformation technique, a system of nonlinear integro-differential equations for the flow angles and the wall angles is formulated. For the case in which the wall geometry is symmetric, a compatibility condition for the system is automatically satisfied. Some numerical solutions to the resulting nonlinear system are presented, showing the shapes of the free surface corresponding to a number of different wall shapes.

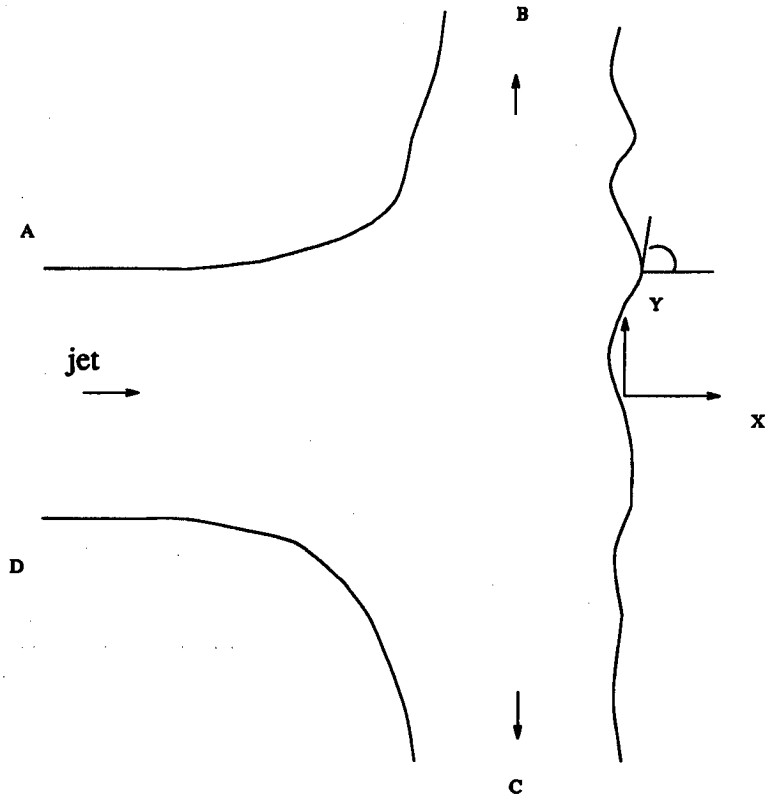

Figure 4–1: The free streamlines AB and CD bounding the jet impinging on an uneven wall

4.2 Mathematical Formulation

The two-dimensional steady irrotational flow of an incompressible inviscid fluid impinging upon an uneven wall is considered(see Fig.4.2). Cartesian coordinates are introduced with the X-axis along the centre line of the approaching jet. The complex variable $Z = X + iY$ is introduced.

Far away from the wall, the incident flow is required to be a uniform stream with constant speed U and thickness $2H$. Far away from the stagnation point upward and downward along the wall, the flow is also a uniform stream and thicknesses there are H_1 and H_2 respectively. By the conservation of mass, we

have $H_1 + H_2 = 2H$. A velocity potential denoted by Φ and a stream function denoted by Ψ are defined such that the complex potential

$$W = \Phi + i\Psi \tag{4.1}$$

is analytic in the domain occupied by the fluid. Bernoulli's equation is applied to both free surfaces on which pressure is constant, so that the fluid speed q takes the constant value U there. Meanwhile the stream function Ψ is chosen to have the value UH on the upper free surface, $-UH$ on the lower free surface, and takes the value $\Psi = \Psi_0$ on the dividing streamline and the wall. For symmetric flows $\Psi_0 = 0$. The complex velocity is defined as

$$V = u - iv = qe^{-i\theta} \tag{4.2}$$

where θ is the angle between the flow direction and the X-axis. The relation between the complex potential and the complex velocity is given by

$$\frac{dW}{dZ} = V. \tag{4.3}$$

This problem is now non-dimensionalized using the substitutions

$$z = x + iy = \frac{X + iY}{H}, \quad w = \phi + i\psi = \frac{\Phi + i\Psi}{UH}, \quad v = \frac{qe^{-i\theta}}{U} = \frac{V}{U} \tag{4.4}$$

and then writing $H_1 = Hh_1$, $H_2 = Hh_2$, so that $h_1 + h_2 = 2$, where $\psi = \pm 1$ on the upper and lower free surfaces, respectively.

We introduce the function ω as follows

$$\omega = \log v = \log \frac{q}{U} - i\theta. \tag{4.5}$$

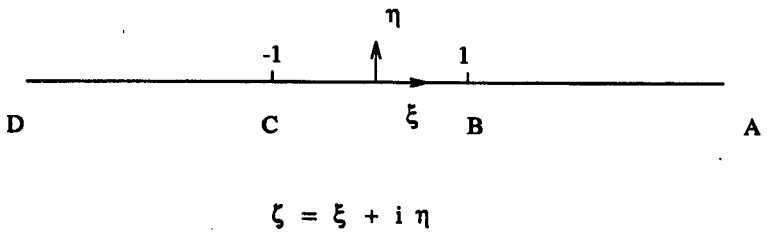

Figure 4–2: The images of A,B,C and D in the reference ζ-plane

4.3 Flow Angles

We seek a mapping of the flow region in the z-plane onto the upper half of a transform plane $\zeta = \xi + i\eta$ and then seek ω as a function of ζ there (see Figure 4–2).

Since ω is an analytic function of ζ, the values of q and θ on the axis $\eta = 0$ are related as Hilbert transforms, so giving

$$\frac{q(\xi)}{U} = \exp\left\{\frac{1}{\pi}\int_{-\infty}^{\infty *} \frac{\theta(t)}{\xi - t}dt\right\} \tag{4.6}$$

where $\int^*$ denotes a principal value integral. Since $q = U$ on the free surface, this gives

$$\frac{1}{\pi}\int_{-\infty}^{\infty *} \frac{\theta(t)}{\xi - t}dt = 0, \qquad 1 <\mid \xi \mid < \infty. \tag{4.7}$$

The above equation (4.7) can be written as

$$\frac{1}{\pi}\int_{-\infty}^{-1 *} \frac{\theta(t)}{\xi - t}dt + \frac{1}{\pi}\int_{1}^{\infty *} \frac{\theta(t)}{\xi - t}dt + \frac{1}{\pi}\int_{-1}^{1} \frac{\theta(t)}{\xi - t}dt = 0, \qquad 1 <\mid \xi \mid < \infty. \tag{4.8}$$

We now define the function $F(\xi)$ by

$$F(\xi) = \frac{1}{\pi}\int_{-1}^{1} \frac{\theta(t)}{\xi - t}dt, \qquad 1 <\mid \xi \mid < \infty, \tag{4.9}$$

so that equation (4.7) becomes

$$\frac{1}{\pi}\int_{-\infty}^{-1 *} \frac{\theta(t)}{\xi - t}dt + \frac{1}{\pi}\int_{1}^{\infty *} \frac{\theta(t)}{\xi - t}dt = -F(\xi), \qquad 1 <\mid \xi \mid < \infty. \tag{4.10}$$

Making the change of variables $t = r^{-1}$, $s = \xi^{-1}$ in (4.10) gives

$$\begin{aligned} -F(s^{-1}) &= \frac{1}{\pi}\int_{-1}^{0*} \frac{s\theta(r^{-1})r^{-1}}{r-s}dr + \frac{1}{\pi}\int_{0}^{1*} \frac{s\theta(r^{-1})r^{-1}}{r-s}dr \\ &= s\frac{1}{\pi}\int_{-1}^{1*} \frac{\theta(r^{-1})r^{-1}}{r-s}dr, \qquad 0 < |s| < 1. \end{aligned} \tag{4.11}$$

Similarly, substituting for ξ in (4.9) gives

$$F(\xi) = F(s^{-1}) = s\frac{1}{\pi}\int_{-1}^{1} \frac{\theta(t)}{1-st}dt = sg(s), \qquad 0 < |s| < 1, \tag{4.12}$$

where we have defined

$$g(s) = \frac{1}{\pi}\int_{-1}^{1} \frac{\theta(t)}{1-st}dt, \qquad 0 < |s| < 1. \tag{4.13}$$

Combining (4.11) and (4.12) then yields the so-called aerofoil equation

$$g(s) = \frac{1}{\pi}\int_{-1}^{1*} \frac{\phi(r)}{s-r}dr, \qquad 0 < |s| < 1, \tag{4.14}$$

which here relates $g(s)$ defined by (4.13) in terms of the flow angle on the wall to $\phi(r) \equiv r^{-1}\theta(r^{-1})$. In order to invert the integral equation (4.14), we first show in Appendix A that $g(s)$ defined by (4.13) is square integrable. Then (see Hochstadt[1973]) one obtains

$$\phi(s) = \frac{c}{\sqrt{1-s^2}} - \frac{1}{\pi}\int_{-1}^{1*} \sqrt{\frac{1-r^2}{1-s^2}}\frac{g(r)}{s-r}dr, \tag{4.15}$$

where c is a constant to be determined later. Moreover, there is an alternative representation

$$\phi(s) = -\frac{1}{\pi}\int_{-1}^{1*} \sqrt{\frac{1-s^2}{1-r^2}}\frac{g(r)}{s-r}dr \tag{4.16}$$

valid subject to the compatibility condition

$$\int_{-1}^{1} \frac{g(s)}{\sqrt{1-s^2}}ds = 0. \tag{4.17}$$

Reinterpreting (4.15) in terms of the free streamline angle $\theta(s^{-1}) = s\phi(s)$ gives

$$s^{-1}\theta(s^{-1})\sqrt{1-s^2} = c - \int_{-1}^{1*} \sqrt{1-r^2}\frac{g(r)}{s-r}dr. \tag{4.18}$$

Since θ remains finite as $s \longrightarrow \pm 1$, we obtain the two expressions

$$c = \int_{-1}^{1} \sqrt{1-r^2}\frac{g(r)}{1-r}dr = -\int_{-1}^{1} \sqrt{1-r^2}\frac{g(r)}{1+r}dr. \tag{4.19}$$

Thus we find that

$$0 = \int_{-1}^{1} \sqrt{1-r^2}\left(\frac{1}{1-r}+\frac{1}{1+r}\right)g(r)dr = 2\int_{-1}^{1}\frac{g(r)}{\sqrt{1-r^2}}dr. \tag{4.20}$$

Consequently, condition (4.17) is satisfied for all wall shapes. Equation (4.18) may be rewritten in terms of $\theta(t)$ ($|t| > 1$) as (see Appendix B)

$$\theta(t) = \pm\frac{1}{\pi}\frac{\sqrt{t^2-1}}{t}\left(\int_{-\infty}^{-1*} - \int_{1}^{\infty*}\right)\frac{1}{\sqrt{\xi^2-1}}\frac{\xi F(\xi)}{\xi - t}d\xi, \qquad |t| > 1, \tag{4.21}$$

where the positive sign applies for $t > 1$ and the negative sign for $t < -1$. Equation (4.21), combined with (4.9), gives a linear relation between the flow angle on the free surface and on the wall in a closed form, but specified in terms of the parameter ξ on the real axis of the ζ-plane.

4.4 Governing Equation

The geometry of the flow region together with the free surface and curved wall boundary is shown in Figure 4.2. The transformation of the flow region to the upper half of the ζ-plane is given by the generalized Schwarz-Christoffel formula

$$\frac{dz}{d\zeta} = -\frac{2}{\pi}\frac{\zeta - a}{\zeta^2 - 1}\exp\left(-\frac{1}{\pi}\int_{-\infty}^{\infty}\frac{\theta(t)}{\zeta - t}dt\right), \qquad \zeta = \xi + i\eta, \quad \eta \geq 0, \tag{4.22}$$

where $\theta(t)$ is the flow angle on either the free surface or the wall, the real value a defines the image in the ζ-plane of the stagnation point of the flow. The transformation outlined here for mapping a simply-connected domain D of general shape on to the upper half-plane, which plays the role of a reference or *canonical* domain,

is obtained from a generalization (see Woods [1961]) of the Schwarz-Christoffel mapping formula with adjustment to allow for the sense of the tangent direction along the boundary.

If the equation for the wall is $x = \kappa(y)$, then

$$\theta_w = \frac{\pi}{2} - \tan^{-1}\kappa'(y) \tag{4.23}$$

is the angle between the tangent to the wall and the x-axis. In equation (4.22), letting $\eta \to 0^+$, one obtains

$$\frac{dz}{d\xi} = -\frac{2}{\pi}\frac{\xi - a}{\xi^2 - 1}\exp\left(-\frac{1}{\pi}\int_{-\infty}^{\infty *}\frac{\theta(t)}{\xi - t}dt + i\theta(\xi)\right). \tag{4.24}$$

Then, integrating the imaginary part of this equation gives

$$y(t) = y(a) + \frac{2}{\pi}\int_a^t \frac{\xi - a}{1 - \xi^2}\exp\left(-\frac{1}{\pi}\int_{-\infty}^{\infty *}\frac{\theta(u)}{\xi - u}du\right)\sin\theta(\xi)d\xi, \qquad |\,t\,| < 1. \tag{4.25}$$

Inserting this into (4.23) relates θ to the parameter t by

$$\theta(t) = \frac{\pi}{2} - \tan^{-1}\kappa'\left(y(a) + \frac{2}{\pi}\int_a^t \frac{\xi - a}{1 - \xi^2}\exp\left(-\frac{1}{\pi}\int_{-\infty}^{\infty *}\frac{\theta(u)}{\xi - u}du\right)\sin\theta(\xi)d\xi\right), \qquad a < t < 1, \tag{4.26}$$

$$\theta(t) = -\frac{\pi}{2} - \tan^{-1}\kappa'\left(y(a) + \frac{2}{\pi}\int_t^a \frac{a - \xi}{1 - \xi^2}\exp\left(-\frac{1}{\pi}\int_{-\infty}^{\infty *}\frac{\theta(u)}{\xi - u}du\right)\sin\theta(\xi)d\xi\right), \qquad -1 < t < a, \tag{4.27}$$

since the flow angle $\theta(t)$ is related to the wall angle $\theta_w(t)$ by

$$\begin{cases} \theta(t) = \theta_w(t), & a < t < 1, \\ \theta(t) = \theta_w(t) - \pi, & -1 < t < a. \end{cases} \tag{4.28}$$

Equations (4.9), (4.21), (4.26) and (4.27) form a system of nonlinear integro-differential equations for this problem. If this system is solved for $\theta(t)$, $|t| < 1$,

then $F(\xi)$, $|\xi| > 1$, is given by (4.9) and $\theta(t)$ for $|t| > 1$ is obtained from equation (4.21). The mapping from the ζ-plane to the physical plane is given by (4.22). The shape of the free surface is determined by (4.24), which, in view of condition (4.7), reduces to

$$\frac{dz}{d\xi} = -\frac{2}{\pi}\frac{\xi - a}{\xi^2 - 1}\exp\left(i\theta(\xi)\right), \qquad 1 < |\xi| < \infty. \tag{4.29}$$

It is unlikely that this system of equations can be solved analytically except for special cases of $\kappa(y)$. In the following section we will discuss them.

4.5 Special Cases

4.5.1 Classic wall shapes

i) Whenever $\theta(t)$ satisfies $\theta(-t) = \theta(t) - \pi$, $0 < t < 1$, the function $F(\xi)$ defined in equation (4.9) can be reduced to

$$F(\xi) = \frac{2\xi}{\pi}\int_0^1 \frac{\theta(t)}{\xi^2 - t^2}dt + \log\frac{\xi}{\xi + 1}, \qquad 1 <| \xi |< \infty, \tag{4.30}$$

which in the simpler case $\theta(t) = \alpha$, $0 < t < 1$, gives

$$F(\xi) = \frac{\alpha}{\pi}\log\frac{\xi - a}{\xi - 1} + \left(\frac{\alpha}{\pi} - 1\right)\log\frac{\xi + 1}{\xi - a} \qquad 1 <| \xi |< \infty. \tag{4.31}$$

This corresponds to a jet impinging on an inclined wall at angle α.

ii) In the symmetric case for which $\theta(t)$ satisfies with $\theta(t) = -\theta(-t)$, $0 < t < 1$, the function $\kappa(y)$ is odd while $F(\xi)$ is even, so it is sufficient to consider only the upper half $t > 1$ of the free surface. Then equation (4.9) can be written as

$$F(\xi) = \frac{2}{\pi}\int_0^1 \frac{t\theta(t)}{\xi^2 - t^2}dt, \qquad 1 <| \xi |< \infty, \tag{4.32}$$

which, for the simplest case $\theta(t) = \alpha$, $0 < t < 1$, describing an ideal jet impinging symmetrically on an infinite wedge having angle 2α, yields

$$F(\xi) = \frac{\alpha}{\pi}\log\frac{\xi^2}{\xi^2 - 1}. \tag{4.33}$$

iii) A special example of both i) and ii) is $\theta(t) = \alpha = \pi/2$, $0 < t < 1$, which corresponds to an ideal jet impinging normally on a infinite wall. This gives

$$F(\xi) = \frac{1}{2}\log\frac{\xi^2}{\xi^2 - 1}. \tag{4.34}$$

In all the above cases leading to (4.31), (4.33) and (4.34), we need not solve the system of integral equations. As the flow angle on the wall is known and $F(\xi)$ is given explicitly, the flow angle on the free streamline is determined directly from (4.21) and then the free streamline shape is computed from (4.29).

iv) More generally, for symmetric flows leading to (4.32) it is natural to choose $y(a) = 0$, while $\theta(t) = \theta_w(t)$ on $0 < t < 1$. Then, equation (4.26) becomes

$$\theta(t) = \frac{\pi}{2} - \tan^{-1}\kappa'\left(\frac{2}{\pi}\int_0^t \frac{\xi}{1-\xi^2}P(\xi)\sin\theta(\xi)d\xi\right) \qquad 0 < t < 1, \tag{4.35}$$

where $P(\xi)$ is defined as

$$P(\xi) = \exp\left(-\frac{2}{\pi}\int_0^{\infty *}\frac{u\theta(u)}{\xi^2 - u^2}du\right), \qquad 0 < \xi < t. \tag{4.36}$$

Taking the real part and the imaginary part of equation (4.29) gives

$$x(\xi) = x(\xi_0) - \frac{2}{\pi}\int_{\xi_0}^{\xi}\frac{\xi}{\xi^2 - 1}\cos\theta(\xi)d\xi, \tag{4.37}$$

$$y(\xi) = y(\xi_0) + \frac{2}{\pi}\int_{\xi}^{\xi_0}\frac{\xi}{\xi^2 - 1}\sin\theta(\xi)d\xi \tag{4.38}$$

for $\xi > 1$, which describe the shape of the streamline forming the upper portion of the free surface.

For numerical computation, it is preferable to rewrite (4.21) as (see Appendix B)

$$\theta(t) = \frac{\left(t^2-1\right)^{\frac{1}{2}}}{\pi}\int_1^{\infty *}\frac{F(\xi)}{(t^2-\xi^2)}\frac{2\xi d\xi}{(\xi^2-1)^{\frac{1}{2}}}, \qquad t > 1, \tag{4.39}$$

and to apply the transformations

$$t^2 - 1 = e^{2u}, \quad \xi^2 - 1 = e^{2v} \tag{4.40}$$

where $-\infty < u, v < \infty$ for $1 < t, \xi < \infty$. Then, equation (5.39) is reduced to

$$\begin{aligned}
\theta\left[\left(1+e^{2u}\right)^{\frac{1}{2}}\right] &= \frac{e^u}{\pi}\int_{-\infty}^{\infty *}\frac{2}{e^{2u}-e^{2v}}F\left[\left(1+e^{2v}\right)^{\frac{1}{2}}\right]e^v dv \\
&= \frac{1}{\pi}\int_{-\infty}^{\infty *}\frac{2F\left[\left(1+e^{2v}\right)^{\frac{1}{2}}\right]}{e^{u-v}-e^{v-u}}dv \\
&= \frac{1}{\pi}\int_{-\infty}^{\infty *}\frac{F\left[\left(1+e^{2v}\right)^{\frac{1}{2}}\right]dv}{\sinh(u-v)}, \qquad -\infty < u < \infty, \quad (4.41)
\end{aligned}$$

while equations (4.37) and (4.38) become

$$x(u) = x(u_0) - \frac{1}{\pi}\int_{u_0}^{u}\cos\theta\left(\left(1+e^{2u}\right)^{\frac{1}{2}}\right)du, \quad (4.42)$$

$$y(u) = y(u_0) + \frac{1}{\pi}\int_{u_0}^{u}\sin\theta\left(\left(1+e^{2u}\right)^{\frac{1}{2}}\right)du. \quad (4.43)$$

In the following subsection we use the above formulae to find an analytic solution for a special case. The agreement of this result with an existing result confirms the mathematical formulation of this Chapter.

4.5.2 A limit case of problem

In this section we derive the analytic solution for a jet impinging normally on a flat wall so as to provide a check for the numerical solution of the strategies outlined above.

The function $F(\xi)$ of (4.34) is obtained after applying transformation (4.40) as

$$F(\xi) = \frac{1}{2}\log\frac{\xi^2}{\xi^2-1} = \frac{1}{2}\log\frac{1+e^{2v}}{e^{2v}} = \frac{1}{2}\log(1+e^{-2v}). \quad (4.44)$$

Substituting (4.44) into (4.41) yields

$$\theta\left[\left(1+e^{2u}\right)^{\frac{1}{2}}\right] = \frac{1}{\pi}\int_{-\infty}^{\infty *}\frac{\frac{1}{2}\log\left(1+e^{-2v}\right)dv}{\sinh(u-v)}, \qquad -\infty < u < \infty. \quad (4.45)$$

To evaluate the improper integral (4.45), we examine

$$\frac{1}{2}\log(1+e^{-2z}) \quad (4.46)$$

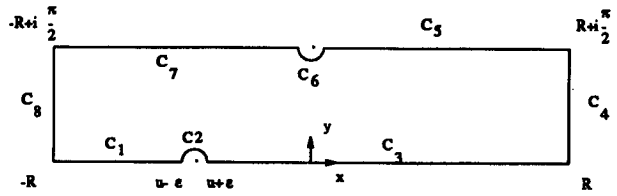

Figure 4–3: The path of integration of c

which is a multivalued function along some lines such as $z = x + i\frac{\pi}{2}$, $x < 0$ with

$$\log(1+e^{-2(x+i\frac{\pi}{2})}) = \begin{cases} \log(1-e^{-2x}), & x > 0 \\ \log(e^{-2x}-1)+i\pi, & x < 0, y = i\frac{\pi}{2}^+ \\ \log(e^{-2x}-1)-i\pi, & x < 0, y = i\frac{\pi}{2}^- \end{cases} \tag{4.47}$$

where "+" and "−" indicate values above the line and below the line respectively. We consider

$$\frac{1}{\pi}\int_c \frac{\frac{1}{2}\log\left(1+e^{-2z}\right)dz}{\sinh(u-z)}, \qquad -\infty < u < \infty, \tag{4.48}$$

where the path of integration c is chosen as shown in Figure 4.5.2

$$c = \begin{cases} c_1, & -R < z < u-\epsilon \\ c_2, & z = u+\epsilon e^{i\alpha}, 0 < \alpha < \pi \\ c_3, & u+\epsilon < z < R \\ c_4, & z = R+i\alpha, 0 < \alpha < \frac{\pi}{2} \\ c_5, & z = x+i\frac{\pi}{2}, \epsilon < x < R \\ c_6, & z = i\frac{\pi}{2}+e^{i\alpha}, 0 > \alpha > -\pi \\ c_7, & z = x+i\frac{\pi}{2}^-, -R < x < -\epsilon \\ c_8, & z = -R+i\alpha, 0 < \alpha < \frac{\pi}{2} \end{cases} \tag{4.49}$$

The integration can be split into eight parts as

$$\begin{aligned} &\frac{1}{\pi}\int_c \frac{\frac{1}{2}\log\left(1+e^{-2z}\right)dz}{\sinh(u-z)} \\ &= \frac{1}{2\pi}\left\{\int_{c_1}+\int_{c_2}+\int_{c_3}+\int_{c_4}+\int_{c_5}+\int_{c_6}+\int_{c_7}+\int_{c_8}\frac{\log\left(1+e^{-2z}\right)dz}{\sinh(u-z)}\right\} \end{aligned} \tag{4.50}$$

which are calculated individually as

$$I_1 = \int_{c_1} \frac{\log\left(1+e^{-2z}\right)dz}{\sinh(u-z)} = \int_{-R}^{u-\epsilon} \frac{\log\left(1+e^{-2x}\right)dx}{\sinh(u-x)} \tag{4.51}$$

$$I_2 = \int_{c_2} \frac{\log\left(1+e^{-2z}\right)dz}{\sinh(u-z)} = \int_{\pi}^{0} \frac{\log\left(1+e^{-2(u+\epsilon e^{i\alpha})}\right)}{\sinh(-\epsilon e^{i\alpha})} i\epsilon e^{i\alpha} d\alpha$$

$$\to i\pi \log(1+e^{-2u}) \quad \text{as } \epsilon \to 0 \tag{4.52}$$

$$I_3 = \int_{u+\epsilon}^{R} \frac{\log\left(1+e^{-2x}\right)dx}{\sinh(u-x)} \tag{4.53}$$

$$I_4 = \int_{R}^{R+i\frac{\pi}{2}} \frac{\log\left(1+e^{-2z}\right)dz}{\sinh(u-z)} \to 0 \quad \text{as } R \to \infty \tag{4.54}$$

$$I_5 = \int_{R}^{\epsilon} \frac{\log\left(1+e^{-2(x+i\frac{\pi}{2})}\right)dx}{\sinh\left(u-(x+i\frac{\pi}{2})\right)}$$

$$= \int_{R}^{\epsilon} \frac{\log\left(1-e^{-2x}\right)dx}{-i\cosh(u-x)} = -i\int_{\epsilon}^{R} \frac{\frac{1}{2}\log\left(1-e^{-2x}\right)dx}{\cosh(u-x)} \tag{4.55}$$

$$I_6 = \int_{c_6} \frac{\log\left(1+e^{-2z}\right)dz}{\sinh(u-z)} = \int_{-\pi}^{0} \frac{\log\left(1+e^{-2(i\frac{\pi}{2}+\epsilon e^{i\alpha})}\right)}{\sinh\left(u-i\frac{\pi}{2}-\epsilon e^{i\alpha}\right)} i\epsilon e^{i\alpha} d\alpha$$

$$= O(\epsilon \log \epsilon) \to 0 \quad \text{as } \epsilon \to 0 \tag{4.56}$$

$$I_7 = \int_{-\epsilon}^{-R} \frac{\log\left(e^{-2x}-1\right)-i\pi}{-i\cosh(u-x)} dx$$

$$= i\int_{-\epsilon}^{-R} \frac{\log\left(e^{-2x}-1\right)}{\cosh(u-x)} dx + \int_{-\epsilon}^{-R} \frac{\pi}{\cosh(u-x)} dx \tag{4.57}$$

$$I_8 = \int_{-R+\frac{\pi}{2}}^{-R} \frac{\log\left(1+e^{-2z}\right)}{\sinh(u-z)} dz \to 0 \quad \text{as } R \to \infty. \tag{4.58}$$

The residue of the integral (4.48) is zero, i.e.,

$$I = \frac{1}{\pi}\int_{c} \frac{\frac{1}{2}\log\left(1+e^{-2z}\right)dz}{\sinh(u-z)} = 0 \tag{4.59}$$

giving

$$I = \int_{-R}^{u-\epsilon} \frac{\log\left(1+e^{-2x}\right)dx}{\sinh(u-x)} + \int_{\pi}^{0} \frac{\log\left(1+e^{-2(u+\epsilon e^{i\alpha})}\right)}{\sinh(-\epsilon e^{i\alpha})} i\epsilon e^{i\alpha} d\alpha$$
$$+ \int_{u+\epsilon}^{R} \frac{\log\left(1+e^{-2x}\right)dx}{\sinh(u-x)} + \int_{R}^{R+i\frac{\pi}{2}} \frac{\log\left(1+e^{-2z}\right)dz}{\sinh(u-z)}$$

$$+O(\epsilon\log\epsilon)-i\int_{\epsilon}^{R}\frac{\frac{1}{2}\log\left(1-e^{-2x}\right)dx}{\cosh(u-x)}+i\int_{-\epsilon}^{-R}\frac{\log\left(e^{-2x}-1\right)}{\cosh(u-x)}dx$$
$$+\int_{-\epsilon}^{-R}\frac{\pi}{\cosh(u-x)}dx+\int_{-R+\frac{\pi}{2}}^{-R}\frac{\log\left(1+e^{-2z}\right)}{\sinh(u-z)}dz=0. \tag{4.60}$$

Letting $\epsilon\to 0$ and $R\to\infty$ and taking real parts of (4.51) yields

$$\int_{-\infty}^{\infty}\frac{\log\left(1+e^{-2x}\right)}{\sinh(u-x)}dx+\int_{0}^{-\infty}\frac{\pi}{\cosh(u-x)}dx=0. \tag{4.61}$$

We then obtain

$$\begin{aligned}&\int_{-\infty}^{\infty}\frac{\log\left(1+e^{-2x}\right)}{\sinh(u-x)}dx=\pi\int_{0}^{\infty}\frac{1}{\cosh(u-x)}dx\\&=\pi\lim_{R\to\infty}\int_{0}^{R}\frac{2de^{u+x}}{1+e^{2(u+x)}}=2\pi\int_{e^{u}}^{e^{R+u}}\frac{dv}{1+v^{2}}\\&=2\pi\lim_{R\to\infty}\left(\tan^{-1}e^{R+u}-\tan^{-1}e^{u}\right)=2\pi\left(\frac{\pi}{2}-\tan^{-1}e^{u}\right).\end{aligned} \tag{4.62}$$

Therefore equations(4.45) and (4.62) give

$$\theta\left((1+e^{2u})^{\frac{1}{2}}\right)=\frac{\pi}{2}-\tan^{-1}e^{u}. \tag{4.63}$$

We can see that

$$\begin{cases}\theta\left((1+e^{2u})^{\frac{1}{2}}\right)\to\theta(1)=\frac{\pi}{2}, & \text{as } \xi\to 1,\quad u\to-\infty,\\ \theta\left((1+e^{2u})^{\frac{1}{2}}\right)\to\theta(\infty)=0, & \text{as } \xi\to\infty,\quad u\to\infty\end{cases} \tag{4.64}$$

which satisfies the asymptotic conditions at infinity.

The shape of the free surface is checked using (4.42) and (4.43)

$$\begin{aligned}x(u) &= x(u_0)-\frac{2}{\pi}\int_{u_0}^{u}\cos\theta\left(\left(1+e^{2u}\right)^{\frac{1}{2}}\right)du\\&=-1-\frac{2}{\pi}\int_{-\infty}^{u}\cos\left(\frac{\pi}{2}-\tan^{-1}e^{u}\right)du\\&=-1-\frac{2}{\pi}\int_{-\infty}^{u}\sin\left(\tan^{-1}e^{u}\right)du\\&=-1-\frac{2}{\pi}\int_{0}^{\tan^{-1}e^{u}}\frac{\sin t}{\tan t\cos^{2}t}dt\\&=-1-\frac{2}{\pi}\int_{0}^{\tan^{-1}e^{u}}\frac{dt}{\cos t}=-1-\frac{2}{\pi}\log\tan\left(\frac{\pi}{4}+\frac{t}{2}\right)\Big|_{0}^{\tan^{-1}e^{u}}\end{aligned}$$

$$
\begin{aligned}
&= -1 - \frac{2}{\pi}\log\tan\left(\frac{\pi}{4} + \frac{\tan^{-1}e^{u}}{2}\right) \\
&= -1 + \frac{2}{\pi}\log\cot\left(\frac{\pi}{4} + \frac{\tan^{-1}e^{u}}{2}\right) \\
&= -1 + \frac{2}{\pi}\log\tan\left(\frac{\pi}{4} - \frac{\tan^{-1}e^{u}}{2}\right) \qquad (4.65)
\end{aligned}
$$

$$
\begin{aligned}
y(u) &= y(u_1) - \frac{2}{\pi}\int_{u_1}^{u} \sin\theta\left(\left(1+e^{2u}\right)^{\frac{1}{2}}\right) du \\
&= 1 - \frac{2}{\pi}\int_{+\infty}^{u} \sin\theta\left(\left(1+e^{2u}\right)^{\frac{1}{2}}\right) du \\
&= 1 - \frac{2}{\pi}\int_{+\infty}^{u} \cos\left(\tan^{-1}e^{u}\right) du \\
&= 1 - \frac{2}{\pi}\int_{\frac{\pi}{2}}^{\tan^{-1}e^{u}} \frac{\cos t}{\tan t\cos^2 t} dt \\
&= 1 - \frac{2}{\pi}\int_{\frac{\pi}{2}}^{\tan^{-1}e^{u}} \frac{dt}{\sin t} = 1 - \frac{2}{\pi}\log\tan\frac{t}{2}\Big|_{\frac{\pi}{2}}^{\tan^{-1}e^{u}} \\
&= 1 - \frac{2}{\pi}\log\tan\frac{\tan^{-1}e^{u}}{2}. \qquad (4.66)
\end{aligned}
$$

Treating the (x, y) coordinates as the functions of θ, using (4.63) in (4.65) and (4.66), yields

$$x(\theta) = -1 + \frac{2}{\pi}\log\tan\frac{\theta}{2}, \qquad (4.67)$$

$$y(\theta) = 1 - \frac{2}{\pi}\log\tan\left(\frac{\pi}{4} - \frac{\theta}{2}\right). \qquad (4.68)$$

These are exactly the form of parametric representation of the shapes given by Milne-Thomson [1968] for a jet impinging normally on a flat plate. This special case of the problems being considered forms a check on the numerical solution procedure given in a later section. In the case that an ideal jet impinges on an infinite wedge with angle 2α, we also have

$$\theta\left(\left(1+e^{2u}\right)^{\frac{1}{2}}\right) = \alpha\left(1 - \frac{2}{\pi}\tan^{-1}e^{u}\right). \qquad (4.69)$$

Therefore if the values $x(u_0)$ and $y(u_1)$ are specified, the analytic solution can also be found by procedures similar to those leading to (4.67) and (4.68).

Moreover, for the case of a jet impinging on an inclined wall at angle α, the parameter a can be given as

$$a = \sin\alpha. \tag{4.70}$$

The equation (4.21), combined with (4.31)and (4.70), gives the flow angle on the free surface in an integral form, which is

$$\begin{aligned}
\theta(t) &= \pm\frac{1}{\pi}\frac{\sqrt{t^2-1}}{t}\left(\int_{-\infty}^{-1*} - \int_1^{\infty*}\right)\frac{1}{\sqrt{\xi^2-1}}\frac{\xi F(\xi)}{\xi - t}d\xi \\
&= \pm\frac{1}{\pi}\frac{\sqrt{t^2-1}}{t}\int_1^{\infty*}\frac{\xi}{\sqrt{\xi^2-1}}\left(\frac{F(\xi)}{t-\xi} + \frac{F(-\xi)}{t+\xi}\right)d\xi \\
&= \pm\frac{1}{\pi}\frac{\sqrt{t^2-1}}{t}\int_1^{\infty*}\frac{\xi}{\sqrt{\xi^2-1}}\left(\frac{\frac{\alpha}{\pi}\log\frac{\xi-a}{\xi-1} + \left(\frac{\alpha}{\pi}-1\right)\log\frac{\xi+1}{\xi-a}}{t-\xi}\right. \\
&\qquad \left. + \frac{\frac{\alpha}{\pi}\log\frac{\xi+a}{\xi+1} + \left(\frac{\alpha}{\pi}-1\right)\log\frac{\xi-1}{\xi+a}}{t+\xi}\right)d\xi
\end{aligned} \tag{4.71}$$

where the positive sign applies for $t > 1$ and the negative sign for $t < -1$, corresponding to the upper free surface and the lower free surface respectively.

4.6 Numerical Solutions

Numerical solutions to the nonlinear problem are given in this section, only in the symmetric case. The integral in (4.32) is discretized by the trapezoidal rule, having step length δ, with error $O(\delta^2)$, where the mesh points are introduced as

$$t_k = k\delta, \quad \theta_k = \theta(k\delta), \quad \xi_j > 1, \quad k = 0, 1, .., N, \tag{4.72}$$

with $N\delta = 1$, so giving

$$F_j = F(\xi_j) \doteq \frac{2\delta}{\pi}\sum_{k=0}^{N} w_k \frac{t_k\theta_k}{\xi_j^2 - t_k^2}, \qquad \xi_j > 1, \tag{4.73}$$

where w_k are chosen as the weights appropriate to the trapezoidal rule. The integral in (4.41) is complicated by the singularities at the point $u_j = v_j$ and by

the infinite range of integration in the integral. The infinite range is accommodated by considering, for u in some interval $-l < u < m$, the division of (4.41) as

$$\theta\left[(1+e^u)^{\frac{1}{2}}\right] = \frac{e^{\frac{u}{2}}}{\pi}\left(\int_{-\infty}^{-B}\frac{1}{e^u-e^v}F\left[(1+e^v)^{\frac{1}{2}}\right]e^{\frac{v}{2}}dv + \int_{-B}^{A}\frac{1}{e^u-e^v}F\left[(1+e^v)^{\frac{1}{2}}\right]e^{\frac{v}{2}}dv + \int_{A}^{\infty}\frac{1}{e^u-e^v}F\left[(1+e^v)^{\frac{1}{2}}\right]e^{\frac{v}{2}}dv\right), \qquad -l<u<m, \tag{4.74}$$

with A and B, for instance, as $3m$ and $3l$, respectively. For $\xi^2 = e^v + 1$, $v > 2M$, the function $F(\xi)$ has behaviour

$$\begin{aligned} F(\xi) &= \frac{2}{\pi}\int_0^1 \frac{t\theta(t)}{\xi^2-t^2}dt \\ &= \frac{2}{\pi\xi^2}\int_0^1 t\theta(t)\left[1+\frac{t^2}{\xi^2}+\cdots\right]dt \\ &= C\xi^{-2}+O(\xi^{-4}) \end{aligned} \tag{4.75}$$

where

$$C = \frac{2}{\pi}\int_0^1 t\theta(t)dt. \tag{4.76}$$

Substituting equation (4.75) into the last integral in equation (4.74) gives

$$\begin{aligned} \int_A^\infty \frac{1}{e^u-e^v}F\left[(1+e^v)^{\frac{1}{2}}\right]e^{\frac{v}{2}}dv &\simeq C\int_A^\infty \frac{e^{\frac{v}{2}}dv}{(e^u-e^v)(1+e^v)} \\ &= C\int_A^\infty \frac{1}{1+e^u}\left(\frac{1}{1+e^v}+\frac{1}{e^u-e^v}\right)e^{\frac{v}{2}}dv \\ &\le C\frac{1+e^{\frac{u}{2}}}{1+e^u}e^{-\frac{A}{2}}. \end{aligned} \tag{4.77}$$

A similar treatment applied to the first integrals in (4.74) gives

$$\int_{-\infty}^{-B}\frac{1}{e^u-e^v}F\left[(1+e^v)^{\frac{1}{2}}\right]e^{\frac{v}{2}}dv \le C\frac{e^{-\frac{B}{2}}\left(2+e^{-\frac{u}{2}}\right)}{1+e^u}. \tag{4.78}$$

Thus, it is readily shown that the sum of the first and the last integrals in (4.74) has bound

$$\begin{aligned} &\frac{e^{\frac{u}{2}}}{\pi}\left(\int_{-\infty}^{-B}\frac{1}{e^u-e^v}F\left[(1+e^v)^{\frac{1}{2}}\right]e^{\frac{v}{2}}dv + \int_A^\infty \frac{1}{e^u-e^v}F\left[(1+e^v)^{\frac{1}{2}}\right]e^{\frac{v}{2}}dv\right) \\ &\simeq \frac{e^{\frac{u}{2}}}{\pi}\left(C\frac{1+e^{\frac{u}{2}}}{1+e^u}e^{-\frac{A}{2}}+C\frac{2+e^{-\frac{u}{2}}}{1+e^u}e^{-\frac{B}{2}}\right) \\ &\le \frac{2C}{\pi}\left(e^{-\frac{A}{2}}+e^{-\frac{B}{2}}\right), \end{aligned} \tag{4.79}$$

so giving

$$\theta\left[(1+e^{u})^{\frac{1}{2}}\right]=\frac{e^{\frac{u}{2}}}{\pi}\int_{-B}^{A}\frac{1}{e^{u}-e^{v}}F\left[(1+e^{v})^{\frac{1}{2}}\right]e^{\frac{v}{2}}dv+O\left(e^{-\frac{A}{2}}+e^{-\frac{B}{2}}\right). \quad (4.80)$$

Then, we truncate the infinite range to $[-B,A]$ which is then divided into three subranges $[-B,u_{j-1}]$, $[u_{j-1},u_{j+1}]$ and $[u_{j+1},A]$. The integrand in (4.80) is regular and can be dealt with by the trapezoidal rule, except in $[u_{j-1},u_{j+1}]$ where it is approximated by using the Taylor expansion around the point u_j. This yields

$$\begin{aligned}\Theta(u_j) \;\equiv\; & \theta\left[(1+e^{u_j})^{\frac{1}{2}}\right]\doteq\frac{e^{\frac{u_j}{2}}}{\pi}\left(\sum_{i=j+1}^{A}\frac{W_i\Delta}{e^{u_j}-e^{v_i}}F\left[(1+e^{v_j})^{\frac{1}{2}}\right]e^{\frac{v_j}{2}}\right.\\ &+\sum_{i=-B}^{j-1}\frac{W_i\Delta}{e^{u_j}-e^{v_i}}F\left[(1+e^{v_j})^{\frac{1}{2}}\right]e^{\frac{v_j}{2}}\\ &+\left.\left(-\frac{\Delta}{2}+\log\frac{1+e^{\frac{\Delta}{2}}}{1+e^{-\frac{\Delta}{2}}}\right)F\left[(1+e^{u_j})^{\frac{1}{2}}\right]+\Delta\frac{F_j'e^{u_j}}{(1+e^{u_j})^{\frac{1}{2}}}\right)\end{aligned} \quad (4.81)$$

where Δ is the step length, $u_j=j\Delta$ for $j=-L,...,M$ with $-L\Delta=-l$, $M\Delta=m$ and W_i are the weights appropriate to the trapezoidal rule used for (4.80). The function F_j' is the derivative of F_j and can be calculated from (4.32). The integral in equation (4.35) can also be dealt with by the same trapezoidal rule as used in (4.32) so giving

$$\theta_k\doteq\frac{\pi}{2}-\tan^{-1}\kappa'\left(-\frac{2\delta}{\pi}\sum_{n=1}^{k}\frac{\tau_n}{\tau_n^2-1}P_n\sin(\theta_n)\right),\quad k=0,1,...,N \quad (4.82)$$

where θ_k and θ_l are defined in (4.81), $\tau_n=n\delta$, for $n=0,1,...,k$. The quantities P_l are the discretized forms of the function $P(\xi)$, with the singularities at points $\xi=t$, $0<t<1$, treated by the same method as used in dealing with the integral in (4.80). This gives

$$P_n=P(\tau_n)\doteq\exp\left(-\frac{2}{\pi}\left[\delta\sum_{k=1,k\neq n}^{N}\frac{t_k\theta_k}{\tau_n^2-t_k^2}-\theta_n'+\Delta\sum_{j=-N1}^{M}\frac{\xi_j\Theta(\xi_j)}{\xi_j^2-t_k^2}\right]\right), \quad (4.83)$$

where $\tau_n = n\delta$ and θ_k is given in (4.81). Moreover θ' is the first derivative of θ and can be calculated by a central difference approximation with error $O(\delta^2)$ while Θ is given by (4.81). Equations (4.42) and (4.43), discretized by a trapezoidal rule, give

$$x(\xi_i) = x(1) - \frac{\Delta}{\pi} \sum_{j=-L}^{i} \cos\Theta(u_j), \tag{4.84}$$

$$y(\xi_i) = y(\infty) + \frac{\Delta}{\pi} \sum_{j=i}^{M} \sin\Theta(u_j) \tag{4.85}$$

for $i = -L, ..., M$. Thus we obtain $N+1$ nonlinear algebraic equations for $N+1$ unknowns from (4.82), combined with equations (4.80), (4.81) and (4.82). This system of equations was solved by using a hybrid Powell method from the NAG library. Equations (4.84) and (4.85) were computed to find the free streamline. In Figure 4–4, we give a comparison with the analytic solution in the case of a jet impinging normally on a flat wall. The free surface shape plotted as a dotted line obtained by using (4.35), (4.41), (4.43) and (4.44) shows good agreement with the analytic result [Milne-Thomson, 1968] shown here by the solid line. In the case of an uneven wall, we chose functions $x = e^{-y^2}$, $x = -e^{-y^2}$ and $x = -\text{sech}\ y$. The step lengths chosen were $\delta = 0.05$, $\Delta = 0.04$ and the computations were performed with $L = 100$, $M = 250$, $A = 3M$ and $B = 3L$ in each case. The resulting free-streamline profiles are shown in Figures 4–5, 4–6 and 4–7.

4.7 Conclusions

In this study, we have investigated the free streamline problem for a jet impinging on various walls. A relation between the flow angle on the free surface and the flow angle on the wall is given. In some special cases, this may be reduced to a simple integral expression. Based on the relation (4.21), a system of equations is formulated which allows for very general boundary shapes. In the special case

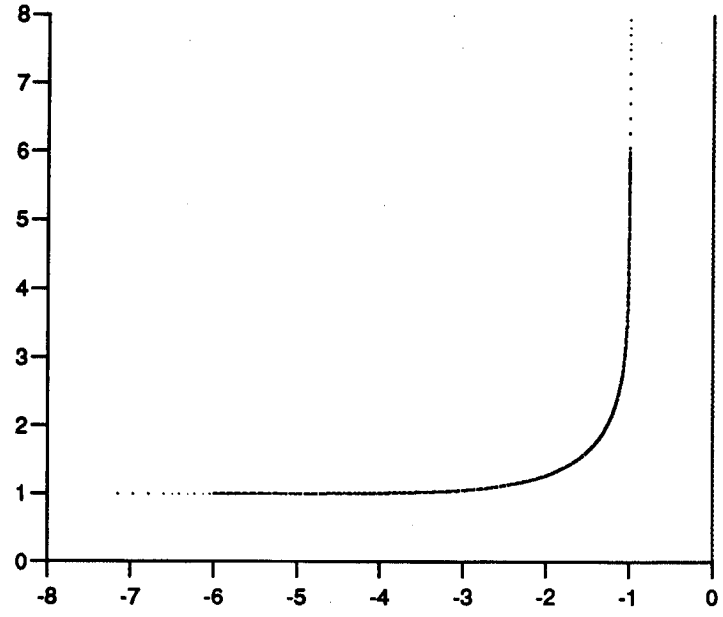

Figure 4–4: One half of a symmetric jet impinging normally on a flat wall $x = 0$ where $(\cdots)$ line represents the analytic result and the (—) line represents the numerical solution.

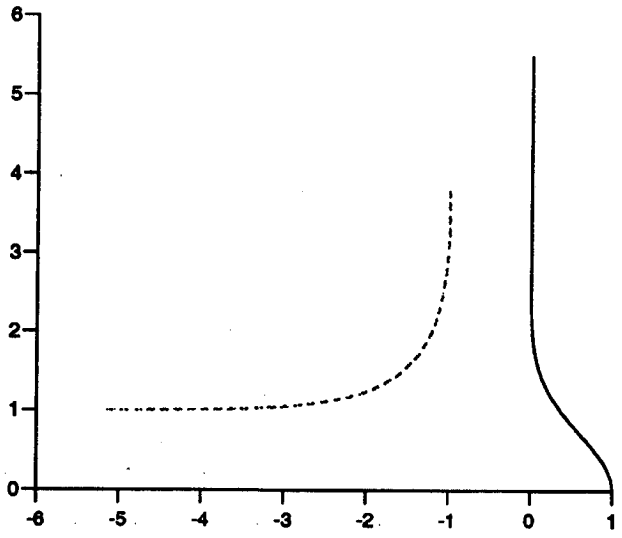

Figure 4–5: A jet of upstream thickness 2 impinging symmetrically on an uneven wall given by $x = e^{-y^2}$

of a jet impinging normally on a plane wall, the analytic solution, a standard analytic formula Milne-Thomson[1968], was rederived. Its utility is tested by comparing numerical computation for a jet impinging normally on a plane wall with those from a standard analytic formula, showing good numerical agreement. Calculations for symmetric jets hitting specific curved walls are shown. Further work to be undertaken will deal with walls in the form of blunted wedges and for boundary conditions corresponding to porous walls. The formulation allows more freedom than that used by King [1990], since it does not use special properties of the hodograph plane.

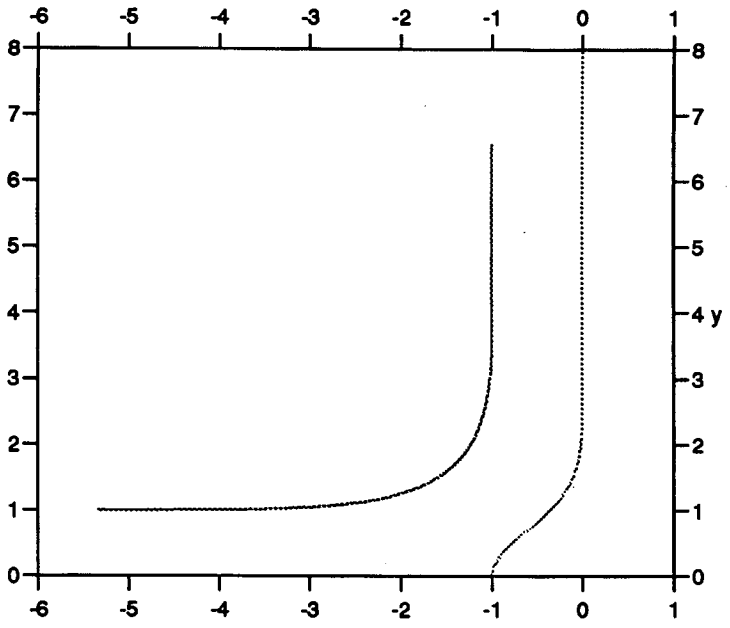

Figure 4–6: Flow impinging on symmetrically an uneven wall given by $x = -e^{-y^2}$

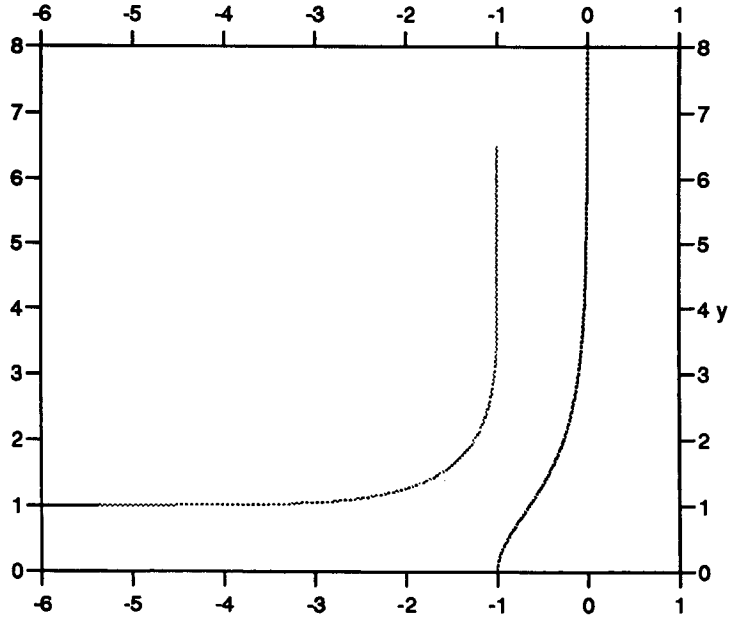

Figure 4–7: Flow impinging symmetrically on an uneven wall given by $x = -\text{sech}y$

Chapter 5

The Impact of a Jet Incident on an Asymmetric Uneven Wall

5.1 Introduction

In this chapter we consider further an ideal jet impinging on an uneven wall in an asymmetric case. The unknown position of the stagnation point introduces much difficulty for computing the free surface shapes. Using the integral form of the momentum equation, we obtain an integral relation between a point in the $\zeta-$plane, which corresponds to the position of the stagnation point in the physical plane, and the flow speed and shape of the wall. The z-plane, the physical plane (see Fig. 5–1), is redefined by

$$z = x + iy = \frac{\pi(X + iY)}{H} \tag{5.1}$$

where H is the width of the incoming jet at $X = -\infty$. The complex potential plane, the w-plane (see Fig. 5–2), is considered as

$$w = \phi + i\psi = \frac{\pi}{UH}(\Phi + i\Psi). \tag{5.2}$$

We re-examine the following equation

$$q(\xi) = \exp\left\{\frac{1}{\pi}\int_{-\infty}^{\infty *} \frac{\theta(t)}{\xi - t}dt\right\}, \tag{5.3}$$

which is obtained by the use of

$$v = \frac{dw}{dz} = qe^{-i\theta}, \quad \omega = \log v = \log q - i\theta, \tag{5.4}$$

where $\log q$ has a singularity at a stagnation point. As assumed in the last chapter, only one stagnation point exists in the flow region. In the reference ζ-plane (see Fig.5–3), the stagnation point is taken as $\zeta = a$. As $\zeta \to a$, we have

$$v \sim (\zeta - a), \tag{5.5}$$

where we assume that the fluid angles of two outgoing streams at the stagnation point differ by π. In the more general case we should have $v \sim (\zeta - a)^{\frac{\beta_1}{\pi}}$ where β_1 is the angle difference(see Birkhoff & Zarantonello [1957]). Let

$$v = \frac{dw}{dz} = (\zeta - a)^{\frac{\beta_1}{\pi}} Q(\zeta), \tag{5.6}$$

where $Q(\zeta) \neq 0$ for all $\zeta = \xi + i\eta$, $\eta \geq 0$. Then for the function

$$\log q = \log |(\zeta - a)^{\frac{\beta_1}{\pi}} Q(\zeta)|, \tag{5.7}$$

the singularity term is

$$\frac{\beta_1}{\pi} \log(\zeta - a), \tag{5.8}$$

so that $\log q$ is readily shown to belong to $L_2[-\infty, \infty]$. Therefore we obtain, from the reciprocity theorem (see Tricomi [1957] or Hochstadt [1973]), the reciprocity formula associated with (5.3)

$$\theta(\xi) = -\frac{1}{\pi}\int_{-\infty}^{\infty *} \frac{\log q}{\xi - t}dt. \tag{5.9}$$

By application of the Bernoulli condition, we have $\log q = 0$ on $\eta = 0$, $|\xi| > 1$ so that equation (5.9) can be reduced to

$$\theta(\xi) = -\frac{1}{\pi}\int_{-1}^{1*} \frac{\log q}{\xi - t}dt. \qquad |\xi| < \infty \tag{5.10}$$

where the integral is a Cauchy principal value on $|\xi| < 1$.

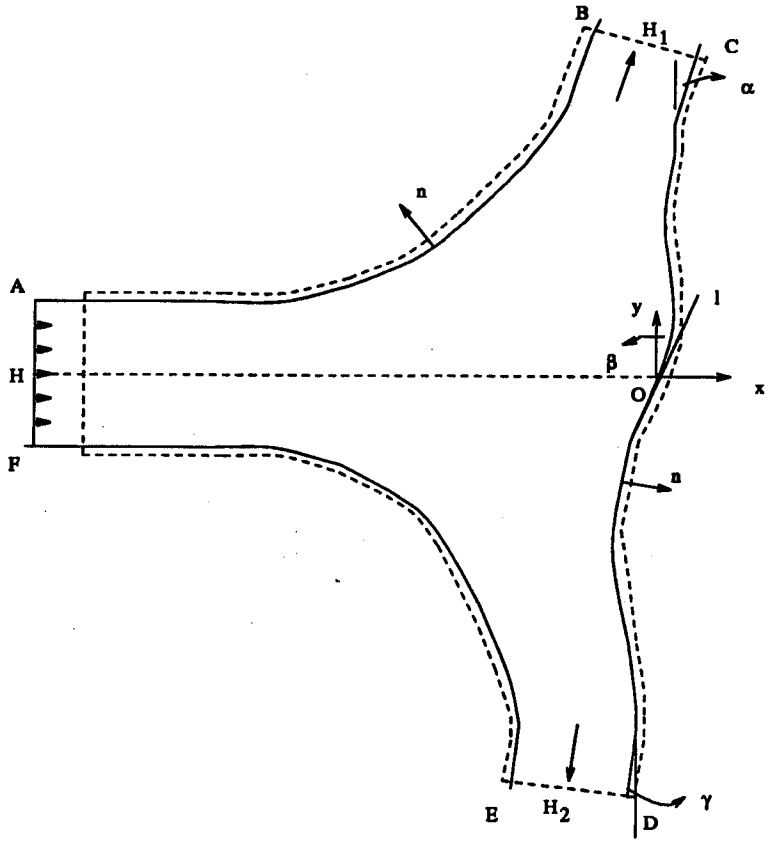

Figure 5–1: The physical-plane of a jet impinging on an asymmetric wall

5.2 Mathematical Analysis of the Problem

The transformation which maps the upper half ζ-plane to the complex potential plane is given as

$$w(\zeta) = -\frac{1+a}{2}\log\frac{1+\zeta}{1+a} - \frac{1-a}{2}\log\frac{\zeta-1}{1-a} + i\pi \tag{5.11}$$

with

$$a = 1 - 2H_1/H. \tag{5.12}$$

However, the parameters a and H_1 are unknown and another condition is needed to determine them. This is provided by an integral form of the momentum

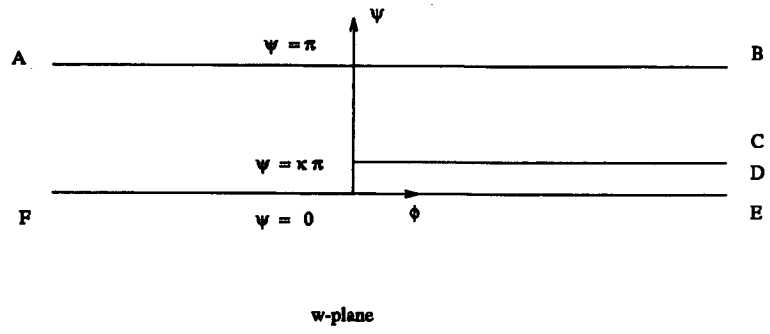

Figure 5–2: The w-plane of a jet impinging on an asymmetric wall

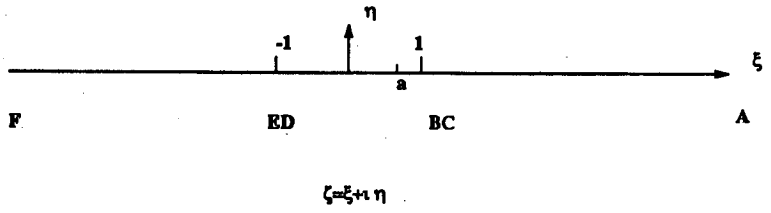

Figure 5–3: The $\zeta = \xi + i\eta$ plane

equation in a chosen direction $\vec{l}$. In an incompressible inviscid fluid the stress is $\sigma_{ij} = -p\delta_{ij}$ and when gravitational effects are neglected in comparison with the momentum of the incoming jets, the integral form of the momentum equation for steady motion around any closed curve τ, from (2.31), is as follows

$$\rho \int (\vec{u} \cdot \vec{l})\vec{u} \cdot \vec{n} ds = -\int p l_j n_j ds \tag{5.13}$$

where $\vec{n}$ is the outeward normal on the closed curve τ, and the integration is taken along the control surface.

For the jet impinging on the asymmetric uneven wall, a control surface is taken to correspond to the curve τ as shown in Fig. 5–1, consisting of the free surface, the solid boundary and lines at right angles to the flow directions at infinity. Taking Ox parallel to the incoming stream, so that the two outgoing streams are inclined at angles α and γ, respectively, to the Oy axis, the choice of $\vec{l}$ as an arbitrary unit

vector $\vec{l} = (\sin\beta, \cos\beta)$ then gives

$$\rho U^2(-H\sin\beta + H_1\cos(\beta-\alpha) - H_2\cos(\gamma-\beta)) = -\int_{\dot{\tau}} P \;\; \vec{n}\cdot\vec{l} \;\; ds - \int_{\ddot{\tau}} P_0 \;\; \vec{n}\cdot\vec{l} \;\; ds \tag{5.14}$$

where $\dot{\tau}$ is the wetted portion of the wall COD, $\ddot{\tau}$ includes the surfaces DE, EF, FA, AB and BC on which the pressure has the uniform value P_0. Since $\tau = \dot{\tau} + \ddot{\tau}$ is a closed surface, we obtain

$$\oint_{\tau} P_0 \;\; \vec{n}\cdot\vec{l} \;\; ds = 0 \tag{5.15}$$

which results in

$$\int_{\dot{\tau}} P_0 \;\; \vec{n}\cdot\vec{l} \;\; ds = -\int_{\ddot{\tau}} P_0 \;\; \vec{n}\cdot\vec{l} \;\; ds. \tag{5.16}$$

Inserting equation (5.16) into (5.14) and then non-dimensionalizing it gives

$$-\sin\beta + h_1\cos(\beta-\alpha) - h_2\cos(\gamma-\beta) = -\frac{1}{\pi}\int_{\dot{\tau}}(p-p_0)\vec{n}\cdot\vec{l}d\bar{s} \tag{5.17}$$

where the transformations are

$$p = \frac{P}{\rho U^2}, \quad p_0 = \frac{P_0}{\rho U^2},$$
$$\bar{s} = \frac{\pi s}{H}, \quad h_1 = \frac{H_1}{H}, \quad h_2 = \frac{H_2}{H}.$$

The mass conservation law implies that

$$1 = h_1 + h_2, \tag{5.18}$$

which, together with (5.12), gives

$$h_1 = \frac{1-a}{2}, \qquad h_2 = \frac{1+a}{2}. \tag{5.19}$$

The Bernoulli condition along the wall gives

$$p - p_0 = \frac{1}{2}(1 - q^2(\xi)), \qquad |\xi| < 1. \tag{5.20}$$

If the wall is given by $x = k(y)$, we have

$$\vec{l} = (l_1, l_2) = (\sin\beta, \quad \cos\beta) \tag{5.21}$$

$$\vec{n} = (n_1, n_2) = \left(\frac{1}{(1+k'^2)^{\frac{1}{2}}}, \quad -\frac{k'}{(1+k'^2)^{\frac{1}{2}}}\right) \tag{5.22}$$

$$d\bar{s} = (1+k'^2)^{\frac{1}{2}} dy. \tag{5.23}$$

Substituting all the equations from (5.19) to (5.23) into (5.17) yields

$$\begin{aligned} -(\sin\beta \quad + \quad & \cos(\gamma-\beta)) + \frac{1-a}{2}(\cos(\beta-\alpha) + \cos(\gamma-\beta)) \\ & = \frac{1}{\pi}\int \frac{1}{2}(1-q^2)(\sin\beta - k'\cos\beta)dy \end{aligned} \tag{5.24}$$

which should hold for all β.

The above equation (5.24) actually implies that

$$2 - (1-a)\sin\alpha + (1+a)\sin\gamma = \frac{1}{\pi}\int (1-q^2)dy, \tag{5.25}$$

$$-(1+a)\cos\gamma + (1-a)\cos\alpha = \frac{1}{\pi}\int (1-q^2)k'dy. \tag{5.26}$$

In the special case $\alpha = \gamma = 0$, these yield

$$2 = \frac{1}{\pi}\int (1-q^2)dy, \tag{5.27}$$

$$2a = -\frac{1}{\pi}\int (1-q^2)k'dy. \tag{5.28}$$

The relation between the flow angle and the slope of the tangent is

$$\theta(\xi) = \begin{cases} \frac{\pi}{2} - \tan^{-1} k'(y), & a < \xi < 1 \\ -\frac{\pi}{2} - \tan^{-1} k'(y), & -1 < \xi < a \end{cases} \tag{5.29}$$

The integral equation (5.10) for $|\xi| < 1$ can be inverted using the finite Hilbert transform, and then written in terms of $\theta(\xi)$ given in (5.29). We obtain

$$\log q = -\frac{1}{\pi}\int_{-1}^{1} \left(\frac{1-t^2}{1-\xi^2}\right)^{\frac{1}{2}} \frac{\theta(t)}{t-\xi}dt + \frac{c}{(1-\xi^2)^{\frac{1}{2}}}, \quad |\xi| < 1. \tag{5.30}$$

The constant c is obtained by multiplying by $\sqrt{1-\xi^2}$ and letting $\xi \to 1$ in this equation, so that

$$c = \frac{1}{\pi} \int_{-1}^{1} (1-t^2)^{\frac{1}{2}} \frac{\theta(t)}{t-1} dt. \tag{5.31}$$

Substituting this expression into equation (5.30) and writing into an alternative form gives

$$q = \exp\left\{ -\frac{1}{\pi} \int_{-1}^{1} \left(\frac{1-t^2}{1-\xi^2} \right)^{\frac{1}{2}} \left(\frac{1}{t-\xi} - \frac{1}{t-1} \right) \theta(t) dt \right\}, \quad |\xi| < 1 \tag{5.32}$$

which reduces to

$$q = \exp\left\{ -\frac{1}{\pi} \sqrt{\frac{1-\xi}{1+\xi}} \int_{-1}^{1} \sqrt{\frac{1+t}{1-t}} \frac{\theta(t)}{t-\xi} dt \right\}, \quad |\xi| < 1. \tag{5.33}$$

The variable y is specified using equation (5.24) as

$$\frac{dy}{d\xi} = -\frac{1}{\pi} \frac{\xi - a}{\xi^2 - 1} (q(\xi))^{-1} \sin\theta(\xi), \quad |\xi| < \infty. \tag{5.34}$$

This may be integrated as

$$y(\xi) = -\frac{\pi}{2} - \int_{-\infty}^{\xi} \frac{t-a}{t^2-1} (q(t))^{-1} \sin\theta(t) dt, \quad |\xi| < 1 \tag{5.35}$$

showing how y is related to θ and q.

The problem now is governed by a system of equations (5.10), (5.28), (5.29) and (5.35). When the system of equations is solved, we obtain $\theta(\xi)$, $|\xi| < 1$ and the parameter a. Equation (6.10) gives the flow angles both on the wall and on the free-surface. Therefore we consider (5.29) and have

$$\frac{dz}{d\xi} = -\frac{1}{\pi} \frac{\xi - a}{\xi^2 - 1} \exp(i\theta(\xi)), \quad |\xi| > 1. \tag{5.36}$$

Taking the real and imaginary parts of (5.36) and integrating gives

$$x(\xi) = x(\xi_0) - \frac{1}{\pi} \int_{\xi_0}^{\xi} \frac{t-a}{t^2-1} \cos\theta(t) dt, \quad |\xi| > 1 \tag{5.37}$$

$$y(\xi) = -\frac{\pi}{2} - \frac{1}{\pi} \int_{-\infty}^{\xi} \frac{t-a}{t^2-1} \sin\theta(t) dt, \quad |\xi| > 1 \tag{5.38}$$

where $x(\xi_0)$ is assumed to be given. This equation then gives the shape of the free-surface.

5.3 The Singularities in the Problem

The integral equation (5.10) is singular whenever $|\xi| \leq 1$. Also, the integrand is singular at the stagnation point $\xi = a$, where $\log q$ has order

$$O(\log(\xi - a)). \tag{5.39}$$

Additionally, equation (5.33) has singularities at $\xi = \pm 1$, since the flow tends to uniform flow with $q = 1$ in both the downstream branches. The special case of flow impinging on an inclined plane is studied in the following section, to motivate approximations near the singular points. The integrand in equation (6.34) has order

$$O((\xi - a)(q(\xi))^{-1}). \tag{5.40}$$

When $\xi \to a$, we have

$$q(\xi) \sim (\xi - a)^{\frac{\beta_1}{\pi}} \tag{5.41}$$

$$(\xi - a)(q(\xi))^{-1} \sim (\xi - a)^{1-\frac{\beta_1}{\pi}}. \tag{5.42}$$

At $\xi = \pm 1$, the integrand also has singularities.

5.4 The Special Case of an Inclined Plane Wall

In the case of a jet impinging on an inclined flat wall with $x = k(y) = y \tan \alpha$, then the choice $\beta = \alpha = \gamma$ in (5.24) gives

$$(1 + a)(\sin \alpha + 1) + (1 - a)(\sin \alpha - 1) = 0 \tag{5.43}$$

which reduces to $a = -\sin \alpha$.

Equation (5.29) can be written as

$$\theta(\xi) = \begin{cases} \frac{\pi}{2} - \alpha, & -\sin\alpha < \xi < 1 \\ -\frac{\pi}{2} - \alpha, & -1 < \xi < -\sin\alpha \end{cases} . \tag{5.44}$$

After determining c in (5.30) from (5.31), we obtain

$$\begin{aligned} q &= \exp\left\{ \frac{1}{\pi} \left[\int_{-1}^{-\sin\alpha} \left(\frac{1-t^2}{1-\xi^2} \right)^{\frac{1}{2}} \frac{\frac{\pi}{2}+\alpha}{t-\xi} dt \right.\right. \\ &\quad \left.\left. - \int_{-\sin\alpha}^{1} \left(\frac{1-t^2}{1-\xi^2} \right)^{\frac{1}{2}} \frac{\frac{\pi}{2}-\alpha}{t-\xi} dt \right] - \frac{\cos\alpha}{(1-\xi^2)^{\frac{1}{2}}} \right\}, \quad |\xi| < 1. \end{aligned} \tag{5.45}$$

The first integral in (5.45) is evaluated as

$$\begin{aligned} I_1 &= \frac{\frac{\pi}{2}+\alpha}{(1-\xi^2)^{\frac{1}{2}}} \int_{-1}^{-\sin\alpha} \frac{(1-t^2)^{\frac{1}{2}}}{t-\xi} dt \\ &= \frac{\frac{\pi}{2}+\alpha}{(1-\xi^2)^{\frac{1}{2}}} \int_{0}^{\frac{\pi}{2}-\alpha} \frac{\sin^2 u}{-\cos u - \xi} du \\ &= \frac{\frac{\pi}{2}+\alpha}{(1-\xi^2)^{\frac{1}{2}}} \int_{0}^{\frac{\pi}{2}-\alpha} \frac{\cos^2 u - \xi^2 - (1-\xi^2)}{\cos u + \xi} du \\ &= \frac{\frac{\pi}{2}+\alpha}{(1-\xi^2)^{\frac{1}{2}}} \int_{0}^{\frac{\pi}{2}-\alpha} \left[\cos u - \xi - \frac{1-\xi^2}{\cos u + \xi} \right] du \\ &= \frac{\frac{\pi}{2}+\alpha}{(1-\xi^2)^{\frac{1}{2}}} \left(\cos\alpha - \xi\left(\frac{\pi}{2}-\alpha\right) - (1-\xi^2) \int_{0}^{\frac{\pi}{2}-\alpha} \frac{du}{\cos u + \xi} \right). \end{aligned} \tag{5.46}$$

Since we can determine the final integral as

$$\int_{0}^{\frac{\pi}{2}-\alpha} \frac{du}{\cos u + \xi} = \frac{1}{(1-\xi^2)^{\frac{1}{2}}} \log \left| \frac{1 + r\tan(\frac{\pi}{4} - \frac{\alpha}{2})}{1 - r\tan(\frac{\pi}{4} - \frac{\alpha}{2})} \right|, \tag{5.47}$$

where

$$r = \left(\frac{1-\xi}{1+\xi} \right)^{\frac{1}{2}}, \tag{5.48}$$

we may substitute it into (5.46), to obtain

$$I_1 = \frac{\frac{\pi}{2}+\alpha}{(1-\xi^2)^{\frac{1}{2}}} \left(\cos\alpha - \xi\left(\frac{\pi}{2}-\alpha\right) - (1-\xi^2) \frac{1}{(1-\xi^2)^{\frac{1}{2}}} \log \left| \frac{1 + r\tan(\frac{\pi}{4} - \frac{\alpha}{2})}{1 - r\tan(\frac{\pi}{4} - \frac{\alpha}{2})} \right| \right). \tag{5.49}$$

Similarly the second integral is obtained as

$$I_2 = \frac{\frac{\pi}{2}-\alpha}{(1-\xi^2)^{\frac{1}{2}}}\left(-\cos\alpha - \xi\left(\frac{\pi}{2}+\alpha\right) + (1-\xi^2)\frac{1}{(1-\xi^2)^{\frac{1}{2}}}\log\left|\frac{1+r\tan(\frac{\pi}{4}-\frac{\alpha}{2})}{1-r\tan(\frac{\pi}{4}-\frac{\alpha}{2})}\right|\right), \tag{5.50}$$

which may be combined with (5.49) to give

$$\begin{aligned} I &= \frac{I_1 - I_2}{\pi} = \frac{1}{\pi}\left[\frac{\pi\cos\alpha}{(1-\xi^2)^{\frac{1}{2}}} - \pi F(r)\right] \\ &= \frac{\cos\alpha}{(1-\xi^2)^{\frac{1}{2}}} - F(r). \end{aligned} \tag{5.51}$$

where

$$F(r) = \log\left|\frac{1+r\tan(\frac{\pi}{4}-\frac{\alpha}{2})}{1-r\tan(\frac{\pi}{4}-\frac{\alpha}{2})}\right|. \tag{5.52}$$

Substituting (5.52) into (5.45) gives

$$\begin{aligned} q(\xi) &= \exp\left\{I - \frac{\cos\alpha}{(1-\xi^2)^{\frac{1}{2}}}\right\} \\ &= \exp\{-F(r)\} = \exp\left\{-F\left(\frac{1-\xi}{1+\xi}\right)\right\} \\ &= \left|\frac{1-r\tan(\frac{\pi}{4}-\frac{\alpha}{2})}{1+r\tan(\frac{\pi}{4}-\frac{\alpha}{2})}\right| \\ &= \left|\frac{(1+\xi)^{\frac{1}{2}} - (1-\xi)^{\frac{1}{2}}\tan(\frac{\pi}{4}-\frac{\alpha}{2})}{(1+\xi)^{\frac{1}{2}} + (1-\xi)^{\frac{1}{2}}\tan(\frac{\pi}{4}-\frac{\alpha}{2})}\right|. \end{aligned} \tag{5.53}$$

We can see that as $\xi \to \pm 1$ then $q \to 1$ while at $\xi = -\sin\alpha$, then $q = 0$. By setting $\xi = \sin\bar{\alpha}$ for $-\pi/2 < \bar{\alpha} < \pi/2$, we obtain

$$\begin{aligned} q(\xi) = q(\sin\bar{\alpha}) &= \left|\frac{1-\tan(\frac{\pi}{4}-\frac{\bar{\alpha}}{2})\tan(\frac{\pi}{4}-\frac{\alpha}{2})}{1+\tan(\frac{\pi}{4}-\frac{\bar{\alpha}}{2})\tan(\frac{\pi}{4}-\frac{\alpha}{2})}\right| \\ &= \frac{\left|\sin\frac{\bar{\alpha}+\alpha}{2}\right|}{\cos\frac{\bar{\alpha}-\alpha}{2}}. \end{aligned} \tag{5.54}$$

Then $\theta(\xi)$ can be found from (5.10) so that the shape of the free surface can be obtained using (6.37) and (6.38). Moreover this special case provides the starting point for numerical solution of cases with nonplanar walls.

5.5 The Numerical Scheme

The integration within equation (5.32) is written as

$$\int_{-1}^{a-\epsilon_1*}\left(\frac{1-t^2}{1-\xi^2}\right)^{\frac{1}{2}}\left(\frac{1}{t-\xi}-\frac{1}{t-1}\right)\theta(t)dt$$
$$+\int_{a-\epsilon_1}^{a+\epsilon_2}\left(\frac{1-t^2}{1-\xi^2}\right)^{\frac{1}{2}}\left(\frac{1}{t-\xi}-\frac{1}{t-1}\right)\theta(t)dt$$
$$+\int_{a+\epsilon_2}^{1*}\left(\frac{1-t^2}{1-\xi^2}\right)^{\frac{1}{2}}\left(\frac{1}{t-\xi}-\frac{1}{t-1}\right)\theta(t)dt \equiv J_1+J_2+J_3, \quad |\xi|<1. \tag{5.55}$$

At $\xi = a$, the flow angle θ has a jump, so that

$$\theta(t) \simeq \begin{cases} \beta_0 & , \quad a < \xi < a+\epsilon_2 \\ \beta_0 - \pi & , \quad a-\epsilon_1 < \xi < a \end{cases} . \tag{5.56}$$

The first term in J_2 can be approximated using (5.56) as

$$\int_{a-\epsilon_1}^{a+\epsilon_2}\left(\frac{1-t^2}{1-\xi^2}\right)^{\frac{1}{2}}\frac{\theta(t)}{t-\xi}dt$$
$$\simeq \frac{1}{(1-\xi^2)^{\frac{1}{2}}}\left[(\beta_0-\pi)\int_{a-\epsilon_1}^{a}\frac{(1-t^2)^{\frac{1}{2}}}{t-\xi}dt+\beta_0\int_{a}^{a+\epsilon_2}\frac{(1-t^2)^{\frac{1}{2}}}{t-\xi}dt\right]$$
$$= \frac{1}{(1-\xi^2)^{\frac{1}{2}}}\left[\beta_0(\sin u_2-\sin u_1)+\pi(\sin u_1-\sin u_0)+\xi(\beta_0(u_2-u_1)+\pi(u_1-u_0))\right]$$
$$-\left(\beta_0\log\left|\frac{1+r\tan\frac{u_2}{2}}{1-r\tan\frac{u_2}{2}}\right|-\beta_0\log\left|\frac{1+r\tan\frac{u_1}{2}}{1-r\tan\frac{u_1}{2}}\right|\right.$$
$$\left.+\pi\log\left|\frac{1+r\tan\frac{u_1}{2}}{1-r\tan\frac{u_1}{2}}\right|-\pi\log\left|\frac{1+r\tan\frac{u_0}{2}}{1-r\tan\frac{u_0}{2}}\right|\right) \tag{5.57}$$

where

$$\cos u_0 = a, \qquad \cos u_1 = a-\epsilon_1, \qquad \cos u_2 = a+\epsilon_2 \tag{5.58}$$

$$r = \left(\frac{1+\xi}{1-\xi}\right)^{\frac{1}{2}}. \tag{5.59}$$

Equation (5.57) shows that as $\xi \to a$,

$$r = \left(\frac{1+\xi}{1-\xi}\right)^{\frac{1}{2}} \to \left(\frac{1+a}{1-a}\right)^{\frac{1}{2}} = \cot\frac{1}{2}u_0, \tag{5.60}$$

giving $J_2 \longrightarrow -\infty$. Therefore $q(\xi) \longrightarrow 0$, which is consistent with $q(a) = 0$.

Singularities of (5.55) at $\xi = \pm 1$ can be treated in a similar way. The variables in the two integrals are changed, for convenience of computation, using two different transformations. In J_1, let

$$(1+a)u_1 = 1 + t, \quad dt = (1+a)du_1 \tag{5.61}$$

and in J_3, let

$$(1-a)u_2 = t - a, \quad dt = (1-a)du_2. \tag{5.62}$$

Then as $\epsilon_1 \to 0$ and $\epsilon_2 \to 0$, the other two integrals in equation (5.55) are changed to

$$\begin{aligned}\lim(J_1 + J_3) \;=\; & \sqrt{\frac{1-\xi}{1+\xi}} \int_0^1 \sqrt{\frac{(1+a)u_1}{2-1+a)u_1}} \frac{\theta((1+a)u_1 - 1))}{(1+a)u_1 - 1 - \xi}(1+a)du_1 \\ & + \sqrt{\frac{1-\xi}{1+\xi}} \int_0^1 \sqrt{\frac{1+a+(1-a)u_2}{(1-a)(1-u_2)}} \cdot \frac{\theta((1-a)u_2 + a))}{(1-a)u_2 + a - \xi}(1-a)du_2, \\ & \qquad\qquad |\xi| < 1. \end{aligned} \tag{5.63}$$

Since u_1 and u_2 are dummy variables, using u to replace them in (5.63) gives

$$\begin{aligned}\lim(J_1 + J_3) \;=\; & \sqrt{\frac{1-\xi}{1+\xi}} \int_0^1 \sqrt{\frac{(1+a)u}{2-1+a)u}} \cdot \frac{\theta_1(u)}{(1+a)u - 1 - \xi}(1+a)du \\ & + \sqrt{\frac{1-\xi}{1+\xi}} \int_0^1 \sqrt{\frac{1+a+(1-a)u}{(1-a)(1-u)}} \cdot \frac{\theta_2(u)}{(1-a)u + a - \xi}(1-a)du, \\ & \qquad\qquad |\xi| < 1 \end{aligned} \tag{5.64}$$

where

$$\begin{cases} \theta_1(u) = \theta((1+a)u - 1) \\ \theta_2(u) = \theta((1-a)u + a) \end{cases}. \tag{5.65}$$

We can see that the integral over $(-1, 1)$ is treated numerically using a collocation method. The interval $[-1, 1]$ is divided into $[-1, a)$ and $(a, 1]$ for which two different discretizations are introduced as

$$\begin{cases} t_i = (1+a)ih_1 - 1, & i = 0, \cdots, M, \quad Mh_1 = 1 \quad \text{on}[-1, a) \\ t_i = a + (i-M)h_2(1-a), & i = M+1, \cdots, N, \quad (N-M)h_2 = 1 \quad \text{on}(a, 1]. \end{cases} \tag{5.66}$$

This scheme applied to (5.64) then gives an approximation to (5.33) which expresses the flow speed along the wall as a function of flow angle θ in a discrete form. In the following method, all the integrals over $(-1,1)$ will be treated using this scheme.

To seek the discrete form of (5.35) which is expressed in term of q and $\theta(\xi)$, we first consider the discrete form of equation (5.10) for $|\xi| > 1$

$$\begin{aligned}\theta(\xi) &= \frac{1}{\pi}\int_{-1}^{1}\frac{\log q}{\xi - t}dt \\ &\simeq \frac{1}{\pi}\left[h_1(1+a)\sum_{i=1}^{M}\frac{\log q(t_i)}{\xi - t_i} + h_2(1-a)\sum_{i=M+1}^{N}\frac{\log q(t_i)}{\xi - t_i}\right]. \qquad (5.67)\end{aligned}$$

The integral in equation (5.35) is divided into three parts

$$\begin{aligned}y(\xi) &= -\frac{\pi}{2} - \frac{1}{\pi}\left[\int_{-\infty}^{-1-\epsilon}\frac{t-a}{t^2-1}\sin\theta(t)dt + \int_{-1-\epsilon}^{-1+\epsilon}\frac{t-a}{t^2-1}(q(t))^{-1}\sin\theta(t)dt\right. \\ &\quad \left.\int_{-1+\epsilon}^{\xi}\frac{t-a}{t^2-1}(q(t))^{-1}\sin\theta(t)dt\right], \quad |\xi| < 1 \qquad (5.68)\end{aligned}$$

where $q = 1$ has been used in the first integrand.

Since, as $\xi \to -1$,

$$q \to 1, \qquad \theta \to \gamma, \qquad (5.69)$$

the second integration is approximated by

$$\int_{-1-\epsilon}^{-1+\epsilon}\frac{t-a}{t^2-1}\sin\gamma dt = \frac{1-a}{2}\sin\gamma\log\frac{2-\epsilon}{2+\epsilon}. \qquad (5.70)$$

The other two integrals are evaluated in different ways. The first integral is further divided into

$$\int_{-\infty}^{-1-\epsilon}\frac{t-a}{t^2-1}\sin\theta(t)dt = \int_{-\infty}^{-1-\epsilon}\frac{t}{t^2-1}\sin\theta(t)dt + a\int_{-\infty}^{-1-\epsilon}\frac{1}{t^2-1}\sin\theta(t)dt. \qquad (5.71)$$

Using the transformations

$$\log(\xi^2-1) = \xi_1, \qquad \log\frac{\xi-1}{\xi+1} = \xi_2 \qquad (5.72)$$

in the integrals respectively gives

$$\begin{aligned}\int_{-\infty}^{-1-\epsilon} \frac{t-a}{t^2-1}\sin\theta(t)dt &= \frac{1}{2}\int_{\log\epsilon(2+\epsilon)}^{\infty} \sin\theta\left(-(1+e^{\xi_1})^{\frac{1}{2}}\right)d\xi_1 \\ &+ \frac{a}{2}\int_0^{\log\left(2+\frac{2}{\epsilon}\right)} \sin\theta\left(\frac{1+e^{\xi_2}}{1-e^{\xi_2}}\right)d\xi_2 \end{aligned} \tag{5.73}$$

where θ is evaluated using (5.67). For the third integral in (5.68), the scheme (5.66) is employed. In the case $\xi < a$, we obtain $\xi = \xi_j$, $j = 1, \cdots, M$

$$\int_{-1+\epsilon}^{\xi} \frac{t-a}{t^2-1}(q(t))^{-1}\sin\theta(t)dt = h_1(1+a)\sum_{i=1}^{j}\frac{\xi_i - a}{\xi_i^2-1}(q(\xi_i))^{-1}\sin\theta(\xi_i). \tag{5.74}$$

In the case that $\xi > a$, $\xi = \xi_j$, $j = M+1, \cdots, N$, the integral is also split into two parts as

$$\begin{aligned}\int_{-1+\epsilon}^{\xi} \frac{t-a}{t^2-1}(q(t))^{-1}\sin\theta(t)dt &= h_1(1+a)\sum_{i=1}^{M}\frac{\xi_i - a}{\xi_i^2-1}(q(\xi_i))^{-1}\sin\theta(\xi_i) \\ &+ h_2(1-a)\sum_{M+1}^{j}\frac{\xi_i - a}{\xi_i^2-1}(q(\xi_i))^{-1}\sin\theta(\xi_i). \end{aligned} \tag{5.75}$$

The equation (5.24) is discretized as

$$\begin{aligned}&\left(-(\sin\beta + \cos(\gamma-\beta)) + \frac{1-a}{2}(\cos(\beta-\alpha)+\cos(\gamma-\beta))\right) \\ &= \frac{1}{2}\left[h_1(1+a)\sum_{i=0}^{M}(1-q_i^2)(\sin\beta - K'(y_i)\cos\beta)P_i\right. \\ &\left.+h_2(1-a)\sum_{i=M+1}^{N}(1-q_i^2)(\sin\beta - K'(y_i)\cos\beta)P_i\right], \end{aligned} \tag{5.76}$$

where

$$y_i = y(\xi_i), \quad P_i = \frac{\xi_i - a}{\xi_i^2-1}(q(\xi_i))^{-1}\sin\theta(\xi_i). \tag{5.77}$$

The discretized forms of (5.25) and (5.26) are obtained by simply letting $\beta = \frac{\pi}{2}$ and $\beta = 0$. We then have

$$y(\xi_j) = -\frac{\pi}{2} - \frac{1}{\pi}\int_{-\infty}^{\xi_j}\frac{\sin\theta(t)}{q(t)}dt, \quad |\xi_j| < 1 \tag{5.78}$$

for $j = 1, 2, \cdots, N-1$. Then substituting these into (5.29) yields

$$\theta(\xi_j) = \begin{cases} -\frac{\pi}{2} - \tan^{-1} k'(y(\xi_j)), & j = 1, \cdots, M \\ \frac{\pi}{2} - \tan^{-1} k'(y(\xi_j)), & j = M+1, \cdots, N-1. \end{cases} \tag{5.79}$$

These equations and (5.76) constitute N algebraic equations containing N unknowns $\theta(\xi_1), \cdots, \theta(\xi_{N-1})$ and the parameter a. The profile of the free surface is obtained from equations (5.37) and (5.38).

5.6 Results

The method is tested by considering a small number of different types of wall shapes. For instance, $x(y) = -ce^{-(y-b)^2}$ and $x(y) = c/(e^{-(y-b)} + e^{y-b})$ where c and b can be chosen. In the case that b is zero,the wall shapes become symmetrical about the x-axis. We found that when $|c| < 1$, the results agree very well with the results obtained using the method developed in Chapter 4 for the symmetric wall shapes. We found that as b increases slightly, the width of the jet going upward is slightly larger than the width of the jet going downward.

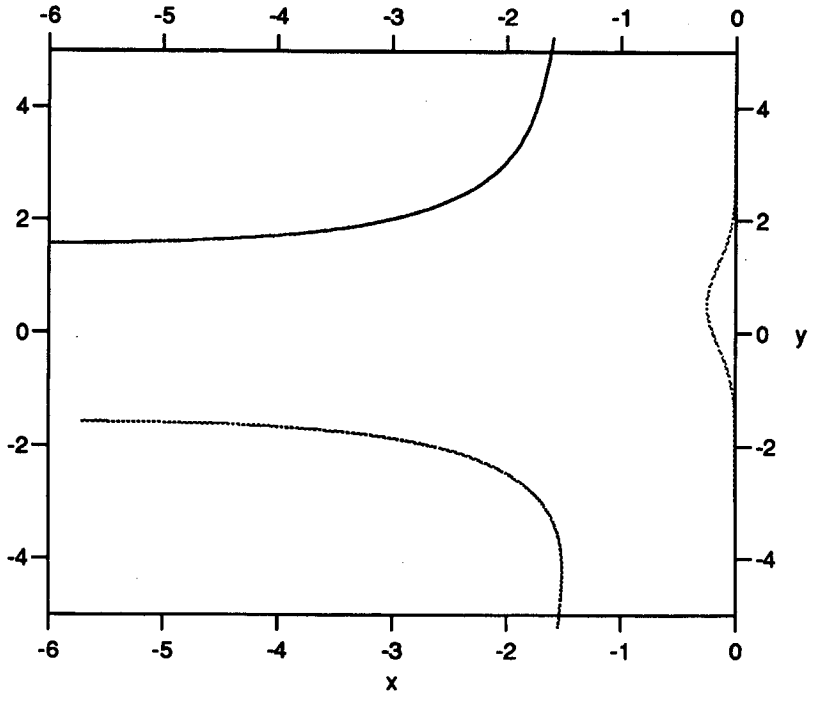

Figure 5–4: $x(y) = -0.25e^{-(y-0.5)^2}$

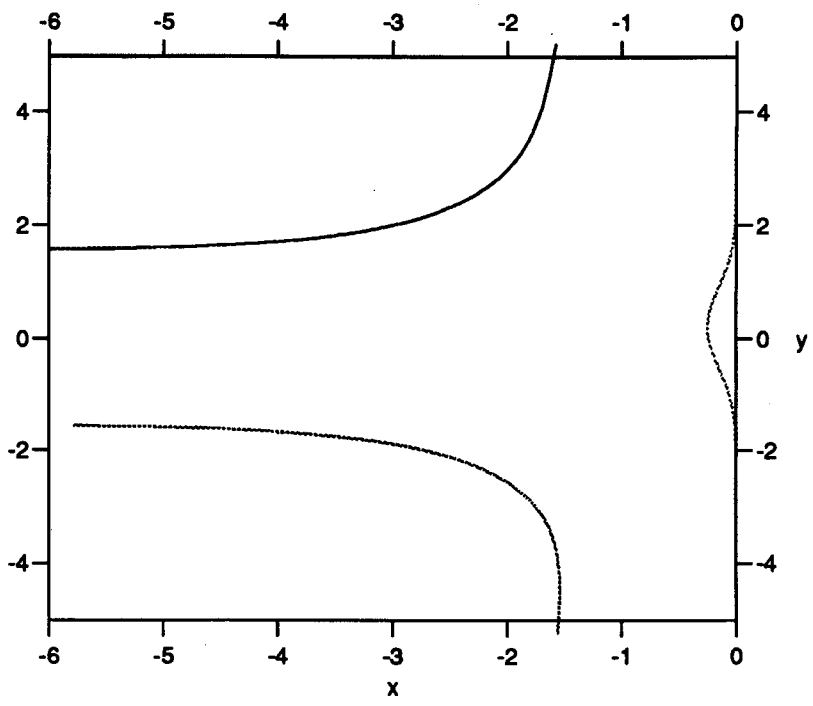

Figure 5–5: $x(y) = -0.25e^{-(y-0.2)^2}$

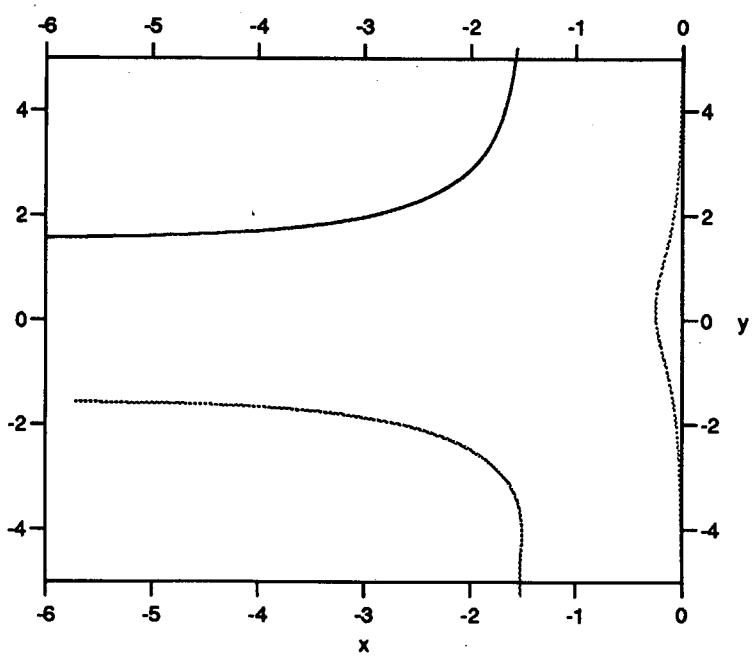

Figure 5–6: The wall function is $x(y) = -0.5\text{sech}(y - 0.2)$.

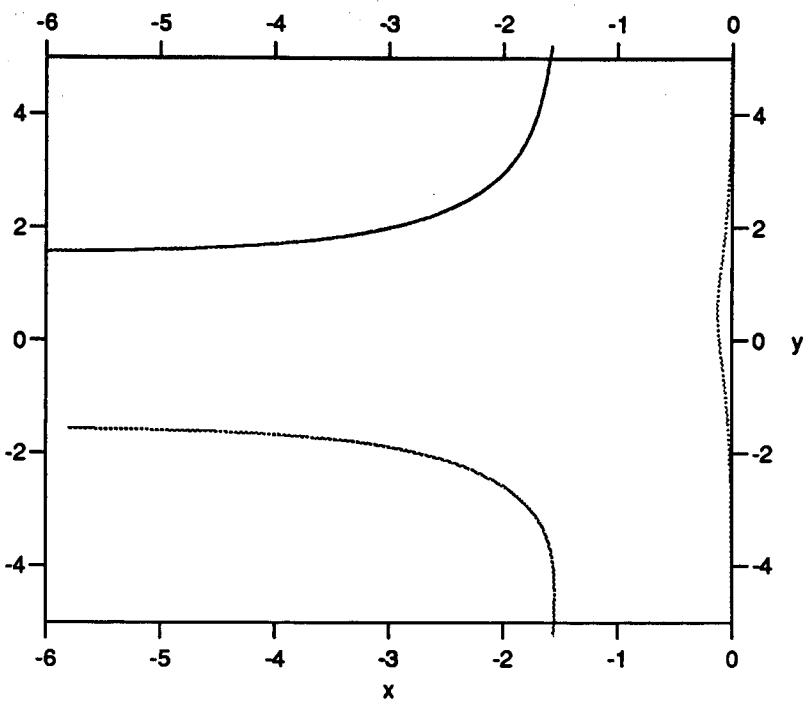

Figure 5–7: $x(y) = -0.25/(e^{(y-0.5)} + e^{-(y-0.5)})$.

Chapter 6

Free Surface Shape of a Jet Passing Through a Porous Film

6.1 Introduction

The problem of determining the free surface of a two dimensional jet of ideal fluid passing through a porous film then impinging on a wall is considered. When a flow occurs through a barrier we say the fluid transpires through the surface.

For the impact of an ideal jet on a porous wall, Jenkins and Barton [1989] investigated numerically the free surface shapes of the jet when the velocity is prescribed. The fixed domain method is used to formulate this physical problem. Since the boundary condition of this problem is complicated, they argued that the classical hodograph technique failed to work. King [1990] examined the same problem but with constant normal velocity across the wetted part of the porous wall by using the extended hodograph technique. This different approach stimulates our work Chapter 3 to give a further effective extension. This chapter concerns the free surface problem of a jet passing through a porous film and then incident on the flat wall. The physical condition across the porous film of the fluid is in analogy to the Darcy's law. The pressure difference is taken as proportional to the normal velocity, which is unknown prior to solving the problem. The velocity also is discontinuous across the film, i.e. the velocity has a jump. Thus the complex

potential plane is divided into two separate parts. Also the hodograph plane is diffcult to map onto a simple reference plane. Our transformation technique does not work very well in this case due to the discontinuity of the pressure and flow velocity. It seems to us that developing the numerical scheme of the formulation of this problem using the generalized Schwartz-Christoffel formula is difficult. In this chapter we use the Cauchy integral formula to deal with this problem. The rest of this chapter is organized as follows. In section 6.2, we formulate this problem using one of the boundary integral methods. Then section 6.3 analyzes the singularities in this problem, while section 6.4 gives the numerical scheme and presents some numerical results.

6.2 Mathematical Formulation of the Problem

The two dimensional steady flow of an incompressible inviscid fluid passing through a porous film then impinging upon a flat wall is considered(see Fig. 6–1). The flow is assumed irrotational on both sides of the film. A Cartesian coordinate system with the X-axis along the flat wall and the Y-axis into the fluid is introduced. The flow is symmetric about the Y-axis. Far away from the wall and along the Y-axis, the flow is required to be a uniform stream with uniform speed U_1 and thickness $2h_1$, while far away from the porous film along the X-axis, the two outgoing flows are uniform with speeds U_2 and $-U_2$ and thickness h_2. A velocity potential Φ and a stream function Ψ are defined such that the complex potential

$$W = \Phi + i\Psi \tag{6.1}$$

is analytic in the domain occupied by the fluid. Because the flow is divided, by the porous film, into two parts, it is convenient to label the two regions. Let D_1 denote the region upstream of the porous film, with $D_2 = D_{21} \cup D_{22}$ the region

downstream of the porous film. We have

$$W = W_j = \Phi_j + i\Psi_j, \qquad Z = X + iY \in D_j \tag{6.2}$$

and the complex velocity is defined as

$$\frac{dW}{dZ} = V = \Phi_X + i\Psi_X = Qe^{-i\theta}, \tag{6.3}$$

$$V = V_j = \frac{dW_j}{dZ}, \qquad Z = X + iY \in D_j \tag{6.4}$$

where θ is the angle between the flow direction and the x-axis while Q is the flow speed.

Since Bernoulli's equation holds in both D_1 and D_2, the flow speed Q has the constant values U_1 and U_2 along the free surface in D_1 and D_2, respectively with a jump occurring at the porous film. The stream function Ψ equals 0 on the dividing streamline along $X = 0$ and $Y = 0$ and takes the constant values $\Psi = \pm U_1 h_1 = \pm U_2 h_2$ on the free surfaces in $X > 0$ and $X < 0$, respectively.

Along the porous film, the mass conservation law implies the continuity of the stream function, so that

$$[\Psi] = \Psi_1 - \Psi_2 = 0, \quad Z = X + iH \text{ and } X \in (-L, L) \tag{6.5}$$

where H is the distance of the porous film from the wall $Y = 0$. The normal component of velocity towards the wall is

$$\Psi_X = \Psi_{1X} = \Psi_{2X}, \quad Z = X + iH \text{ and } X \in (-L, L). \tag{6.6}$$

It is assumed that the pressure drop is proportional to Ψ_X, so giving

$$P_1 - P_2 = K\Psi_X \quad , \tag{6.7}$$

where P_i is pressure in the region D_i and the constant K is the impermeability of the porous film.

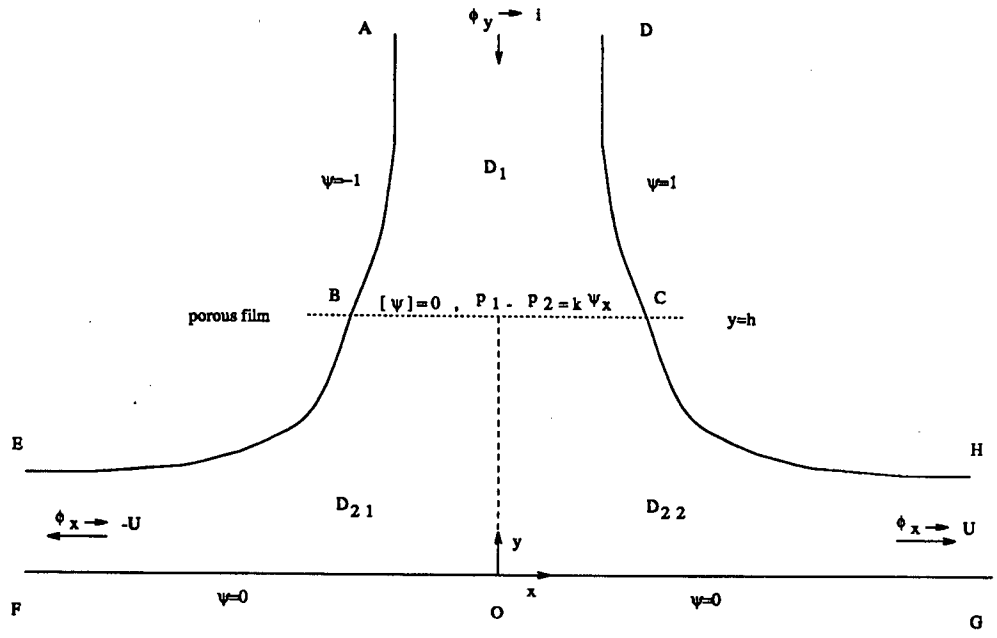

Figure 6–1: The non-dimensional physical-plane for a jet impinging on a porous film

Non-dimensionalization is performed using the substitutions

$$\left.\begin{aligned} z = x + iy = \frac{X + iY}{h_1}, \quad w = \frac{W}{U_1 h_1}, \quad w'(z) = \frac{W'(Z)}{U_1}, \quad p = \frac{2P}{\rho U_1^2}, \\ q = \frac{Q}{U_1}, \quad h = \frac{H}{h_1}, \quad U = \frac{U_2}{U_1} = \frac{h_1}{h_2}, \quad k = \frac{2K}{\rho U_1}. \end{aligned}\right\} \tag{6.8}$$

The dimensionless physical plane is shown in Fig. 6–1. The dimensionless governing equation and boundary conditions therefore are

$$\Delta^2 \psi = 0, \qquad z \in D_1 \cup D_2 \tag{6.9}$$

$$\nabla\phi \rightarrow (\pm U, 0), \qquad x \rightarrow \pm\infty \tag{6.10}$$

$$\nabla\phi \rightarrow (0, 1), \qquad y \rightarrow \infty \tag{6.11}$$

$$p_1 - p_2 = k\psi_x, \quad \psi_{1x} = \psi_{2x}, \qquad z = x + ih, \mid x \mid \leq \pm l \tag{6.12}$$

$$\left.\begin{aligned} p_1 + q_1^2 = 1, \qquad z \in D_1, \\ p_2 + q_2^2 = U^2, \qquad z \in D_2 \end{aligned}\right\} \tag{6.13}$$

where $p_i (i = 1, 2)$ is the non-dimensional pressure in domain $D_i (i = 1, 2)$ and $q_i (i = 1, 2)$ is the non-dimensional speed in domain $D_i (i = 1, 2)$ respectively.

We introduce three analytic functions as

$$v_1 = \frac{dw_1}{dz} - i, \quad z \in D_1 = \{z | z = x + iy, \quad y > h\}; \tag{6.14}$$

$$v_2 = \frac{dw_2}{dz} + U, \quad z \in D_{21} = \{z | z = x + iy, \quad x < 0, \quad y < h\}; \tag{6.15}$$

$$v_3 = \frac{dw_2}{dz} - U, \quad z \in D_{22} = \{z | z = x + iy, \quad x > 0, \quad y < h\}. \tag{6.16}$$

Along the free surfaces we also have

$$\frac{d\phi_1}{ds} = 1, \quad \frac{d\phi_2}{ds} = U \tag{6.17}$$

where s is arclength. Integrating the above equations (6.17) and setting $\phi = s = 0$ at the porous film $y = h$ gives

$$\phi_1 = s, \quad \phi_2 = Us \tag{6.18}$$

along the free surface in the regions D_1 and D_2. Since, along any streamline,

$$\frac{dz}{ds} = e^{i\theta} \quad , \tag{6.19}$$

we may integrate with respect to distance along both portions DC and CH of the free streamline to obtain

$$x(s) = \int_0^s \cos\theta(t)dt - 1, \quad y(s) = \int_0^s \sin\theta(t)dt + h. \tag{6.20}$$

Applying Cauchy's theorem to v_1, v_2 and v_3 respectively in D_1, D_{21} and D_{22} gives the relations between the velocity on the free surface and on the film. We will treat them as follows.

First, we have

$$\oint_{l_1} \frac{v_1 dz}{z - (x + ih)} = 0 \tag{6.21}$$

where the closed curve l_1 is $\overline{ABC_dCDA}$ shown in Fig.6–2. Let $z_j = x_j + iy_j$ $(j = 1, 2, 3, 4)$ denote z on $\overline{AB}$,$\overline{BC}$, $\overline{CD}$ and $\overline{DA}$ respectively.

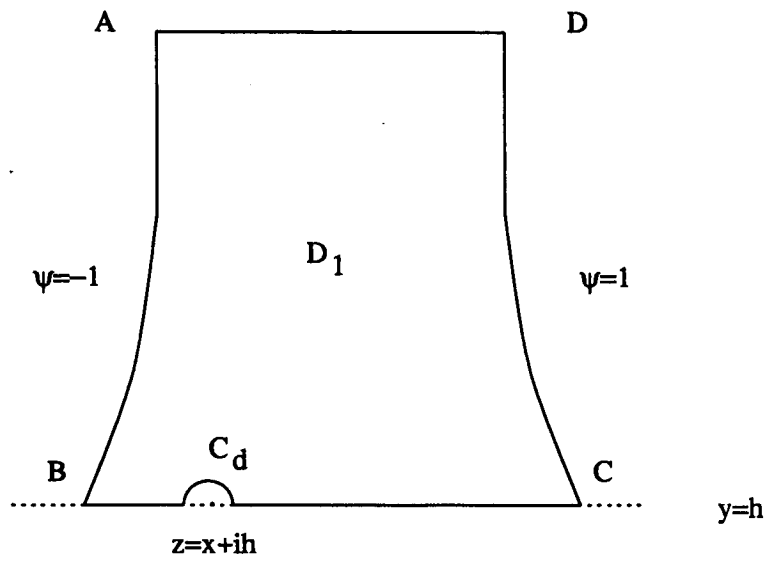

Figure 6–2: The integral route l_1

The integral around the semi-circle $C_d = \{z_d | z_d - (x+ih) = \epsilon e^{i\Theta}, 0 < \Theta < \pi\}$, as $\epsilon \to 0$, gives

$$\int_{C_d} \frac{v_1 dz_d}{z_d - (x+ih)} = \int_{\pi}^{0} \frac{v_1 i\epsilon e^{i\Theta} d\Theta}{\epsilon e^{i\Theta}} \longrightarrow -i\pi v_1(x+ih). \tag{6.22}$$

The integral on $\overline{DA}$, as $|z_4| \to \infty$, has

$$\int_{DA} \frac{v_1 dz_4}{z_4 - (x+ih)} \longrightarrow 0. \tag{6.23}$$

Thus, equation (6.21) reduces to

$$i\pi v_1(x+ih) = \int_{AB} \frac{v_1 dz_1}{z_1 - (x+ih)} + \int_{BC}^{*} \frac{v_1 dx_2}{x_2 - x} + \int_{CD} \frac{v_1 dz_3}{z_3 - (x+ih)}, \tag{6.24}$$

where, thereafter, the sign $\int^*$ represents the Cauchy principal value.

Since along any streamline ψ is constant, the variable z can be treated as a function of the velocity potential ϕ or equivalently, from equation (6.18), as a function of the arclength s. Because $\overline{AB}$ and $\overline{CD}$ are symmetric about the y-axis, we obtain

$$\left.\begin{aligned} x_1(s) = -x_3(s) \equiv x(s), \quad y_1(s) = y_3(s) \equiv y(s), \\ \theta_1(s) = -\pi - \theta_3(s) \equiv \theta(s) \end{aligned}\right\} \tag{6.25}$$

where $x_1(0) = -x_3(0) = l$ and $y_1(0) = y_3(0) = h$. Based on the above discussion, equation (6.24) reduces to

$$
\begin{aligned}
& i\pi v_1(x+ih) \\
&= \int_{-\infty}^{0} \frac{(e^{-i\theta}-i)e^{i\theta}ds}{x(s)+iy(s)-(x+ih)} + \oint_{-l}^{l} \frac{v_1 dx_2}{x_2-x} + \int_{0}^{-\infty} \frac{(e^{i\theta}+i)e^{-i\theta}ds}{-x(s)+iy(s)-(x+ih)} \\
&= \int_{-\infty}^{0} \left[\frac{1-ie^{i\theta}}{x(s)+iy(s)-(x+ih)} + \frac{1+ie^{-i\theta}}{x(s)-iy(s)+(x+ih)} \right] ds \\
&+ \int_{-l}^{l*} \frac{v_1 dx_2}{x_2-x}.
\end{aligned} \tag{6.26}
$$

Taking the imaginary part of the above equation (6.26) gives

$$
\phi_{1x} = \frac{1}{\pi} \int_{-l}^{l*} \frac{\psi_{1x}}{x_2-x} dx_2 + F_1(x,h) \tag{6.27}
$$

where

$$
\begin{aligned}
F_1(x,h) &= \frac{1}{\pi} \Im \left\{ \int_{-\infty}^{0} \left[\frac{1-ie^{i\theta}}{x(s)+iy(s)-(x+ih)} + \frac{1+ie^{-i\theta}}{x(s)-iy(s)+(x+ih)} \right] ds \right\} \\
&\quad - \frac{1}{\pi} \log \frac{l-x}{l+x} \\
&= \frac{1}{\pi} \int_{-\infty}^{0} \left[-\frac{(x(s)-x)\cos\theta(s) + (y(s)-h)(1+\sin\theta(s))}{(x(s)-x)^2+(y(s)-h)^2} \right. \\
&\quad \left. + \frac{(x(s)+x)\cos\theta(s) + (y(s)-h)(1+\sin\theta(s))}{(x(s)+x)^2+(y(s)-h)^2} \right] ds - \frac{1}{\pi} \log \frac{l-x}{l+x}
\end{aligned} \tag{6.28}
$$

and $\Im$ denotes the imaginary part.

The significance of equation (6.27) is that it gives a relation between ϕ_{1x} and ψ_{1x} along the porous film.

To seek a similar relation below the porous film, we consider, without loss generality, $x < 0$ along the porous film and obtain

$$
\oint_{l_2} \frac{v_2 dz}{z-(x+ih)} = 0, \tag{6.29}
$$

$$
\oint_{l_3} \frac{v_3 dz}{z-(x+ih)} = 0 \tag{6.30}
$$

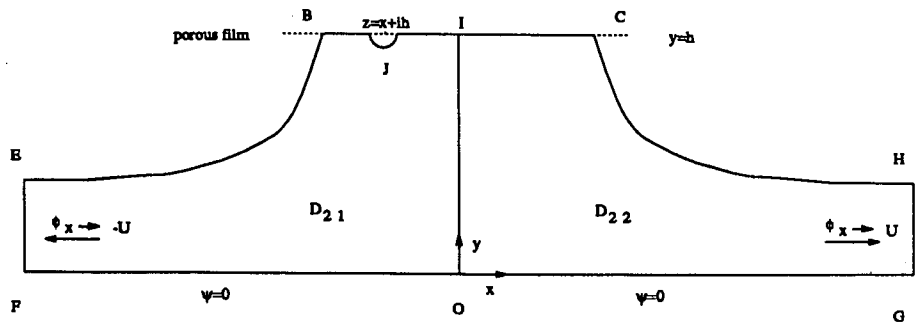

Figure 6–3: The paths of integration l_2 and l_3

where the closed path of integration l_2 is $\overline{BEFOIJB}$ and the l_3 is $\overline{CIOGHC}$. Both these curves are shown in Fig. 6–3.

From equation (6.29), we obtain

$$\int_{BE} \frac{v_2 dz}{z-(x+ih)} + \int_{EF} \frac{v_2 dz}{z-(x+ih)} + \int_{FO} \frac{v_2 dz}{z-(x+ih)} + \int_{OI} \frac{v_2 dz}{z-(x+ih)} + \int_{IJB} \frac{v_2 dz}{z-(x+ih)} = 0. \tag{6.31}$$

On $\overline{EF}$, as $|z| \to \infty$, the integral has the behaviour

$$\int_{EF} \frac{v_2 dz}{z-(x+ih)} \longrightarrow 0.$$

The integral along the porous film has

$$\int_{IJB} \frac{v_2 dz}{z-(x+ih)} \longrightarrow -\int_{-l}^{0*} \frac{v_2 dz}{z-(x+ih)} - i\pi v_2(x+ih),$$

as the radius of the semi-circle tends to 0.

After setting $v_2 = -q(x) + U$ on the flat wall $\overline{FO}$ and using equation (6.19) along $\overline{BE}$, we obtain

$$i\pi v_2(x+ih) = \int_0^\infty \frac{(e^{-i\theta}+1)Ue^{i\theta}ds}{x_1(s)+iy_1(s)-(x+ih)} - \int_{-l}^{0*} \frac{v_2 dx_2}{x_2-x} + \int_{-\infty}^{0} \frac{-q(\bar{x})+U}{\bar{x}-(x+ih)} d\bar{x} + \int_0^h \frac{v_2(iy)idy}{iy-(x+ih)}. \tag{6.32}$$

Similarly, equation (6.30) reduces to

$$-\int_0^\infty \frac{(e^{-i\theta}-1)Ue^{i\theta}ds}{x_3(s)+iy_3(s)-(x+ih)} + \int_l^0 \frac{v_3 dx_2}{x_2-x} +$$

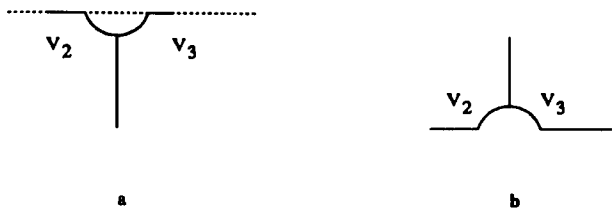

Figure 6–4: The paths of integration around the points $z = 0$ and $z = ih$

$$+\int_0^\infty \frac{q(\bar{x}) - U}{\bar{x} - (x + ih)} d\bar{x} - \int_0^h \frac{v_3(iy) i dy}{iy - (x + ih)} = 0. \qquad (6.33)$$

Because of symmetry, we have the same argument as we had in obtaining equation (6.26) along the free surfaces on the upper stream region. Moreover, we also have $v_2(iy) - v_3(iy) = 2U$ along the central line $\overline{OI}$.

Thus, equations (6.32) and (6.33) give

$$\begin{aligned} i\pi v_2(x + ih) &= \int_0^\infty \frac{(e^{-i\theta} + 1) U e^{i\theta} ds}{x_1(s) + iy_1(s) - (x + ih)} - \int_0^\infty \frac{(e^{-i\theta_3} - 1) U e^{i\theta_3} ds}{x_3(s) + iy_3(s) - (x + ih)} \\ &\quad - \int_{-l}^{0*} \frac{v_2 dx_2}{x_2 - x} + \int_l^0 \frac{v_3 dx_2}{x_2 - x} + \int_0^h \frac{2U i dy}{iy - (x + ih)} \\ &\quad + \int_{-\infty}^0 \frac{-q(\bar{x}) + U}{\bar{x} - (x + ih)} d\bar{x} + \int_0^\infty \frac{q(\bar{x}) - U}{\bar{x} - (x + ih)} d\bar{x} \\ &= \int_0^\infty \left[\frac{(e^{-i\theta} + 1) U e^{i\theta}}{x(s) + iy(s) - (x + ih)} + \frac{(e^{i\theta} + 1) U e^{-i\theta}}{x(s) - iy(s) + (x + ih)} \right] ds \\ &\quad - \int_l^{l*} \frac{(\phi_{2x} + i\psi_{2x}) dx_2}{x_2 - x} + U \log \left[\left(\frac{l}{x} \right)^2 - 1 \right] + 2U \log \frac{x}{x + ih} \\ &\quad + \int_{-\infty}^0 \frac{-q(\bar{x}) + U}{\bar{x} - (x + ih)} d\bar{x} + \int_0^\infty \frac{q(\bar{x}) - U}{\bar{x} - (x + ih)} d\bar{x}. \qquad (6.34) \end{aligned}$$

The approach to the expression (6.34) is slightly altered when $x = 0$ as indicated in Fig. 6–4(a). Taking the imaginary part of (6.34) gives

$$\phi_{2x} = -\frac{1}{\pi} \int_{-l}^{l*} \frac{\psi_{2x}}{x_2 - x} dx_2 + F_2(x, h) \qquad (6.35)$$

where

$$F_2(x, h) = \frac{1}{\pi} \Im \left\{ \int_0^\infty \left[\frac{1 + e^{i\theta}}{x(s) + iy(s) - (x + ih)} + \frac{1 + e^{-i\theta}}{x(s) - iy(s) + (x + ih)} \right] U ds + \right.$$

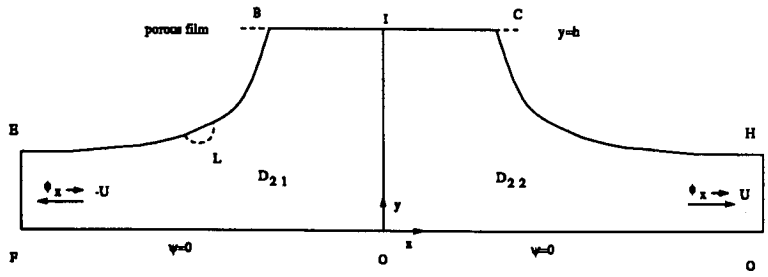

Figure 6–5: The path of integration

$$
\begin{aligned}
&+\int_{-\infty}^{0}\frac{-q(\bar{x})+U}{\bar{x}-(x+ih)}d\bar{x}+\int_{0}^{\infty}\frac{q(\bar{x})-U}{\bar{x}-(x+ih)}d\bar{x}+2U\log\frac{x}{x+ih}\Bigg\}-U\\
=\;&\frac{1}{\pi}\int_{0}^{\infty}\Bigg[\frac{(x(s)-x)\sin\theta(s)-(y(s)-h)(1+\cos\theta(s))}{(x(s)-x)^2+(y(s)-h)^2}\\
&-\frac{(x(s)+x)\sin\theta(s)-(y(s)-h)(1+\cos\theta(s))}{(x(s)+x)^2+(y(s)-h)^2}\Bigg]Uds\\
&+\Im\Bigg\{\int_{0}^{\infty}\frac{2\bar{x}}{\bar{x}^2-(x+ih)^2}(q(\bar{x})-U)d\bar{x}+2U\log\frac{x}{x+ih}\Bigg\}-U\\
=\;&\frac{1}{\pi}\int_{0}^{\infty}\Bigg[\frac{(x(s)-x)\sin\theta(s)-(y(s)-h)(1+\cos\theta(s))}{(x(s)-x)^2+(y(s)-h)^2}\\
&-\frac{(x(s)+x)\sin\theta(s)-(y(s)-h)(1+\cos\theta(s))}{(x(s)+x)^2+(y(s)-h)^2}\Bigg]Uds\\
&\int_{0}^{\infty}\frac{4h\bar{x}x}{(\bar{x}^2-x^2+h^2)^2+(2hx)^2}(q(\bar{x})-U)d\bar{x}-2U\tan^{-1}\frac{h}{x}+U.
\end{aligned}
\tag{6.36}
$$

The other three equations for $\theta(x(s),y(s)) = \theta(s)$ and $q(x)$ are needed to complete this formulation. Similarly to equations (6.26) and (6.34), we obtain respectively

$$
\begin{aligned}
&i\pi(e^{i\theta(s)}-i)\\
&=\int_{-\infty}^{0*}\frac{1-ie^{i\theta(s_1)}}{x(s_1)+iy(s_1)-(x(s)+iy(s))}ds_1+\int_{-l}^{l}\frac{v_1dx_1}{x_1+ih-(x(s)+iy(s))}\\
&-\int_{-\infty}^{0}\frac{1+ie^{-i\theta(s_1)}}{-x(s_1)+iy(s_1)-(x(s)+iy(s))}ds_1, \qquad s<0,
\end{aligned}
\tag{6.37}
$$

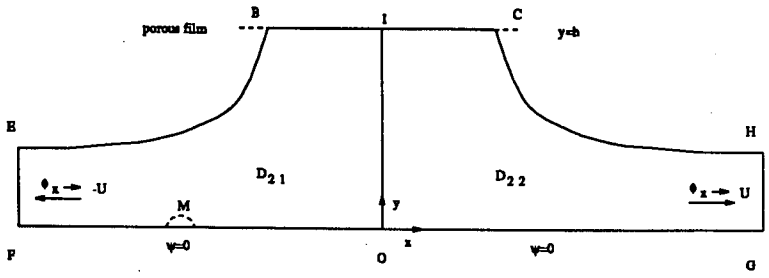

Figure 6–6: The path of integration

$$
\begin{aligned}
& i\pi U(e^{i\theta(s)}+1) \\
&= \int_0^{\infty *}\left[\frac{1+e^{i\theta(s_1)}}{x(s_1)+iy(s_1)-(x(s)+iy(s))}+\frac{1+e^{-i\theta}(s_1)}{x(s_1)-iy(s_1)+x(s)+iy(s))}\right]Uds_1 \\
&+\int_0^{\infty}\frac{2\bar{x}}{\bar{x}^2-(x(s)+iy(s))^2}(q(\bar{x})-U)d\bar{x}-\int_{-l}^{l}\frac{\phi_{2x}+i\psi_{2x}}{x_2+ih-(x(s)+iy(s))}dx_2 \\
&+U\log((x(s)+iy(s)-ih)^2-l^2)-2U\log(-(x(s)+iy(s)), \quad s>0
\end{aligned}
\tag{6.38}
$$

where the path of integration involving the semi-circle on $\overline{BE}$(see Fig. 6–5) is slightly different from the previous one (see Fig. 6–3) with the semi-circle on $\overline{IB}$, and

$$
\begin{aligned}
& -i\pi(q(x)-U) \\
&\qquad = \int_0^{\infty}\left[\frac{1+e^{i\theta(s_1)}}{x(s_1)+iy(s_1)-x}+\frac{1+e^{-i\theta(s_1)}}{x(s_1)-iy(s_1)+x}\right]Uds_1 \\
&\qquad +\int_0^{\infty *}\frac{2\bar{x}}{\bar{x}^2-x^2}(q(\bar{x})-U)d\bar{x}-\int_{-l}^{l}\frac{\phi_{2x}+i\psi_{2x}}{x_2+ih-x}dx_2 \\
&\qquad +U\log((x-ih)^2-l^2), \quad x<0
\end{aligned}
\tag{6.39}
$$

where the path of integration has a similar explanation to that above(see Fig. 6–6).

The imaginary parts of equations (6.37), (6.38) and (6.39) are respectively

$$
\pi\cos\theta(s) = \int_{-\infty}^{0*}\frac{(x(s)-x(s_1))\cos\theta(s_1)+(y(s)-y(s_1))(1+\sin\theta(s_1))}{(x(s)-x(s_1))^2+(y(s)-y(s_1))^2}ds_1
$$

$$+ \int_{-\infty}^{0} \frac{(x(s)+x(s_1))\cos\theta(s_1) - (y(s)-y(s_1))(1+\sin\theta(s_1))}{(x(s)+x(s_1))^2+(y(s)-y(s_1))^2} ds_1$$
$$+ \int_{-l}^{l} \frac{\psi_{1x}(x_1-x(s)) - \phi_{1x}(h-y(s))}{(x_1-x(s))^2+(h-y(s))^2} dx_1, \quad s<0, \tag{6.40}$$

$$\begin{aligned}
\pi\cos\theta(s) &= \int_0^{\infty *} \left[\frac{-\sin\theta(s_1)(x(s)-x(s_1)) + (1+\cos\theta(s_1))(y(s)-y(s_1))}{(x(s)-x(s_1))^2+(y(s)-y(s_1))^2} \right. \\
&- \left. \frac{\sin\theta(s_1)(x(s)+x(s_1)) - (1+\cos\theta(s_1))(y(s)-y(s_1))}{(x(s)+x(s_1))^2+(y(s)-y(s_1))^2} \right] ds_1 \\
&+ \int_0^{\infty} \frac{4\bar{x}x(s)y(s)(q(\bar{x})-U)}{(\bar{x}^2-(x^2(s)-y^2(s)))^2+4x^2(s)y^2(s)} \frac{d\bar{x}}{U} \\
&- \int_{-l}^{l} \frac{\psi_{2x}(x_2-x(s)) - \phi_{2x}(h-y(s))}{(x_2-x(s))^2+(h-y(s))^2} \frac{dx_2}{U} \\
&+ \tan^{-1}\frac{y(s)-h}{x(s)-l} + \tan^{-1}\frac{y(s)-h}{x(s)+l} - 2\tan^{-1}\frac{y(s)}{x(s)}, \quad s>0
\end{aligned} \tag{6.41}$$

and

$$\begin{aligned}
\pi(q(x)-U) &= \int_0^{\infty} \left[\frac{\sin\theta(s_1)(x-x(s_1)) + (1+\cos\theta(s_1))y(s_1)}{(x-x(s_1))^2+y^2(s_1)} \right. \\
&+ \left. \frac{\sin\theta(s_1)(x(s_1)-x) - (1+\cos\theta(s_1))y(s_1)}{(x+x(s_1))^2+y^2(s_1)} \right] U ds_1 \\
&+ \int_{-l}^{l} \frac{\psi_{2x}(x_2-x) - \phi_{2x}h}{(x_2-x)^2+h^2} dx_2 \\
&+ U\left\{ \tan^{-1}\frac{h}{x-l} + \tan^{-1}\frac{h}{x+l} \right\}.
\end{aligned} \tag{6.42}$$

We can see that as $x \to \infty$, the left-hand side of (6.42) tends to 0, then $q(x) \to U$.

The physical condition (6.12) and Bernoulli's condition (6.13) imply that

$$p_1 - p_2 = 1 - U^2 - (\phi_{1x}^2 - \phi_{2x}^2), \quad \text{for} \quad z = x+ih, \ |x|<l \tag{6.43}$$

and

$$1 - U^2 - (\phi_{1x}^2 - \phi_{2x}^2) = k\psi_x, \quad \text{for} \quad z = x+ih, \ |x|<l. \tag{6.44}$$

Substituting (6.27) and (6.35) into the above equation (6.44) gives

$$\begin{aligned}
&\left(\frac{1}{\pi} \int_{-l}^{l*} \frac{\psi_{1x}}{x_2-x} dx_2 + F_1(x,h) \right)^2 - \left(-\frac{1}{\pi} \int_{-l}^{l*} \frac{\psi_{2x}}{x_2-x} dx_2 + F_2(x,h) \right)^2 \\
&= 1 - U^2 - k\psi_x
\end{aligned} \tag{6.45}$$

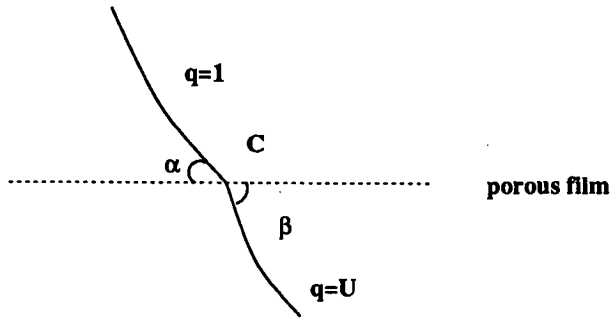

Figure 6–7: The flow angles at film

which reduces further to

$$\left(\frac{1}{\pi}\int_{-l}^{l*}\frac{2\psi_x}{x_2-x}dx_2 + F_1(x,h) - F_2(x,h)\right)\cdot(F_1(x,h)+F_2(x,h))$$
$$= 1 - U^2 - k\psi_x. \tag{6.46}$$

The width of the wetted portion of the fluid jet across the porous film is unknown. However, the Mass Conservation Law implies that, along the porous film,

$$\int_{-l}^{l}\psi_x(x)dx = 2. \tag{6.47}$$

Thus the free surface problem for a fluid jet passing through the film and then impinging on the wall is governed by equations (6.40), (6.41), (6.42), (6.46) and (6.47), together with (6.28) and (6.36).

The parameter U is determined as part of the solutions to the system of equations in which the height of the film h and the impermeability constant k are specified. When the fluid passes through the porous film, the fluid angle along the free surface also has a jump. Let α denote the fluid angle along the free surface at the film in the upstream region, β the fluid angle at the film in the downstream region shown in Fig. 6–7. The continuity of normal velocity gives

$$\sin\alpha = U\sin\beta \tag{6.48}$$

from which α and β may be found as

$$\phi_{1x}(x,h) \longrightarrow \phi_{1x}(l,h) = \cos\alpha, \quad \text{as} \quad x \longrightarrow l, \tag{6.49}$$

$$\frac{\phi_{2x}(x,h)}{\psi_x(x,h)} \longrightarrow \frac{\phi_{2x}(l,h)}{\psi_x(l,h)} = -\tan\beta, \quad \text{as} \quad x \longrightarrow l. \tag{6.50}$$

We also have from $U = |dw/dz|$ on CH, the formula

$$U^2 = \phi_{2x}^2(l,h) + \psi_x^2(l,h). \tag{6.51}$$

6.3 The Singularities in the Integrals

There exist a few singularities in taking the integrals around corners as well as in the Cauchy principal value integral. We first consider, from equation (6.27),

$$\begin{aligned} I_0 &= \int_{x-\epsilon}^{x+\epsilon} \frac{\psi_x(x_2)}{x_2 - x} dx_2 \\ &= \int_{x-\epsilon}^{x+\epsilon} \frac{\psi_x(x_2) - \psi_x(x)}{x_2 - x} dx_2 + \psi_x(x) \int_{x-\epsilon}^{x+\epsilon} \frac{dx_2}{x_2 - x} \\ &= \psi_x(x+\epsilon) - \psi_x(x-\epsilon) + O(\epsilon^3) \end{aligned} \tag{6.52}$$

where the integrand is expanded using Taylor series up to $O(\epsilon^2)$. This technique can also apply to (6.35) and we do not repeat the similar analysis.

In equation (6.27), the integral near $x = -l$ is

$$\begin{aligned} \int_{-l+\epsilon}^{-l+h_0} \frac{\psi_x}{x_2 - (-l)} dx_2 &= \int_{-l+\epsilon}^{-l+h_0} \frac{\psi_x(x_2) - \psi_x(-l)}{x_2 - (-l)} dx_2 + \psi_x(-l) \int_{-l+\epsilon}^{-l+h_0} \frac{dx_2}{x_2 + l} \\ &= \int_{-l+\epsilon}^{-l+h_0} \psi_{xx}(-l)(h_0 - \epsilon) + \psi_x(-l) \int_{-l+\epsilon}^{-l+h_0} \frac{dx_2}{x_2 + l} + O(h_0^2) \\ &= \psi_x(-l+h) - \psi_x(-l+\epsilon) + \psi_x(-l) \int_{\epsilon}^{h_0} \frac{du}{u}. \end{aligned} \tag{6.53}$$

At the same point, $F_1(x,h)$ in (6.28) also has a singularity. We consider

$$\begin{aligned} I_1 &= -\frac{1}{\pi} \int_{-h_1}^{0} \frac{(x(s) - x)\cos\theta(s) + (y(s) - h)(1 + \sin\theta(s))}{(x(s) - x)^2 + (y(s) - h)^2} ds \\ &= -\frac{1}{\pi} \int_{-h_1}^{0} \frac{\frac{x(s) - x}{s}\cos\theta(s) + \frac{y(s) - h}{s}(1 + \sin\theta(s))}{\left(\frac{x(s) - x}{s}\right)^2 + \left(\frac{y(s) - h}{s}\right)^2} \frac{ds}{s}. \end{aligned} \tag{6.54}$$

The integrand may be approximated by a using Taylor series up to second order as

$$\frac{x(s)-(-l)}{s} \sim x'(-l)+\frac{x''(-l)}{2}s+O(|s|^2), \tag{6.55}$$

$$\frac{y(s)-h}{s} \sim y'(-l)+\frac{y''(-l)}{2}s+O(|s|^2). \tag{6.56}$$

Substituting (6.55) and (6.56) into (6.54), we have

$$\begin{aligned} I_1 &= -\frac{1}{\pi}\int_{-h_1}^{0} \frac{\left(x'(-l)+\frac{x''(-l)}{2}s\right)\cos\theta(s)+\left(y'(-l)+\frac{y''(-l)}{2}s\right)(1+\sin\theta(s))+O(|s|^2)}{(x'(-l))^2+2x'(-l)\frac{x''(-l)}{2}s+(y'(-l))^2+2y'(-l)\frac{y''(-l)}{2}s+O(|s|^2)}\frac{ds}{s} \\ &= -\frac{1}{\pi}\int_{-h_1}^{0} \frac{\cos\theta(0)\cos\theta(s)+\sin\theta(0)\sin\theta(s)+\sin\theta(0)+\frac{y''(-l)}{2}s+O(|s|^2)}{1+O(|s|^2)}\frac{ds}{s} \\ &= -\frac{1}{\pi}\int_{-h_1}^{0}\left(\cos\theta(0)\frac{\cos\theta(s)-\cos\theta(0)}{s}+\sin\theta(0)\frac{\sin\theta(s)-\sin\theta(0)}{s}+\frac{1+\sin\theta(0)}{s}\right)ds \\ &\quad -\frac{y''(-l)}{2}h_1+O(|s|^2). \end{aligned} \tag{6.5}$$

The singular term in this integral is due to the integrand $1/s$ and after using Taylor series on the other terms, this integral reduces further to

$$\begin{aligned} I_1 &= -\frac{1}{\pi}\left(\int_{-h_1}^{\epsilon}\frac{1+\sin\theta(\epsilon)}{s}ds-\frac{y''(-l)}{2}h_1\right)+O(|s|^2) \\ &= (1+\sin\theta(\epsilon))\int_{\epsilon}^{h_1}\frac{s}{ds}+\frac{y'(-h_1)-y'(\epsilon)}{2}+O(|s|^2) \\ &= \frac{1}{\pi}\left(\log\frac{h_1}{u}\Big|_{u\to 0}+\sin\theta(\epsilon)\int_{\epsilon}^{h_1}\frac{ds}{s}+\frac{y'(-h_1)-y'(\epsilon)}{2}\right)+O(|h_1|^2). \end{aligned} \tag{6.58}$$

The last term in (6.28) as $x \to -l$ cancels with $-\log u$ as $u \to 0$ in this equation. Since $\sin\theta(\epsilon) \to -\psi_x(-l)$ as $\epsilon \to 0$, the singularity of the second term in this equation cancels the last term in (6.53). Thus we show that the singularity at the corner in (6.27) is approximated by

$$\begin{aligned} &\psi_x(-l+h)-\psi_x(-l)+\psi_x(-l)\log h_0+\log h_1 \\ &+\sin\theta(0)\log h_1+\frac{y'(-h_1)-y'(\epsilon)}{2}. \end{aligned} \tag{6.59}$$

Applying similar analysis to the singularity in (6.35) gives

$$I_2 = \frac{1}{\pi}\int_0^{h_2} \frac{\frac{x(s)-x}{s}\sin\theta(s) - \frac{y(s)-h}{s}(1+\cos\theta(s))}{\left(\frac{x(s)-x}{s}\right)^2 + \left(\frac{y(s)-h}{s}\right)^2}\frac{ds}{s}$$

$$= \frac{1}{\pi}\left(\theta'(0)h_2 - y'(0)(\log h_2 - \log\epsilon) - y''(0)\frac{h_2}{2}\right) + O(|h_2|^2), \quad (6.60)$$

where the term with $\log\epsilon$ cancels with the same term shown in (6.53). Using a similar method on the Cauchy principal value integral in (6.40) yields

$$I_3 = \int_{s-\epsilon}^{s+\epsilon} \frac{\frac{x(s)-x(s_1)}{s-s_1}\cos\theta(s) + \frac{y(s)-y(s_1)}{s-s_1}(1+\sin\theta(s))}{\left(\frac{x(s)-x(s_1)}{s-s_1}\right)^2 + \left(\frac{y(s)-y(s_1)}{s-s_1}\right)^2}\frac{ds_1}{s-s_1}$$

$$= -\frac{y''(s)}{2}2\epsilon + O(\epsilon^2). \quad (6.61)$$

All the above analysis may be used in the following section in computing.

6.4 Numerical Method and Results

We first make a guess of the shape of the free surface, for instance, we could take the shape of the free surface of a jet impinging on a wall as a start. The equation (6.46) is solved to obtain the normal speed along the porous film

$$\psi_{x1}, \psi_{x2}, \cdots, \psi_{xm}, l. \quad (6.62)$$

We substitute these into equations (6.40) and (6.41). Solving these equations yields

$$\theta_{1,1}, \theta_{1,2}, \cdots, \theta_{1,N1}$$
$$\theta_{2,1}, \theta_{2,2}, \cdots, \theta_{2,N2} \quad (6.63)$$

for the upper and lower free surfaces. We obtain the shapes of the free surface using (6.20) and we therefore have (6.28) and (6.36). We then substitute these into

(6.44) to solve this equation again to get a new normal speed along the porous film. Thus we complete the first iteration. The discretized forms of equations (6.20) are

$$x(s_i) = \Delta \sum_{j=0}^{i} \omega_j \cos\theta_j - 1, \quad y(s_i) = \Delta \sum_{j=0}^{i} \Omega_j \sin\theta_j + h \tag{6.64}$$

where Δ is the step length, ω_j and Ω_j are the weights.

The integral domains along the free surface are truncated using $(s_{N_1}, 0)$ for $(-\infty, 0)$ and $(0, s_{N_2})$ for $(0, \infty)$. The integral on $[-l, l]$ is transformed using $x = \hat{x} \cdot l$ where $\hat{x} \in [-1, 1]$.

The mesh points are respectively

$$\hat{x}_i = (i-1)\Delta, \quad i = 1, \cdots, K, \quad \Delta = \frac{1}{K-1},$$
$$\text{on the porous film,} \tag{6.65}$$

$$s_{1j} = -(j-1)\Delta_1, \quad j = 1, \cdots, N_1, \quad -(N_1 - 1)\Delta = s_{N_1},$$
$$\text{on the upper free surface,} \tag{6.66}$$

$$s_{2j} = (j-1)\Delta_2, \quad j = 1, \cdots, N_2, \quad (N_2 - 1)\Delta = s_{N_2},$$
$$\text{on the lower free surface,} \tag{6.67}$$

$$\bar{x}_i = (i-1)\Delta_3, \quad i = 1, \cdots, N_3, \quad (N_3 - 1)\Delta = \bar{x}_{N_3},$$
$$\text{on the flat wall } y = 0. \tag{6.68}$$

The discretized form of equation (6.46) is

$$\left(\frac{1}{\pi}\left(\sum_{j=1}^{i-1} \hat{\psi}_{xj} \frac{2\hat{x}_i\Delta}{\hat{x}_j^2 - \hat{x}_i^2} + \sum_{j=i+1} K\hat{\psi}_{xj} \frac{2\hat{x}_i\Delta}{\hat{x}_j^2 - \hat{x}_i^2} + \int_{\hat{x}_{i-1}}^{\hat{x}_{i+1}*} \hat{\psi}_x \frac{2\hat{x}_i d\hat{x}}{\hat{x}^2 - \hat{x}_i^2}\right) + F_1(\hat{x}_i l, h) - F_2(\hat{x}_i l, h)\right)$$
$$(F_1(\hat{x}_i l, h) + F_2(\hat{x}_i l, h)) = 1 - U^2 - k\hat{\psi}_{xi},$$
$$i = 1, \cdots, K \tag{6.69}$$

where the discretized functions $F_1(\hat{x}_i l, h)$ and $F_2(\hat{x}_i l, h)$ can be obtained using (6.28) and (6.36). The integral term is treated using (6.52) in section 6.3.

The discretized form of equation (6.40) is

$$
\begin{aligned}
&\pi\cos\theta(s_{1j}) = \\
&\Delta_1\sum_{i=1}^{j-1}\omega_i\frac{(x(s_{1j})-x(s_{1i}))\cos\theta(s_{1i})+(y(s_{1j})-y(s_{1i}))(1+\sin\theta_i)}{(x(s_{1j})-x(s_{1i}))^2+(y(s_{1j})-y(s_{1i}))^2} \\
&+\Delta_1\sum_{j+1}^{N_1}\omega_i\frac{(x(s_{1j})-x(s_{1i}))\cos\theta(s_{1i})+(y(s_{1j})-y(s_{1i}))(1+\sin\theta(s_{1i}))}{(x(s_{1j})-x(s_{1i}))^2+(y(s_{1j})-y(s_{1i}))^2} \\
&+\Delta_1\sum_{i=1}^{N_1}\omega_i\frac{(x(s_{1j})+x(s_{1i}))\cos\theta(s_{1i})-(y(s_{1j})-y(s_{1i}))(1+\sin\theta(s_{1i}))}{(x(s_{1j})+x(s_{1i}))^2+(y(s_{1j})-y(s_{1i}))^2} \\
&+\Delta\sum_{i=1}^{K}\hat{\Omega}_i\left[\frac{\hat{\psi}_{1xi}(\hat{x}_i l-x_j(s))-\hat{\phi}_{1xi}(h-y_j(s))}{(\hat{x}_i l-x_j(s))^2+(h-y_j(s))^2}\right. \\
&\left.-\frac{\hat{\psi}_{1xi}(\hat{x}_i l+x_j(s))-\hat{\phi}_{1xi}(h-y_j(s))}{(\hat{x}_i l+x_j(s))^2+(h-y_j(s))^2}\right]+\int_{s_{j-1}}^{s_{j+1}*}\frac{G_1(s_{1j},s)}{s_j-s}ds
\end{aligned}
\tag{6.70}
$$

where $\hat{\phi}_x = \phi_x(\hat{x}l, y)$, $\hat{\psi}_x = \psi_x(\hat{x}l, y)$ and

$$
G_1(s_{1j},s) = \frac{\frac{x(s_{1j})-x(s)}{s_{1j}-s}\cos\theta(s)+\frac{y(s_{1j})-y(s)}{s_{1j}-s}(1+\sin\theta(s))}{\left(\frac{x(s_{1j})-x(s)}{s_{1j}-s}\right)^2+\left(\frac{y(s_{1j})-y(s)}{s_{1j}-s}\right)^2}. \tag{6.71}
$$

The integral term in (6.70) is treated using (6.61) in section 6.3.

The discretized form of equation (6.41) is

$$
\begin{aligned}
&\pi\cos\theta(s_{2j}) = \\
&\Delta_2\sum_{i=1}^{j-1}\hat{\omega}_i\frac{-(x(s_{2j})-x(s_{2i}))\sin\theta(s_{2i})+(y(s_{2j})-y(s_{2i}))(1+\cos\theta_i)}{(x(s_{2j})-x(s_{2i}))^2+(y(s_{2j})-y(s_{2i}))^2} \\
&+\Delta_2\sum_{j+1}^{N_2}\hat{\omega}_i\frac{-(x(s_{2j})-x(s_{2i}))\sin\theta(s_{2i})-(y(s_{2j})-y(s_{2i}))(1+\cos\theta(s_{2i}))}{(x(s_{2j})-x(s_{2i}))^2+(y(s_{2j})-y(s_{2i}))^2} \\
&-\Delta_2\sum_{i=1}^{N_2}\hat{\omega}_i\frac{(x(s_{2j})+x(s_{2i}))\sin\theta(s_{2i})-(y(s_{2j})-y(s_{2i}))(1+\cos\theta(s_{2i}))}{(x(s_{2j})+x(s_{2i}))^2+(y(s_{2j})-y(s_{2i}))^2} \\
&+\frac{4\Delta_3}{U}\sum_{i=1}^{N_3}\delta_i\frac{\bar{x}_i x(s_{2j})y(s_{2j})(q(\bar{x}_i)-U)}{(\bar{x}_i^2-x^2(s_{2j})+y^2(s_{2j}))^2+4x^2(s_{2j})y^2(s_{2j})} \\
&-\frac{\Delta}{U}\sum_{i=1}^{K}\Omega_i\left[\frac{\hat{\psi}_{2xi}(\hat{x}_i l-x_j(s))-\hat{\phi}_{2xi}(h-y(s_{2j}))}{(\hat{x}_i l-x(s_{2j}))^2+(h-y(s_{2j}))^2}\right.
\end{aligned}
$$

$$-\frac{\hat{\psi}_{2xi}(\hat{x}_i l + x(s_{2j})) - \hat{\phi}_{2xi}(h - y(s_{2j}))}{(\hat{x}_i l + x(s_{2j}))^2 + (h - y(s_{2j}))^2}\Bigg] + \int_{s_{2(j-1)}}^{s_{2(j+1)^*}} \frac{G_2(s_{2j}, s)}{s_{2j} - s} ds$$
$$+ \tan^{-1}\frac{y(s_{2j}) - h}{x(s_{2j}) - l} + \tan^{-1}\frac{y(s_{2j}) - h}{x(s_{2j}) + l} - 2\tan^{-1}\frac{y(s_{2j})}{x(s_{2j})}, \tag{6.72}$$

where

$$G_2(s_{2j}, s) = \frac{-\dfrac{x(s_{2j}) - x(s)}{s_{2j} - s}\sin\theta(s) + \dfrac{y(s_{2j}) - y(s)}{s_{2j} - s}(1 + \cos\theta(s))}{\left(\dfrac{x(s_{2j}) - x(s)}{s_{2j} - s}\right)^2 + \left(\dfrac{y(s_{2j}) - y(s)}{s_{2j} - s}\right)^2} \tag{6.73}$$

and $q(\bar{x}_i)$ can be obtained from

$$\begin{aligned}
\pi(q(\bar{x}_i) - U) &= \Delta_2 \sum_{j=1}^{N_2} \hat{\omega}_j \left[\frac{\sin\theta(s_{2j})(\bar{x}_i - x(s_{2j})) + (1 + \cos\theta(s_{2j}))y(s_{2j})}{(\bar{x}_i - x(s_{2j}))^2 + y^2(s_{2j})}\right. \\
&+ \left.\frac{\sin\theta(s_{2j})(x(s_{2j}) - \bar{x}_i) - (1 + \cos\theta(s_{2j}))y(s_{2j})}{(\bar{x}_i + x(s_{2j}))^2 + y^2(s_{2j})}\right] U \\
&+ \sum_{k=1}^{K} \Delta l \left[\frac{\psi_{2x}(x_k l - \bar{x}_i) - \phi_{2x} h}{(x_k l - \bar{x}_i)^2 + h^2} - \frac{\psi_{2x}(x_k l + \bar{x}_i) - \phi_{2x} h}{(x_k l + \bar{x}_i)^2 + h^2}\right] \\
&+ U\left\{\tan^{-1}\frac{h}{\bar{x}_i - l} + \tan^{-1}\frac{h}{\bar{x}_i + l}\right\}.
\end{aligned} \tag{6.74}$$

For the case that the parameter $h = 4.8$, we chose $N_1 = 20$ and $N_2 = 40$ and $K = 10$. We also selected different impermeability constants with $k = 0.11$ and $k = 0.20$. The results are shown in Figure 6–8. In Figure 6–9, we can see clearly that immediately before jets pass through the film, the computed shapes of the free surface become swollen and then after the jets pass through the film, the shapes of the free surface become slightly contracted. For $h = 5.8$ and $k = 0.11$, Figure 6–12 also shows that the width of the jet becomes slightly large around the film. We also compute the jet passing through the film at height $h = 5.8$ and $k = 0.18$, shown in Figure 6–13. A comparison of these two jets for $h = 5.8$, with $k = 0.11$ and $k = 0.18$ is shown in Figure 6–14.

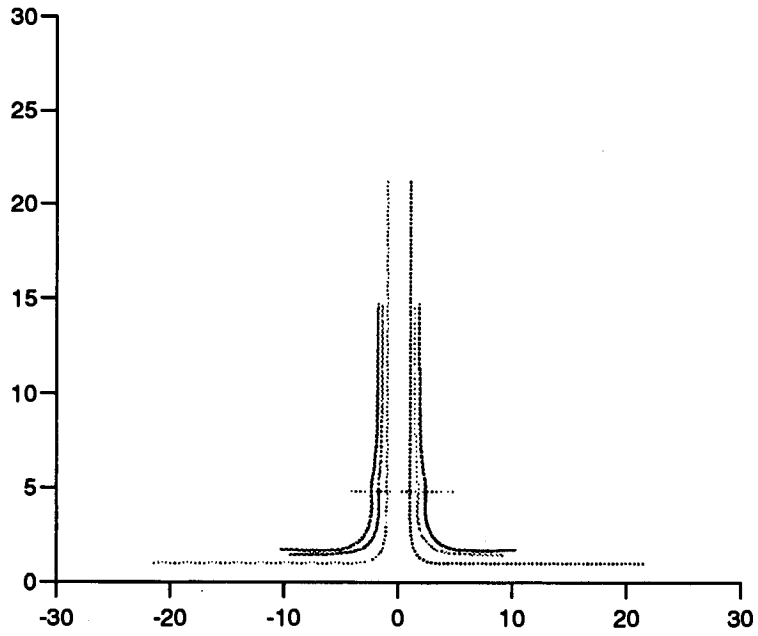

Figure 6–8: The physical-plane of a jet passing through a porous film at height $h = 4.8$ and then impinging on a flat wall where the outside lines correspond to impermeability constant $k = 0.2$, the inside lines correspond to $k = 0$ and the lines between them correspond to $k = 0.11$.

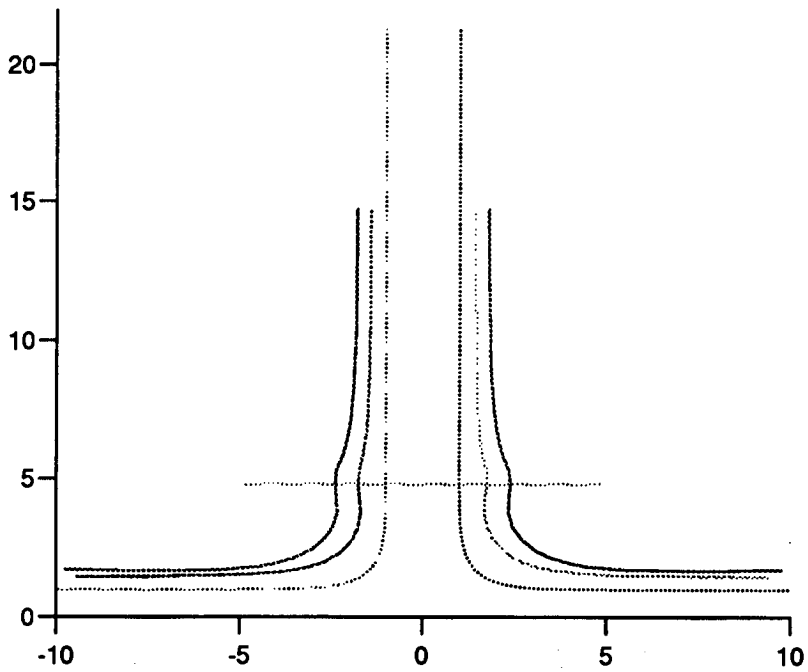

Figure 6–9: The physical-plane of Figure 6-8 is in the different scale.

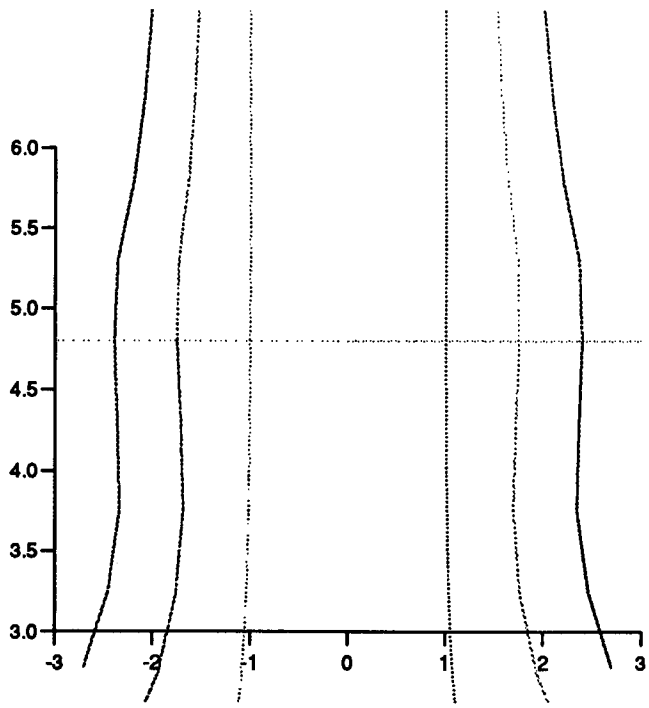

Figure 6–10: The part around film of the Figure 6-8.

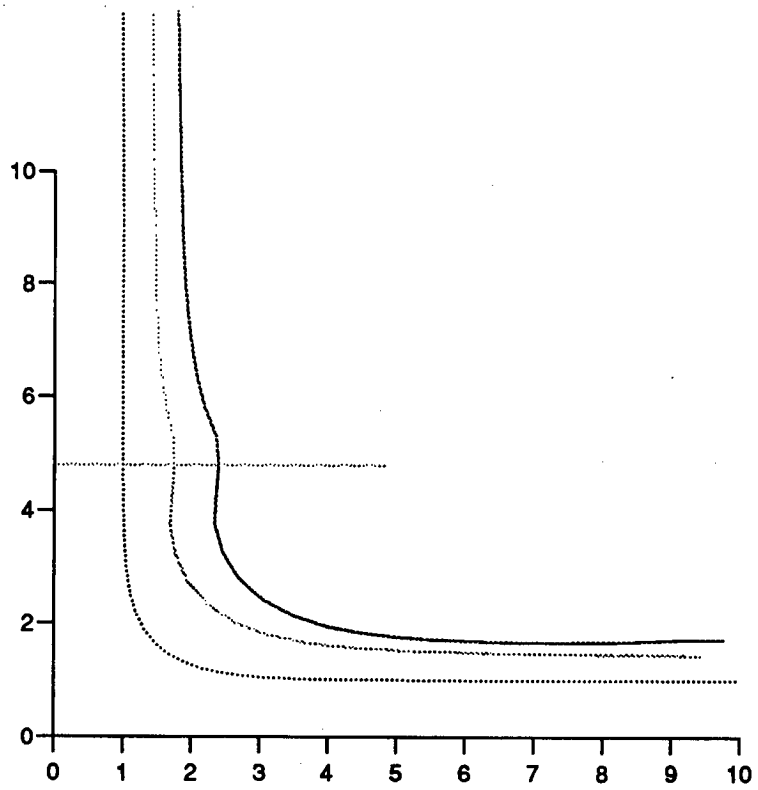

Figure 6–11: The right part of Figure 6-8.

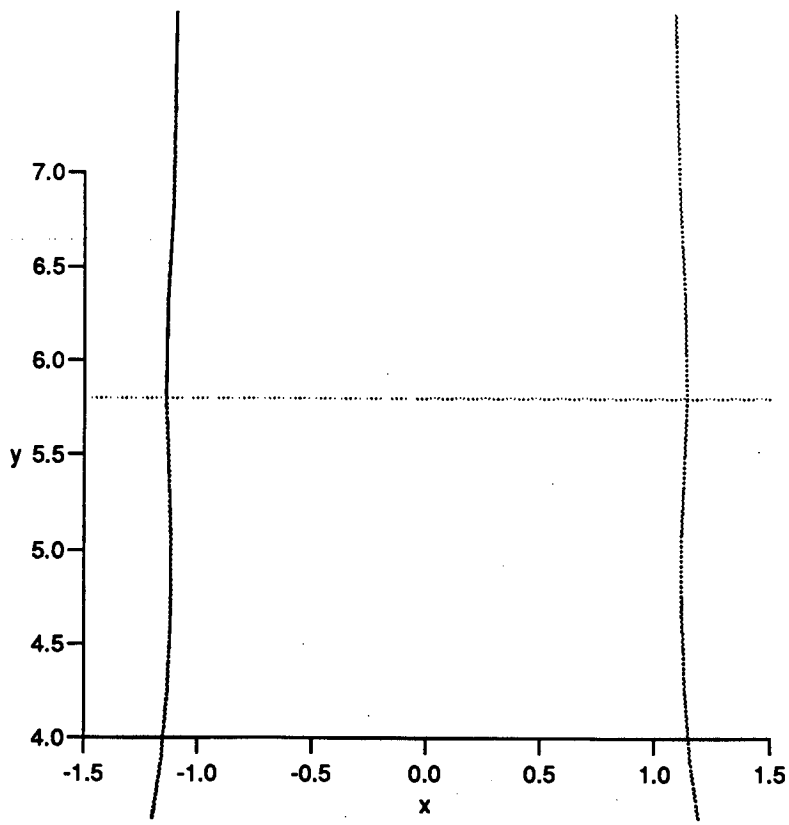

Figure 6–12: A jet passing through a porous film at height $h = 5.8$ and then impinging on a flat wall with impermeability constant $k = 0.11$.

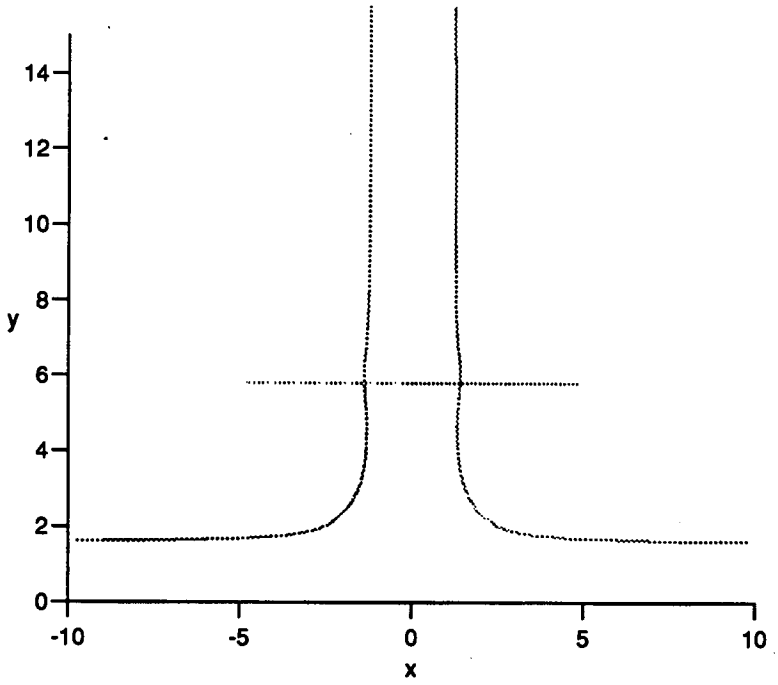

Figure 6–13: A jet passing through a porous film at height $h = 5.8$ and then impinging on a flat wall with impermeability constant $k = 0.18$.

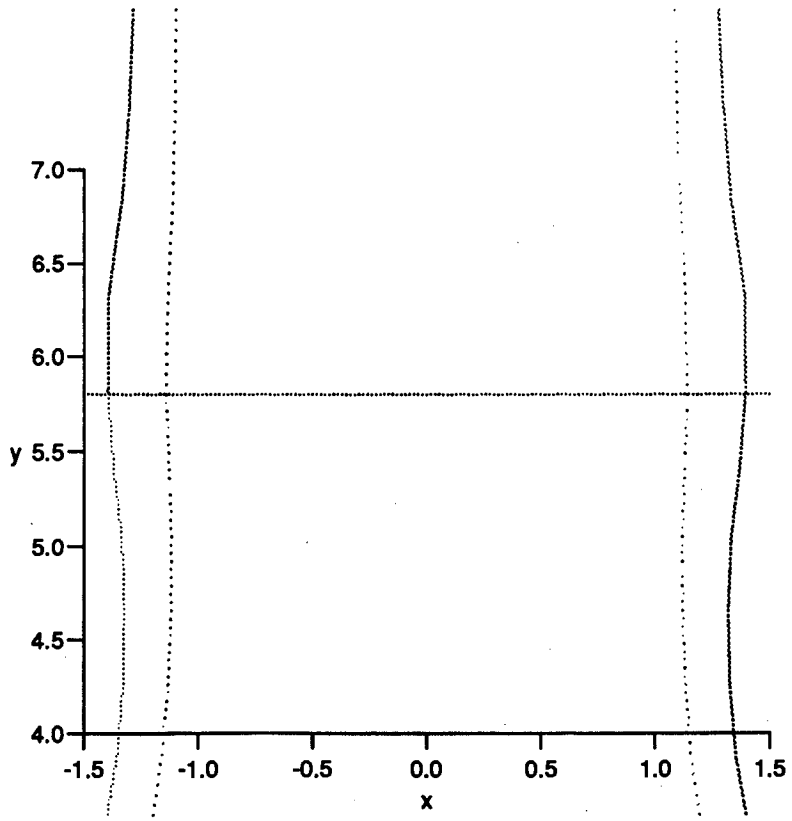

Figure 6–14: Two jets passing through a porous film ($h = 5.8$) and then impinging on a flat wall with $k = 0.18$ (—) and $k = 0.11$ ($\cdots$).

Chapter 7

Conclusions and Remarks

This study is mainly concerned with the free surface problem of a jet impinging on various objects. When the problems of jet impact on a porous wall with prescribed normal speed, of an ideal jet incident on an uneven wall and of a fluid jet passing through a porous film were considered, we could try to use classical hodograph methods by which many free surface problems in fluid mechanics have been previously solved. However, since the boundary conditions are complicated, the relevent hodograph planes no longer have simple geometric shapes. The mapping which transforms the hodograph planes onto a reference plane becomes difficult, if not impossible, to find. The generalized Schwartz-Christoffel formula, given by Woods in 1955, has been extensively used by King and Bloor recently. This technique, however, can be applied in many free surface problems with complicated boundary conditions. We used such transformations in the formulation of a jet incident on a porous wall through which the normal flow velocity is prescribed and of a jet flow impinging on an uneven wall. In the former case, we extended King's method to the case when the jet flow on the wetted part of wall has non-constant normal velocity. The problem is formulated by a system of integral equations. In the case of constant normal velocity, the problem reduces to a single nonlinear integral equation. A numerical scheme is provided. For a few different non-constant

normal velocities, the free surface shapes were computed, showing that our method is plausible and practicable. The formulation has also been developed to consider the effect of gravity, which indicates an alternative computation method other than the fixed domain method. In the case of a jet impinging on an uneven wall, the transformation technique and boundary integral method are used to formulate the problem. We first employed a solution of an integral equation to obtain some analytic results, among which a jet impinging on a flat wall is revisited. In the symmetric case the problem is formulated by a system of integro-differential equations.

When the wall is asymmetric, to determine the position of the stagnation point, an integral form of the momentum equation is used to give a condition which shows how the wall shape affects the location of the stagnation point. This is a necessary ingredient of the formulation and of the computation.

Steady two-dimensional free surface jet flow passing through the porous film has also been investigated analytically and numerically. The Cauchy boundary integral technique used to reduce the physical problem to a system of integral equations, can also be used to deal with any polygonal or curved boundary. The numerical solutions show that, as the impermeability increases, the width of the blocked upper flow around the film grows wider. The flow immediately behind the porous film tends to contract, which indicates the average normal velocity is growing there. The boundary integral method used to formulate the physical problem may be applied to other free surface problems of obstructed fluid flow. Because of the discontinuity of the flow velocity and pressure, the complex potential plane and hodograph plane are divided into two parts, therefore the hodograph method fails to attack this problem. Although the generalized Schwartz-Christoffel formula can apply to it, the formulation leads to a difficult numerical problem.

Appendix A

The flow angle $\theta(t)$ on the wall satisfies $|\theta(t)| < \pi$ so that from (4.13) one obtains

$$g(x) \leq \frac{1}{\pi}\int_{-1}^{1}\frac{\pi}{1-xt}dt = G(x) = -\frac{1}{x}\log\frac{1-x}{1+x}. \tag{A1}$$

To show that $g(x)$ is square integrable, we let $G_1(x) = x^{-1}\log(1-x)$, and then show that $G_1(x)$ is square integrable on $[-1,1]$. $G_1(x)$ has singularities at $x = 0, 1$, but

$$\begin{aligned}\int_{-1}^{1}|G_1(x)|^2dx &= \int_{-1}^{1}\frac{1}{x^2}(\log(1-x))^2dx \\ &= \int_{c}^{1}\frac{1}{x^2}(\log(1-x))^2dx + \int_{-1}^{c}\frac{1}{x^2}(\log(1-x))^2dx, \end{aligned}\tag{A2}$$

where c is an arbitrary constant in $(0,1)$. The integrand in the second integral of $(A2)$ is bounded, while the first integral may be rearranged as

$$\begin{aligned}I_1 &= \int_{c}^{1}\frac{1}{x^2}(\log(1-x))^2dx \\ &= \frac{1-c}{c^2}[(\log(1-c))^2] - 2\int_{c}^{1}\frac{(1-x)(\log(1-x))^2}{x^3}dx \\ &\quad -2\int_{c}^{1}\frac{\log(1-x))}{x^2}dx, \end{aligned}\tag{A3}$$

where the last integral in (A3) is

$$\begin{aligned}\int_{c}^{1}\frac{1}{x^2}\ln(1-x)dx &= \left[\left(-\frac{1}{x}+1\right)\right]_{c}^{1} - \int_{c}^{1}\left(\frac{x-1}{x}\right)\frac{-1}{1-x}dx \\ &= 0 - \frac{c-1}{c}\ln(1-c) - \int_{c}^{1}\frac{dx}{x} \\ &= -\frac{c-1}{c}\ln(1-c) + \ln c \\ &= \frac{1}{c}\ln(1-c) + \ln\left(\frac{c}{1-c}\right). \end{aligned}\tag{A4}$$

The integrands in $(A3)$ are bounded functions on $[c,1]$. Consequently the integral I_1 is bounded so showing that $G_1(x)$ is square integrable. Similarly, $G_1(-x)$ is square integrable so that $G(x) = -[G_1(x) + G_1(-x)]$ is square integrable.

Appendix B

Since equations (4.15) and (4.16) are equivalent, we treat only equation (4.16). Substituting (4.11) into (4.16) and interpreting ϕ in term of θ through $\theta(s^{-1}) = s\phi(s)$ gives

$$\begin{aligned}\xi\theta(\xi) &= -\frac{1}{\pi}\left[\int_{\infty}^{1*}\left(\frac{\xi^2-1}{(t^2-1)\xi^2}\right)^{\frac{1}{2}}\frac{\xi g(t^{-1})}{t-\xi}(-dt)\right. \\ &\qquad \left.+\int_{-1}^{-\infty*}\left(\frac{\xi^2-1}{(t^2-1)\xi^2}\right)^{\frac{1}{2}}\frac{\xi g(t^{-1})}{t-\xi}dt\right]. \qquad \text{(B1)}\end{aligned}$$

For $\xi > 1$, equation(B1) becomes

$$\begin{aligned}\xi\theta(\xi) &= -\frac{1}{\pi}\left[\int_{1}^{\infty*}\left(\frac{\xi^2-1}{(t^2-1)}\right)^{\frac{1}{2}}\frac{g(t^{-1})}{t-\xi}dt - \int_{-\infty}^{-1*}\left(\frac{\xi^2-1}{(t^2-1)}\right)^{\frac{1}{2}}\frac{g(t^{-1})}{t-\xi}dt\right] \\ &= \frac{1}{\pi}(\xi^2-1)^{\frac{1}{2}}\left(\int_{-\infty}^{-1*}-\int_{1}^{\infty*}\right)\frac{1}{(t^2-1)^{\frac{1}{2}}}\frac{tF(t)}{t-\xi}dt, \quad \xi > 1. \qquad \text{(B2)}\end{aligned}$$

In the latter equality of (B2), equation (12) is used to replace $g(t^{-1})$ by $tF(t)$. For $\xi < -1$, similarly one obtains

$$\xi\theta(\xi) = -\frac{1}{\pi}(\xi^2-1)^{\frac{1}{2}}\left(\int_{-\infty}^{-1*}-\int_{1}^{\infty*}\right)\frac{1}{(t^2-1)^{\frac{1}{2}}}\frac{tF(t)}{t-\xi}dt, \quad \xi < -1. \qquad \text{(B3)}$$

In the symmetric case, equation (B2) can be written as

$$\begin{aligned}\theta(\xi) &= \frac{(\xi^2-1)^{\frac{1}{2}}}{\pi\xi}\int_{1}^{\infty*}\frac{1}{(t^2-1)^{\frac{1}{2}}}\left(\frac{1}{\xi-t}+\frac{1}{\xi+t}\right)tF(t)dt \\ &= \frac{(\xi^2-1)^{\frac{1}{2}}}{\pi}\int_{1}^{\infty*}\frac{1}{(t^2-1)^{\frac{1}{2}}}\frac{2t}{\xi^2-t^2}F(t)dt \\ &= \frac{1}{\pi}\frac{(\xi^2-1)^{\frac{1}{2}}}{\xi-1}\int_{1}^{\infty*}\frac{1}{(t^2-1)^{\frac{1}{2}}}\frac{2t(\xi-1)}{\xi^2-t^2}F(t)dt \\ &= \frac{1}{\pi}\left(\frac{\xi+1}{\xi-1}\right)^{\frac{1}{2}}\int_{1}^{\infty*}\frac{1}{(t^2-1)^{\frac{1}{2}}}\left(\frac{t-1}{\xi-t}+\frac{t+1}{\xi+t}\right)F(t)dt \\ &= \frac{1}{\pi}\left(\frac{\xi+1}{\xi-1}\right)^{\frac{1}{2}}\int_{1}^{\infty*}\left[\left(\frac{t-1}{t+1}\right)^{\frac{1}{2}}\frac{F(t)}{\xi-t}+\left(\frac{t+1}{t-1}\right)^{\frac{1}{2}}\frac{F(t)}{\xi+t}\right]dt, \\ &\qquad 1 < \xi < \infty. \qquad \text{(B4)}\end{aligned}$$

References

Batchelor, G. B. 1969 *Introduction to Fluid Dynamics*, Cambridge University Press.

Belward, S. R. and Forbes, L. K. 1993 Fully non-linear two layer flow over arbitrary topography *J. Eng. Math.* **27** 419-432

Benjamin, T. B., 1970 Upstream influence *J. Fluid Mech.*, **40**, 49-79

Benjamin, T. B. and Lighthill, M. J. 1954 On cnoidal waves and bores. *Proc. Roy. Soc. Lond.*, , **Ser. A 224**, 448-460

Birkhoff, G. and Zarantonello, E. H., 1957 *Jets, Wakes and Cavities*, Academic, New York

Bloor, M. I. G., 1978 Large amplitude surface waves. *J. Fluid Mech.*, **84**, 167-179

Boutrous, Y. Z. and El-Malek, M., 1987 *Comput. Math. Appl. Mech. Engng* , **65**, 215

Brodesky, S., 1923 *Proc. Roy. Soc. Lond.*, **Ser. A 102**, 542-553

Byatt-Smith, J. G. B., 1970 An exact integral equation for steady surface waves *Proc. Roy. Soc. Lond.*, **A. 315** , 405-418

Cokelet, E. D., 1977 Steep gravity waves in water of arbitrary uniform depth *Phil. Trans. R. Soc. Lond.* , **A286**, 183

Crapper, D. G., 1957 An exact solution for progressive capillary waves of arbitrary amplitude. *J. Fluid Mech.*, **2**, 532-540

Davis, P. J. and Rabinowitz, P., 1984 *Methods of Numerical Integration* (2nd edition). Academic Press, New York

Dias, F. and Christodoulides, P., 1991 Ideal jet flow under gravity *Phys. Fluids*, **A3**, 1711-1717

Dias, F., Ekrat, A. R. and Trefethen, L. N., 1987 Ideal jet flow in two dimensions. *J. Fluid Mech.*, **185**, 275-288

Dias, F. and Ekrat, A. R., 1992 Ideal jet flow with a stagnation streamline. *Eur. J. Mech.* , **B11**, 233-247

Dias, F. and Tuck, E. O., 1991 Weirflow and water fall *J. Fluid Mech.*, **230**, 525-539

Dias, F. and Vanden-Broeck, J.-M., 1989 Open channel flows with submerged obstruction. *J. Fluid Mech.*, **206**, 155-190

Dias, F. and Vanden-Broeck, J.-M., 1990 Flows emerging from a nozzle and falling under gravity. *J. Fluid Mech.*, **213**, 465-477

Dias, F. and Vanden-Broeck, J.-M., 1993 Nonlinear bow flows with spray. *J. Fluid Mech.*, **255**, 91-102

Dobrovol'skaya, Z. N., 1969 On some problems of similarity flow of fluid with a free surface. *J. Fluid Mech.*, **36**, 805-829

Forbes, L. K., 1981 On the wave resistance of a submerged semi-elliptical body. *J. Engineering Math.*, **Vol. 15** 287-298

Forbes, L. K., 1989 Two layer critical flow over a semi-circular obstruction. *J. Engineering Math.*, **Vol. 23** 325-342

Forbes, L. K. and Schwartz, L. W., 1982 Free surface flow over a semi-circular obstruction. *J. Fluid Mech.*, **114**, 299-314

Gerber, R., 1955 *J. Math. Pure Appl.*, **9**, 185

Gurevich, M. I., 1965 *Theory of Jets in an Ideal Fluid*, Academic, New York

Hochstadt, H., 1973 *Integral Equations*, Wiley-Interscience, New York

Hocking, G. C., 1988 Infinite Froude number solutions to the problem of a submerged source or sink. *J. Austral. Math. Soc.*, **Ser. B29**, 401-409

Hunter, J. K. and Vanden-Broeck, J. M. 1983 Solitary and periodic gravity-capillary waves of finite amplitude. *J. Fluid Mech.*, **134**, 205-219

Jenkins, D. R. and Barton, N. G., 1989 Computation of the free surface shape of an inviscid jet incident on a porous wall. *IMA J. Appl. Math.*, **41**, 193-206

Keller, J. B., 1990 On unsymmetrically impinging jets. *J. Fluid Mech.*, **211**, 653-655

Kelvin, W., 1886 On stationary waves in flowing water. *Phil. Mag*, **22(5)**, 445

King, A. C. and Bloor, M. I. G., 1987 Free surface flow over a step. *J. Fluid Mech.*, **182**, 193-208

King, A. C. and Bloor, M. I. G., 1988 A note on the free surface induced by a submerged source at infinite Froude number *J. Austral. Math. Soc.*, **Ser. B30** 147-156

King, A. C. and Bloor, M. I. G., 1989 A semi-inverse method for free-surface flow over a submerged body. *Q. Jl Mech. Appl. Math.*, **Vol. 42** 183-202

King, A. C. and Bloor, M. I. G., 1990 Free-surface flow of a stream obstructed by an arbitrary bed topography. *Q. Jl Mech. Appl. Math.*, **Vol. 43** 87-106

King, A. C. and Bloor, M. I. G., 1990 Free streamline flow over curved topography. *Quart. Appl. Math.*, **XLVIII 2**, 281-293

King, A. C., 1990 A note on the impact of a jet on a porous wall. *IMA J. Appl.Math.*, **45**, 139-146

Lamb, H., 1932 *Hydrodynamics* (6th edition) , Cambridge Univ. Press

Longuet-Higgins, M. S., 1989 Capillary-gravity waves of solitary type on deep water. *J. Fluid Mech.*, **200**, 451-470

Martin, H. , Heat and mass transfer between impinging gas jets and solid surfaces. 1977 *Advances in Heat Transfer* (Edited by J.P. Hartneff and T.F. Irvine) Vol 13 pp 1-60 Academic Press, New York

Milne-Thomson, L. M., 1968 *Theoretical Hydrodynamics*, 5th edition Macmillan & Co Ltd, London

Naghdi, P. M. and Vonsarnpigoon, 1986 The downstream flow beyond an obstacle *J. Fluid Mech.*, **162**, 223-236

Ockendon, H. and Tayler, A. B., 1983 *Inviscid Fluid Flows.* Springer-Verlag, Berlin

Olmstead, W. E. and Raynor, S., 1964 Depression of an infinite liquid surface by an incompressible gas jet. *J. Fluid Mech.*, **19**, 561-576

Schwartz, L. W., 1974 Computer extension and analytic continuation of Stokes' for gravity waves *J. Fluid Mech.*, **62** 553-578

Schwartz, L. W., 1981 Nonlinear solution for an applied overpressure on a moving stream *J. Eng. Math.*, **15** No. 2 147-156

Schwartz, L. W. and Vanden-Broeck, J.-M., 1979 Numerical solution of the exact equations for capillary-gravity waves. *J. Fluid Mech.*, **95** 119-139

Stevens, J. and Webb, B.W., 1992 Measurements of the free surface flow structure under an impinging, free liquid jet. *J. Heat Transfer* Trans. ASME **114**(1), 79-84

Stokes, G. G., 1847 On the theory of oscillatory waves. *Trans. Camb. Phil. Soc.*, **8**, 441

Stokes, G. G., 1880 Supplement to a paper on the theory of oscillatory waves. In *Mathematical and Physical Papers*, **Vol. 1**, Cambridge Univ. Press

Tricomi F. G., 1957 *Integral Equations*, Interscience, New York

Tuck, E. O., 1987 Efflux from a slit in a vertical wall *J. Fluid Mech.*, **176** 253-264

Tuck, E. O and Vanden-Broeck, J.-M., 1984 A cusplike free-surface flow due to a submerged source or sink *J. Austral. Math. Soc.* , **Ser. B25** 443-450

Vanden-Broeck, J.-M., 1980 Nonlinear stern waves *J. Fluid Mech.*, **96** 603-611

Vanden-Broeck, J.-M., 1993 Two-dimensional jet aimed vertically upwards *J. Austral. Math. Soc.* , **Ser. B34**, 393-400

Vanden-Broeck, J.-M. and Keller J. B., 1987 Weir flows *J. Fluid Mech.*, **176** 283-293

Vanden-Broeck, J.-M. and Keller J. B., 1989 Surfing on solitary waves *J. Fluid Mech.*, **198** 115-125

Vanden-Broeck, J.-M. and Dias, F., 1991 Nonlinear free-surface flows past a submerged inclined flat plate. *Phys. Fluids*, **A3(12)**, 2995-3000

Vanden-Broeck, J.-M., Schwartz, L. W. and Tuck, E. O., 1978 Divergent low Froude number series expansion of nonlinear free surface flow problem *Proc. Roy. Soc. Lond.*, **Ser. A 361**, 207-224

Wehausen, J. V. and Laitone, E. V., 1960 In*Handbuch der Physik*, **Vol. 9**, Springer, Berlin

Woods, L. C., 1958 Some generalizations of the Schwartz-Christoffel mapping formula. *Appl. Sci. Res.*, **B 7**, 89-101

Woods, L. C., 1961 *The Theory of Subsonic Plane Flow*, Cambridge Univ. Press